Detection of Lipopolysaccharide Pyrogens by Molecularly Imprinted Polymers

A thesis submitted in accordance with the conditions governing candidates for the degree of Philosophiae Doctor in Cardiff University

By

Jenna Louise Bowen

(M.Pharm)

June 2011

Welsh School of Pharmacy

Cardiff University

ProQuest LLC
789 East Eisenhower Parkway
P.O. Box 1346
Ann Arbor, MI 48106-1346

Acknowledgements

I would firstly like to thank my supervisors, Drs Chris Allender and Mark Gumbleton. Thank you both for all of the encouragement, support and guidance you have provided me with over the past four years. I could not have wished for better mentors, I have enjoyed every minute of my PhD.

Funding from the Royal Pharmaceutical Society of Great Britain Academic Excellence Awards is gratefully acknowledged.

A huge thank you goes to members of the Allender & Gumbleton laboratories past and present especially Jimmy for the early lessons in polymer chemistry, for teaching me my one Swedish phrase (Hallå din utvecklingsstörda apa!) and for his 'melodic' music in the lab, Marc for being a fantastic lab partner and for serenading me whilst I worked, Mat for always being on hand to give advice and support throughout my entire PhD and for all things 'Mac', Ghaith for the endless entertainment provided over lunch breaks and the emergency chocolate bars and Yvonne for helping to make my time in the lab so enjoyable.

Thanks are extended to Mrs Sarah Davies and all technical staff at the department and to Dr Charles Heard for providing me with my early research experience.

I would also like to express my gratitude to collaborators from outside of the department; Dr Phil Davies in the School of Chemistry for use of the FTIR and to Dr Jonathan Bartley, School of Chemistry for conducting Raman analysis on magnetite samples.

Last, but by no means least, a huge thank you to my family who have unfailingly supported and encouraged me throughout my studies.

Summary

Lipopolysaccharide (LPS) is commonly implicated in the development and rapid progression of sepsis however no efficient diagnostic assay currently exists. The over-arching aim of this project was therefore to develop a novel biomimetic peptide-polymer hybrid system capable of recognising and binding LPS in a variety of biologically relevant environments.

Target selective peptides (both commercially available and synthesised) have been used as high affinity 'functional monomers' in a molecular imprinting approach. To reduce the concept to practice, a bi-functionalised resin was prepared so as to allow the use of two independent surface attachment strategies. Controlled polymer growth was initiated from surface bound iniferter groups whilst the attachment of the peptide was achieved through amine-amine imidoester linkages or via azide-alkyne "click" chemistry. Polymyxin, a small, conformationally constrained cyclic peptide that possesses high affinity for lipopolysaccharide (LPS) was used to provide proof-of-principle.

Polymyxin resins, produced via the immobilisation of alkyne derivitised polymyxin B on the surface of azidomethyl polystyrene via "click" chemistry, were able to efficiently bind LPS from aqueous solutions with an apparent K_d of ~ 0.2 μM. Although the development of the peptide - polymer hybrid system using these resins appeared somewhat unsuccessful, whether the observed reduction in binding is due to changes in the B_{max} or the K_d of the resin remains to be elucidated. The assay performed with the polymerisation samples produced using resin displaying polymyxin immobilised via a dimethyl adipimidate linker, suggest that the hypothesised approach is feasible but that optimisation of a number of variables is needed before definitive results can be obtained.

Table of Contents

List of Figures

List of Tables

Chapter One : General Introduction

1.1 Lipopolysaccharide

1.1.1 General Overview

In 2004, the Infectious Diseases Society of America published a report highlighting the disparity between the dwindling number of new antimicrobial therapies and the increasing occurrence of bacteria resistant to multiple antibiotic classes (1). For a growing number of Gram negative infections there are no effective antimicrobial interventions either available or in the advanced stages of development (2,3). With the emergence of multi-drug resistant pathogens, in an ageing population with an increased number of immuno-compromised patients, it is not surprising that infective diseases are becoming ever more prevalent.

Sepsis is defined as "a life threatening condition that arises when the body's response to an infection injures its own tissues and organs" (4). It is a leading cause of death in non-coronary intensive care units worldwide with mortality rates of up to 50%. In the UK it is responsible for more deaths per year than breast and bowel cancer combined and the associated economic burden on the healthcare system is significant (5). Despite this, it remains under-recognised and poorly understood because of inadequate diagnostic assays and a lack of scientifically targeted clinical treatments.

Lipopolysaccharide is commonly implicated in the development and rapid progression of sepsis, even when the causative pathogen is of Gram-positive or fungal origin (6,7). Its presence in the blood is associated with elevated mortality rates (8), however it is not routinely tested for in the clinical setting.

1.1.2 Structure of Lipopolysaccharide

In the late 1800's the term "endotoxin" was used by Pfeiffer to describe the heat-stable, pyrogenic toxin associated with *Vibrio cholera* (9), however it wasn't until some 50 years later that the structure of these toxins could begin to be elucidated. With the development of extraction and purification techniques, endotoxin was found to consist of lipid and polysaccharide regions and hence the term lipopolysaccharide (LPS) was coined (10). Today, LPS is known to consist of three distinct regions; Lipid A, core regions and an O-specific antigen region (Figure 1.1). Each of these regions contributes to both the three-dimensional structure of LPS and its observed toxicity *in vivo*. Lipopolysaccharide occupies approximately 75 % of the surface area of the outer leaflet of the outer membrane of Gram-negative bacteria, with the lipid A region forming an integral part of the membrane while the polysaccharide portion extends outwards from the cell (11).

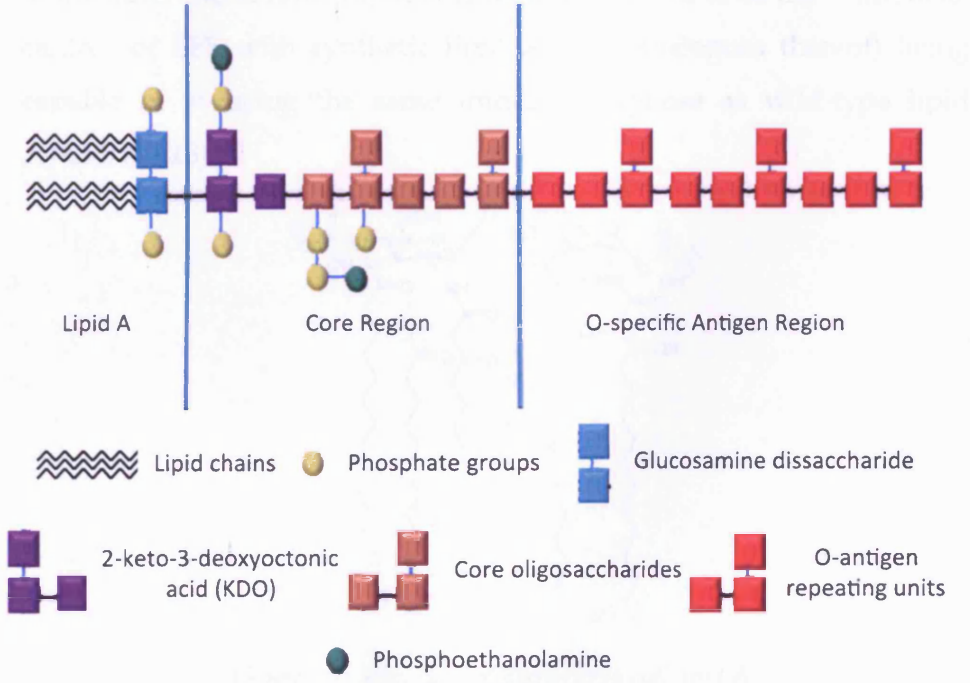

Figure 1.1: Generalised structure of lipopolysaccharide.

Over the past two decades, the structure of lipopolysaccharide has been reviewed extensively by Raetz (12,13), Rietschel (11), Holst (14), Morrison and Ryan (15), Caroff (10) and Lerouge (16). The following section will summarise the key features of each of the three distinct regions of this biomacromolecule.

1.1.2.1 Lipid A

Each of the enzymes responsible for the biosynthesis of lipid A from a uridine diphosphate-*N*-acetylglucosamine precursor, are encoded for by a single gene-copy that are highly conserved across the majority of Gram-negative species (13). As a result, this hydrophobic portion is the most preserved region of the LPS moiety between bacterial species consisting of a fatty acid substituted bisphosphorylated glucosamine disaccharide (Figure 1.2). This region is a prerequisite for viability in Gram-negative bacteria and functions to anchor LPS in the outer leaflet of the outer membrane. Lipid A is widely believed to be the "endotoxic centre" of LPS with synthetic lipid A (and analogues thereof) being capable of inducing the same immune response as wild-type lipid A/LPS (17,18).

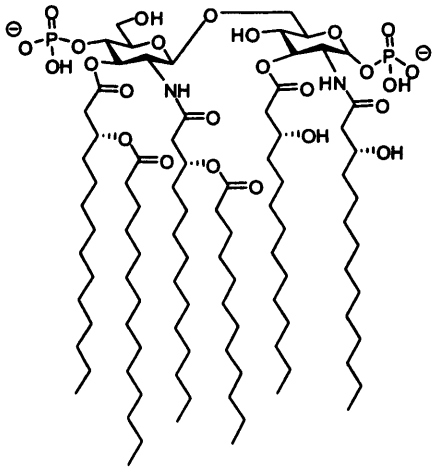

Figure 1.2: Structure of Escherichia coli lipid A.

Although lipid A is the most conserved region of LPS, inter-species variation in the number of carbon atoms and degree of hydroxylation of the acyl chains, as well as the type of hexosamine disaccharide and degree of phosphorylation of the sugar exist (19). The general structure of enterobacteriaceae lipid A encompasses six (*E.coli)* or seven (*Salmonella spp.)* acyl chains that are attached via ester and amide linkages at the C3/3′ and C2/2′ positions of the glucosamine disaccharide (GlcN) respectively. The acyl chains typically consist of between 10 and 16 carbons, with hydroxylation or substitution at C3. The phosphorylation of the glucosamine unit gives the region an overall negative charge that is important for stabilisation of the outer membrane and also for LPS interaction with host proteins. The 6′ position of the second GlcN residue is the location of the glycosydic linkage that connects lipid A to the saccharide region of the molecule.

Several studies have examined the effect of lipid A and its macromolecular conformation on the toxicity associated with a particular bacterial strain. In terms of *in vivo* endotoxic activity, an asymmetric hexaacyl lipid A (as shown for *E. coli* in Figure 1.2) attached to a phosphorylated disaccharide that adopts an overall conical shape is optimal (19,20). Increasing or decreasing the number of acyl chains, omitting the phosphate groups from the glucosamine sugar or reducing the disaccharide unit to a monosaccharide each significantly reduce the biological activity of lipid A (11). It is hypothesised that this is due to interaction with alternative members of the Toll-like receptor family that induce fewer pro-inflammatory cytokines or fail to be activated upon binding of LPS altogether (20). In fact tetraacyl species that form cylindrical structures such as the LPS found in some species of *Rhodobacter* and the lipid A precursor 1a, can function as antagonists to LPS induced activation of macrophages (21).

1.1.2.2 Core regions

The *inner core* consists of two LPS specific sugars, *L*-glycero-*D*-manno heptose and 2-keto-3-doxyoctonic acid (KDO) that are linked to the glucosamine disaccharide of the lipid A moiety (Figure 1.3). The heptose residues have been identified in the majority of Gram-negative bacterial species, however KDO is unique and invariably present in all LPS. In terms of bacterial viability, the lipid A region plus one or two KDO sugars are essential for cell survival (15). The phosphorylation of KDO and inner core sugars leads to an accumulation of negative charges at the membrane of Gram-negative bacteria that is important for the stabilisation of the outer membrane via the interaction with divalent cations and also, to some degree, influences the three-dimensional shape and hence endotoxic activity of the lipid A region (22). The anionic groups are also the initial point of interaction between LPS and host proteins.

Whilst the *outer core* is significantly more variable than the inner region, it typically consists of three common hexose sugars i.e. glucose, galactose and glucosamine. Overall, the core region is usually conserved within a bacterial genus but remains structurally distinct from the cores expressed by other genii e.g. *Salmonella, Shigella* and *Escherichia* have similar but not identical core regions.

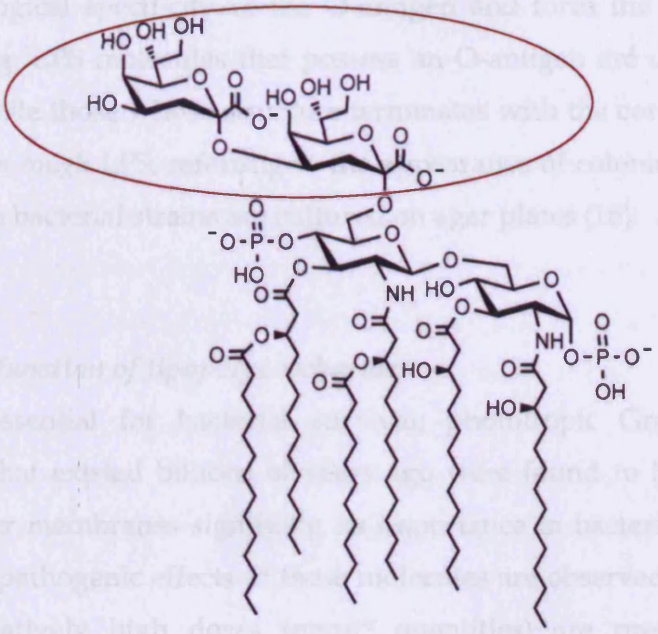

Figure 1.3: Structure of lipid A plus two 2-keto-3-deoxyoctonic acid (KDO) sugars (circled).

1.1.2.3 O-specific antigen region

This region is attached via the terminal sugar of the outer core region. It is highly immunogenic as it protrudes from the bacterial surface and therefore functions as the 'point of contact' between the bacteria and the host system. There exist huge interspecies and intrastrain variations in the composition of this region, however the general structure consists of a repeating pattern of sugar units, typically between three and five sugars long with anything from zero to forty repeats of the unit, that contain dideoxyhexose sugars which are unique to the region (16). The multitude of positions within the repeating unit that the sugar can occupy, coupled with the type of ring structure, the conformation it adopts and the chemical linkages between residues gives rise to the variations observed (23). The overall structure of this region, coupled with particular sugars in the unit, especially the terminal ones, confer

immunological specificity of the O-antigen and form the basis of O-serotyping. LPS molecules that possess an O-antigen are described as *smooth* while those whose structure terminates with the core region are defined as *rough* LPS, referring to the appearance of colonies when the respective bacterial strains are cultured on agar plates (16).

1.1.3 The function of lipopolysaccharide

LPS is essential for bacterial survival; phototropic Gram-negative bacteria that existed billions of years ago were found to have LPS in their outer membranes signifying its importance in bacterial existence (11). The pathogenic effects of these molecules are observed in humans when relatively high doses ($ngml^{-1}$ quantities) are present in the circulatory system, however low doses of LPS are believed to be beneficial to the host in helping to maintain a basal level of immune attentiveness (14). Endogenously, it is estimated that there is a much as 25 g of LPS in the human gastrointestinal tract (6). Although this is an essential feature of normal biology, during times of infection the mucosal barrier can become compromised allowing translocation of these native sources from the GI tract to the systemic circulation. Therefore LPS is ubiquitous in sepsis even when the causative agent is of Gram-positive or fungal origin (6,24).

In Gram-negative bacteria LPS is an effective diffusional barrier, much like the stratum corneum in humans, protecting the bacterium against host defense strategies, bile acids and hydrophobic antibiotics, allowing only low molecular weight, hydrophilic molecules to permeate (14). Additionally it impedes phagocytosis of the cell and may also function as a bacterial adhesin (25,26).

1.1.4 Recognition of lipopolysaccharide by host

Wherever there is potential for bacterial growth and division there is likely to be LPS in the environment. A wide variety of environments therefore exist in which there is a potential for exposure to LPS via inhalation, ingestion or direct entry into the circulatory system (27). Once LPS has entered the circulation it causes increased permeability of the vascular endothelium, facilitating its entry into the tissue. This plus oedema leads to a decreased blood volume that subsequently causes hypotension and tissue ischaemia. Ischaemia can cause the integrity of the mucosal barrier of the gut to become compromised, allowing the influx of endogenous LPS into the systemic circulation, thus amplifying the problem (24).

When lipopolysaccharide is released from the bacterial cell during growth, division or cell lysis, it is recognised as a pathogen associated molecular pattern (PAMP) by pattern recognition receptors (PRR's) (28). Activation of these receptors that are expressed on innate immune cells and principally by mononuclear phagocytes, leads to an exaggerated systemic immune response that is disproportionate to the initial antigenic insult. Such recognition of LPS by the host system leads to a cascade of events that results in the production of cytokines and other inflammatory mediators (Figure 1.4). Actions of the activated immune cells, combined with the effect of the inflammatory cytokines leads to the development of the clinical symptoms associated with infection e.g. fever, endothelial damage, peripheral vascular dilatation, coagulation disorders and myocardial depression which can eventually produce multiorgan failure, shock and death of the host. The organ systems most affected are the brain, heart, kidneys, liver and lung giving rise to altered levels of mental alertness, myocardial depression, acute renal and hepatic failure and respiratory distress syndromes (29).

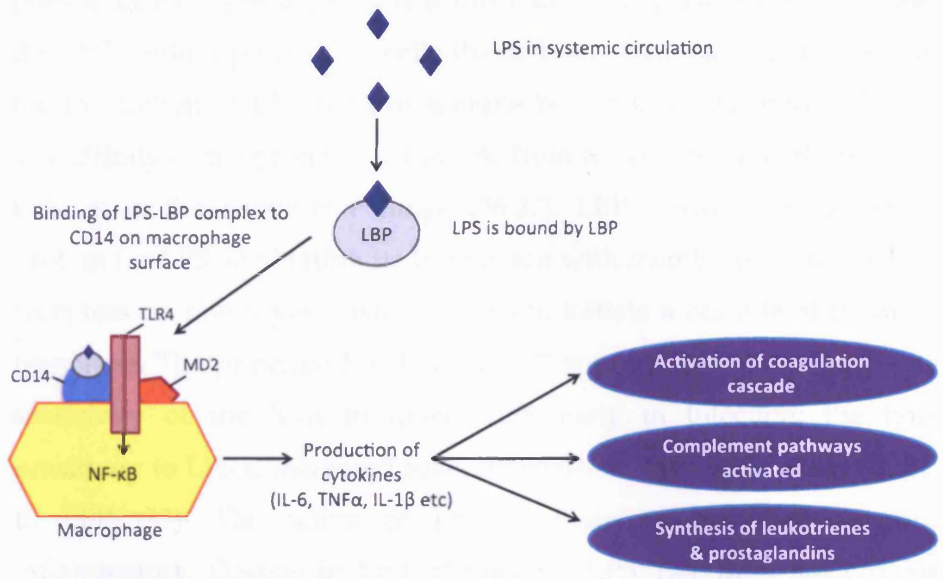

Figure 1.4: Schematic of the immunological response observed following infection of host with LPS. Following activation of the TLR4 receptor complex, nuclear translocation of nuclear factor kappa B (NF-κB) occurs, resulting in the production of pro-inflammatory cytokines such as tumour necrosis factor alpha (TNFα) and a variety of interleukins (e.g. IL-6 and IL-1β). Subsequent activation of other pathways precipitate the insult to the host system. (LPS = lipopolysaccharide; LBP = lipopolysaccharide binding protein; CD14= cluster of differentiation 14, a protein expressed on the surface of macrophages which functions as a receptor for the LPS-LBP complex; TLR4 = toll-like receptor 4, a type of pattern recognition receptor; MD2 = extracellular molecule associated with TLR4) .

1.1.4.1 Recognition of LPS by serum proteins

There are a number of endogenous proteins that recognise and bind LPS when it is present in the bloodstream. Lipopolysaccharide binding protein (LBP) is a 60 KDa glycoprotein synthesised by hepatocytes that is constitutively present in normal serum at a concentration of ~ 0.5 - 10 μgml^{-1}. Following induction of an acute phase reaction, this level can increase to in excess of 200 μgml^{-1} (30-33). Basic amino acid residues clustered at the far end of the amino terminal mediate the initial

electrostatic interactions with the negatively charged lipid A/KDO portion of the molecule (31). It is this half of the protein that possesses the LPS binding properties while the carboxyl terminal is implicated in the interaction of LPS with membrane bound CD14 receptors (34,35). The affinity of the protein for lipid A, from rough and smooth forms of LPS, is in the nanomolar range (36,37). LBP functions as a carrier protein for LPS, facilitating its interaction with membrane bound CD14 receptors on monocytes/macrophages to initiate a cascade of immune responses. The principal function of LBP appears to be to enhance the sensitivity of the host to detect LPS early in infection; the host sensitivity to LPS is increased several orders of magnitude when bound to LBP (33). The action of LBP is therefore described as pro-inflammatory. Despite its high affinity for LPS, LBP does not possess any direct antimicrobial activity (38).

Bactericidal/permeability increasing protein (BPI) is another native protein that interacts with LPS in serum. It has a molecular weight of approximately 55 KDa and is found predominantly in the azurophilic granules of polymorphonuclear neutrophils (PMNs) (33,39). PMNs are granulocytes that are released from the bone marrow in response to complement proteins. They are recruited to the site of infection where they phagocytose invading organisms and kill them intracellularly. Upon ingestion of the micro-organism, degranulation of the granulocytes occur resulting in the release of toxic nitrogen oxides, cationic proteins and defensins that can kill bacteria, proteolytic enzymes and lysozyme (40). Whereas LBP is constitutively expressed in the liver, there is no significant endogenous level of BPI in the circulation (low $ngml^{-1}$) prior to induction of an acute phase reaction, since there are few polymorphonuclear neutrophils present and hence little neutrophil derived BPI (41). The protein has good sequence

homology with LBP (~45% amino acid sequence identity (Figure 1.5)) (33,42) however the two proteins have very disparate activities.

BPI:

^{82}Asn-Ala-Asn-Ile-Lys-Ile-Ser-Gly-Lys-Trp-Lys-Ala-Gln-Lys-Arg-Phe-Leu-Lys-Met-Ser-Gly-Asn-Phe-Asp-Leu-Ser-Ile^{108}

LBP:

^{91}Trp-Lys-Val-Arg-Lys-Ser-Phe-Phe-Lys-Leu-Gln-Gly-Ser-Phe-Asp-Val-Ser-Val^{108}

Figure 1.5: Specific peptide sequences of BPI and LBP that demonstrate highest LPS binding activity. (Highlighted residues indicate homology between the two proteins.) Generally a repeating sequence of alternating polar and non-polar amino acid residues in both sequences is observed, in addition to an overall positive charge (32,42)

Unlike LBP, BPI is anti-inflammatory. The affinity of BPI for LPS is approximately 20 – 100 fold higher than LBP (39,43,44) and it possesses both antibacterial and anti-endotoxin activities; properties that are a consequence of the highly cationic nature of BPI (net charge of ~ +12) (39,45). Binding of BPI to live Gram-negative bacteria is facilitated via electrostatic interactions with LPS in the outer membrane. As the affinity of this peptide for LPS is significantly greater than that of the stabilising divalent cations, BPI effectively displaces the Mg^{++}/Ca^{++} ions to bring about destabilisation and hence increased permeability, of the outer membrane. Other effects of this interaction include hydrolysis of cellular phospholipids by phospholipases and interruption of cell division. Following an increased incubation period, BPI brings about cell kill by perturbing the inner membrane of the bacterium (46). Studies using the amino-terminal half of BPI have demonstrated that it is this domain that is responsible for both antibacterial and anti-

endotoxin properties (43,47). Whilst the carboxy-terminal possesses little/no antibacterial activity, it plays a significant role in the neutralisation of endotoxin. It is unable to interact with membrane bound CD14 and therefore incapable of initiating the subsequent cascade of immune/inflammatory responses that is observed with the LPS-LBP complex, instead it promotes adhesion of bacterial cells and aggregates of LPS to the surface of neutrophils and monocytes to promote phagocytosis and clearance of LPS from the systemic circulation (48,49).

A soluble form of the membrane bound receptor CD14 (sCD14) also constitutively exists in serum (50). Several isoforms of this receptor are released from the surface of macrophages and monocytes in response to a variety of stimuli (51). At high concentrations, sCD14 appears to act as a decoy receptor for LPS, preventing binding to membrane bound CD14 and subsequent activation of the signalling cascade (52-54). It is thought to further neutralise the effects of LPS via a role in the transfer of LPS to high-density lipoproteins (55,56). However at lower concentrations, in cells that do not naturally express the membrane bound form of the receptor, it has been shown to enhance the response to LPS (57,58).

1.1.4.2 Recognition of LPS by membrane-bound receptors: The CD14-TLR4-MD2 complex

CD14 (cluster of differentiation antigen 14) a 55 KDa glycosylphospatidylinositol (GPI) anchored protein, was first recognised to have a role in the *in vivo* sensing of LPS in 1990 by Wright and colleagues (59). Inhibition of LPS induced TNFα was observed when cells were exposed to anti-CD14 antibody, thus suggesting a role of this receptor in the induction of inflammatory mediators following

exposure to endotoxin. The CD14 receptor is expressed on the surface of macrophages, monocytes and neutrophils and binds LPS both in association with the serum protein LBP and as monomeric LPS (52). As it is a member of the GPI family of cellular proteins it lacks signalling capacity due to the absence of a transmembrane domain. It was therefore hypothesised that CD14 must be interacting with a second receptor to bring about the induction of inflammatory mediators (60).

The Toll-like receptors (TLRs) are a family of 10 pattern recognition receptors expressed on the surface of macrophages and also intracellularly (61). The involvement of the TLRs, specifically TLR4, in the recognition of LPS was first described by the group of Bruce Beutler in 1998 when genetic mapping of C3H/HeJ mice demonstrated a mutation in the gene encoding for TLR4 (62,63). As a consequence, these mice are hyporesponsive to LPS stimulation due to the presence of a defective TLR4 protein (62,64). TLR4, the first of the human Toll-like receptors to be identified, is a homodimeric, transmembrane receptor that is capable of facilitating intracellular signalling to initiate the induction of inflammatory mediators (65). CD14 functions as a co-receptor for TLR4. Following binding of the LPS-LBP complex by membrane bound CD14, the distance between CD14 and TLR4 decreases affording appropriate presentation of the endotoxin molecule (66). A further accessory molecule, MD2, is required for full activation of the immune system by endotoxin. Although the function of MD2 has not been fully elucidated, its absence results in a significant reduction in the inflammatory response following LPS stimulation (67). It has been suggested that MD2 facilitates the dimerisation and cellular distribution of TLR4 (67-69).

The induction of inflammatory mediators resulting from the formation of the CD14-TLR4-MD2 complex proceeds via a number of adapter molecules including myeloid differentiation primary-response protein

88 (MyD88) and IL-1R-associated kinases (IRAKs) (70,71). The consequence of this signaling cascade is the nuclear translocation of nuclear factor-κB (NF- κB) resulting in the transcription of a variety of pro-inflammatory cytokines and chemokines, including TNF α, IL-6 and IL-1β amongst others (Figure 1.4) (72).

1.1.4.3 Intracellular recognition of LPS

Another member of the pattern recognition receptor family, the NOD (nucleotide binding and oligomerisation domain) like receptors (NLRs), are also implicated in the recognition of Gram-negative bacteria and LPS (73). The NLRs share many similarities with the TLRs, for example they both possess leucine-rich repeats and initiate similar signalling cascades, however these receptors are located exclusively intracellularly (74). They appear to act as a secondary defense mechanism should the membrane bound TLR be absent or unresponsive to a pathogenic stimuli (72). Previously, the receptors NOD1 and NOD2 were thought to be involved in the recognition of LPS (65), however it would appear the activation was due to contamination of the LPS preparation with petidoglycan (72); NOD1 does primarily sense Gram-negative bacteria, however its ligand is not LPS. Another member of the NLR family, NLRP3, has recently been implicated in the intracellular recognition of LPS (72).

1.1.5 Current treatment options for Gram negative infections and associated sepsis.

Suspected bacteraemia is initially treated with empirical antibiotic therapy until positive blood cultures can be obtained. Although antibiotic therapy has been shown to be more effective if started early (75), the choice of anti-infective is critical as some promote the release of

LPS from the bacterial surface through their lytic action (76,77), thus potentiating the clinical condition. Polymyxin B (discussed in more depth in Chapter Three) is an antimicrobial peptide that displays high affinity for LPS and is therefore not only bactericidal but also a potent anti-endotoxin. Its use nowadays is somewhat limited however as a consequence of associated neuro- and nephrotoxicity. The mainstay of current treatment is mainly supportive therapies with the aim of restoring hypovolaemia via fluid boluses to help rectify hypotension and increase tissue perfusion. Glucocorticoid therapy, anti-cytokine and anti-endotoxin therapies have been met with limited success (78) although drotrecogin alfa (Xigris®) a recombinant form of protein C, has been licensed for use in severe sepsis. In a worldwide clinical trial (PROWESS) drotrecogin alfa demonstrated an overall reduction in 28 day mortality compared to placebo (79), however there is an increased risk of bleeding during treatment and a recent Cochrane Review suggests that treatment with Xigris should be avoided (80). Therapeutic targeting of a single point in the immune-inflammatory cascade is likely to have little effect on the overall outcome; a plethora of treatments or a means of more effective removal of LPS from the circulation is likely to be needed to have an impact. In addition, the ability to diagnose sepsis during the early stages with continuous realtime progression monitoring would revolutionise the treatment of sepsis. A 6 - 10% increase in risk of death is observed for every hour that sepsis remains undiagnosed (81).

1.1.6 Detection of lipopolysaccharide

In the 1940's the rabbit pyrogen test was introduced to allow for the detection of endotoxin contamination of pharmaceutical products (82,83). The febrile response of a rabbit following injection of the formulation was monitored; if the rise in temperature exceeded that

outlined in previously established limits the solution was deemed to contain endotoxin at an unacceptable level. Although this test mimics the human response to endotoxin, there are significant limitations associated with this assay. Not only is the process time consuming, expensive and subject to animal welfare issues, certain formulations/pharmaceutical products cannot be tested in this way due to associated severe toxicity or as a result of the drug itself modulating the temperature of the animal, for example, antipyretics (84). As a result, the rabbit pyrogen test has largely been superseded by the Limulus amoebocyte lysate (LAL) assay. Developed by Levin and Bang in the 1960's (85,86), the assay relies on the coagulation of haemocytes from the horseshoe crab, *Limulus polyphemus,* on exposure to lipopolysaccharide (87). Factor C, the main factor sensitive to LPS in the clotting cascade, is activated by endotoxin that in turn activates factor B, thus activating a clotting enzyme that subsequently converts coagulogen into the insoluble coagulin (88). Although easier to perform than the rabbit pyrogen test, interference from drugs and other test substances is possible and therefore careful sample preparation is vital (89). A study to assess the suitability of the assay for the initial diagnosis of peritonitis in peritoneal dialysis patients by Hausmann *et al.* (90) found that despite the assay being very efficient at distinguishing between Gram-positive and Gram-negative infections, false positive results were obtained in some patients as a result of a fungal peritoneal infection. It is a component of the cell wall of the fungus (β glucans) that is able to activate clotting enzymes in the amoebocyte cells by interacting with factor G (91). Although the LAL assay has found considerable use in the detection of endotoxin in pharmaceutical formulations, its use in the clinical setting is limited due to non-specific sequestration of LPS by serum proteins and cellular components (92).

Spectral diagnostics have recently developed an endotoxin activity assay (EAA) that was approved by the FDA (93) as a result of a multinational clinical trial (MEDIC, (6)). The assay indirectly measures LPS, relying on the priming of host neutrophils by LPS-antibody complexes to generate a chemiluminescent response via the oxidation of luminol. The assay is semi-quantitative indicating whether endotoxin level is low, intermediate or high (94).

1.1.7 Removal of lipopolysaccharide

Due to the potent biological activity of LPS, the FDA have imposed an endotoxin limit of 5 EU/kg for intravenous formulations and 0.2 EU/kg for those intended for intrathecal use (1 EU is equivalent to ca. 100 pg of LPS) (95). The risk of contamination should be minimised during the manufacture stage as LPS is a ubiquitously stable macromolecule, resistant to extremes of temperature and pH (96,97) and its removal is therefore somewhat cumbersome. Conventional autoclaving and sterilisation techniques fail to inactivate endotoxin, with prolonged exposure to temperatures in excess of 180 °C or extremes of pH required (98). Such conditions often have a detrimental effect on the formulation in question. Chromatographic clean-up (96,99,100), two-phase extractions (101) and ultrafiltration (102,103) have all been investigated as alternative methods for the removal of endotoxin, with varying degrees of success.

1.2 Molecular Imprinting

1.2.1 Conventional Imprinting

Molecular imprinting, as a means of achieving molecular recognition through the generation of molecule specific cavities within a synthetic material, was first demonstrated in the 1940s in the laboratories of double Nobel Laureate Linus Pauling. Ironically, it was his theory of antibody production (104), later shown to be incorrect, that led Dickey, one of Pauling's research students, to investigate whether silica gels could be prepared with pre-defined substrate selectivity (105). Following these early studies it was not until the 1970s that Wulff first demonstrated molecular imprinting in an organic polymer (106). The approach was popularised in the early 1990s when the work of Mosbach on antibody mimicry was published in Nature (107). The general protocol for producing such receptor mimics is outlined schematically in Figure 1.6.

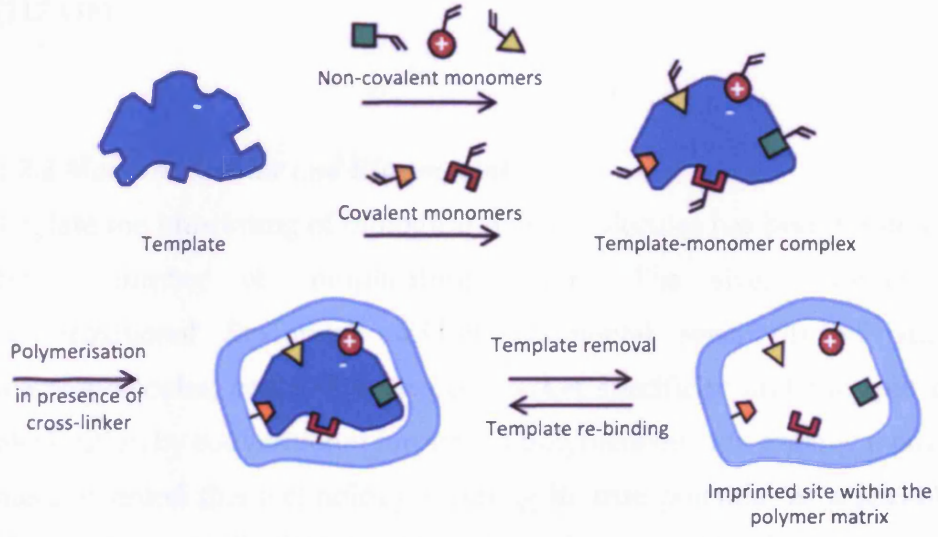

Figure 1.6: Schematic representation of the molecular imprinting process (modified from (108)).

Molecularly imprinted polymers (MIPs) have the potential to serve as efficient, robust, cost effective synthetic alternatives to antibodies. Typically, MIPs have been generated using relatively small, highly functional molecules as templates, for example beta-blockers, corticosteroids and hormones. Such systems are efficient in re-binding and separating the target molecule from complex mixtures, however affinities are generally an order of magnitude or more below those achieved with commercially available antibodies. The field of molecular imprinting has been reviewed extensively both in peer-reviewed journals (108-112) and in dedicated textbooks (113-116).

All too often the preparation of such materials is a poorly controlled, random, affair that results in a population of heterogeneous binding sites. Consequently, reproducibility is poor, binding capacities are low and non-specific binding problematic (see review references above). Furthermore, nearly all of the high affinity data reported in the literature is carried out in non-polar solvents whilst the aqueous compatibility of traditional imprinted polymer formats is, at best, poor (117,118).

1.2.2 Macromolecular and Bio-imprinting

To date the imprinting of biological macromolecules has been hindered by a number of complicating factors. The size, complexity, conformational flexibility and environmental sensitivity of such macromolecules, coupled with poor target specificity and the lack of recognition by conventional imprinted polymers outside organic media, has prevented this technology reaching its true potential as a feasible alternative to antibodies as recognition elements (119-121). However, some success has been achieved in the field through careful design and optimisation of the imprinted system.

Conventional bulk imprinting approaches and the synthesis of imprinted soft gels both suffer from inefficient removal of the template and poor mass transfer upon re-incubation with their target species (122). As a result, efforts have primarily focused on the use of surface imprinting approaches to allow for unhindered access to recognition sites. Early studies employed metal ion co-ordinated imprinting as an approach for the recognition of proteins (123-125). Although the systems were efficient at rebinding their templates, this imprinting technique requires the use of metal-ion coordinating monomers such as N-(4-vinyl)-benzyl iminodiacetic acid and proteins that express histidine residues on their surface. The application of this methodology is therefore somewhat limited. Hierarchial imprinting has also been used to generate recognition elements for peptides. This technique involves the immobilisation of peptidic targets to the surface of a porous, sacrificial solid support such as silica, followed by polymerisation of monomers within the pores and subsequent removal of the support. This allows for the generation of surface confined binding sites that are more homogenous than those generated in conventional imprinted polymer systems (126,127). This homogeneity arises from the fact that the template is immobilised during the imprinting process and is therefore less flexible. The main drawback of such approaches is the necessity for harsh conditions (e.g. the use of glass etchants such as ammonium hydrogen fluoride) to bring about removal of the solid support.

In 2000 - 2001, Rachkov and Minoura demonstrated the epitope approach to molecular imprinting for the first time (128,129). They imprinted a tetra-peptide sequence from the natural peptidic hormone, oxytocin, in acetonitrile (97%)/water (3%). Importantly recognition of the full peptide could be achieved through the imprinting of an exposed epitope from its structure, thus demonstrating the feasibility of

this approach in the area of protein/bio-imprinting. The polymers performed well in chromatographic evaluation studies where the mobile phase consisted mainly of acetonitrile (95%) however when the amount of water in the mobile phase was increased to 70%, significant reductions in retention time were observed due to the loss of hydrogen bonding interactions between the template and the polymer. Further increasing the water content to 90% led to increased retention times due to ionic and/or hydrophobic interactions dominating. The system was sensitive to pH and ionic concentration of the aqueous mobile phase. The polymers were produced by conventional bulk polymerisation and therefore, although they demonstrated effectiveness in recognising the templated tetra-peptide sequence and the natural 9-mer peptide oxytocin, larger targets are likely to suffer from inefficient mass transfer upon rebinding. The Shea group further progressed this technique, achieving recognition of larger protein structures (cytochrome C, bovine serum albumin and alcohol dehydrogenase) through the imprinting of a nonapeptide sequence isolated from the C-terminus of the protein (130). Unlike the work of Rachkov and Minoura, a surface imprinting approach was adopted to generate thin molecularly imprinted films. The nonapeptides were immobilised on a silicon surface and a solution of monomers photochemically polymerised on the surface. The polymer-modified surfaces were soaked in buffer overnight to separate the polymer films from the support, thus generating micron thick films capable of recognising not only the template nonapeptide but also the full protein under native (aqueous buffer) conditions. The MIP films selectively bound their target protein from mixtures composed of five different proteins. Rebinding studies with the BSA MIP film using nonapeptides derived from BSA in which a single amino acid had been substituted resulted in complete loss of recognition, demonstrating the specificity for the system for its template.

Recently the same group demonstrated the use of molecularly imprinted polymers in an *in vivo* system for the first time (131). The polymers, imprinted with the 26 amino acid peptide Melittin from bee venom, demonstrated affinities in the picomolar range that was comparable to those achieved with antibodies (132,133). To achieve such affinities for a biological macromolecule, through polymerisation in wholly aqueous conditions, is a significant advancement for the field of molecular imprinting. The nanoparticles, synthesised using an optimised monomer/cross-linker combination identified during a prior screening study, were capable of neutralising the toxic, fatal effects of Melittin when injected into live mice.

1.3 Scope of thesis

The over-arching aim of this project was to develop a peptide-polymer hybrid system capable of recognising and binding LPS in a variety of biologically relevant environments. The ability to detect endotoxin on admission to hospital and to be able to continuously monitor levels throughout treatment would offer significant clinical benefits. Furthermore, it was hoped that technology developed would provide a platform for the development of novel therapeutic agents for the treatment of Gram-negative infections and associated sepsis.

We hypothesised that through the integration of target specific peptide receptors, into the backbone of a polymer support, the issues surrounding the imprinting of biomacromolecules could be circumvented. Our approach would require that a template selective peptide would be surface immobilised (Figure 1.7 a) and encouraged into its binding conformation through exposure to the template (Figure 1.7 b). Subsequently, following addition of monomers (Figure 1.7 c), this complex would be locked in place by a polymerisation or capture stage (Figure 1.7 d). Finally the removal of the template would expose the peptide, but leave it secured in its binding conformation, essentially lining a portion or the entirety of the polymer cavity. Rebinding of the template would result due to reciprocal peptide-template and polymer-template interactions (Figure 1.7 e). By analogy with conventional 'co-polymer' molecular imprinting, the peptide performs the role of a 'super' functional monomer in that it demonstrates affinity and selectivity for the target *prior* to polymerisation. Whilst possessing the robustness and adaptability of conventionally imprinted polymers, synthesis of these materials would not rely on organic solvents and would be prepared and applied in aqueous environments. Furthermore, this strategy builds upon the success achieved with

surface imprinting and template immobilisation techniques. It is therefore envisaged that the binding sites should be readily accessible and homogenous in nature, thus allowing for efficient recognition and mass transfer kinetics.

From a conventional molecular imprinting perspective, a number of 'templating' processes would occur during pre-polymerisation/ polymerisation and all would contribute to the formation and function of the resulting imprinted site. Firstly interaction between the template and the peptide controls and dictates peptide conformation prior to formation of a pre-polymerisation complex with monomer species. Importantly pre-polymerisation interactions are also established between the peptide and monomers and also, depending on the size of the template relative to the size of the peptide and the degree of polymerisation from the surface, exposed (non-peptide complexed) parts of the template with monomer species. The subsequent capture of these complexes results in an imprinted site where the peptide is effectively sandwiched, in its binding conformation, between template and polymer whilst sections of the template are involved in conventional monomer residue-template interactions.

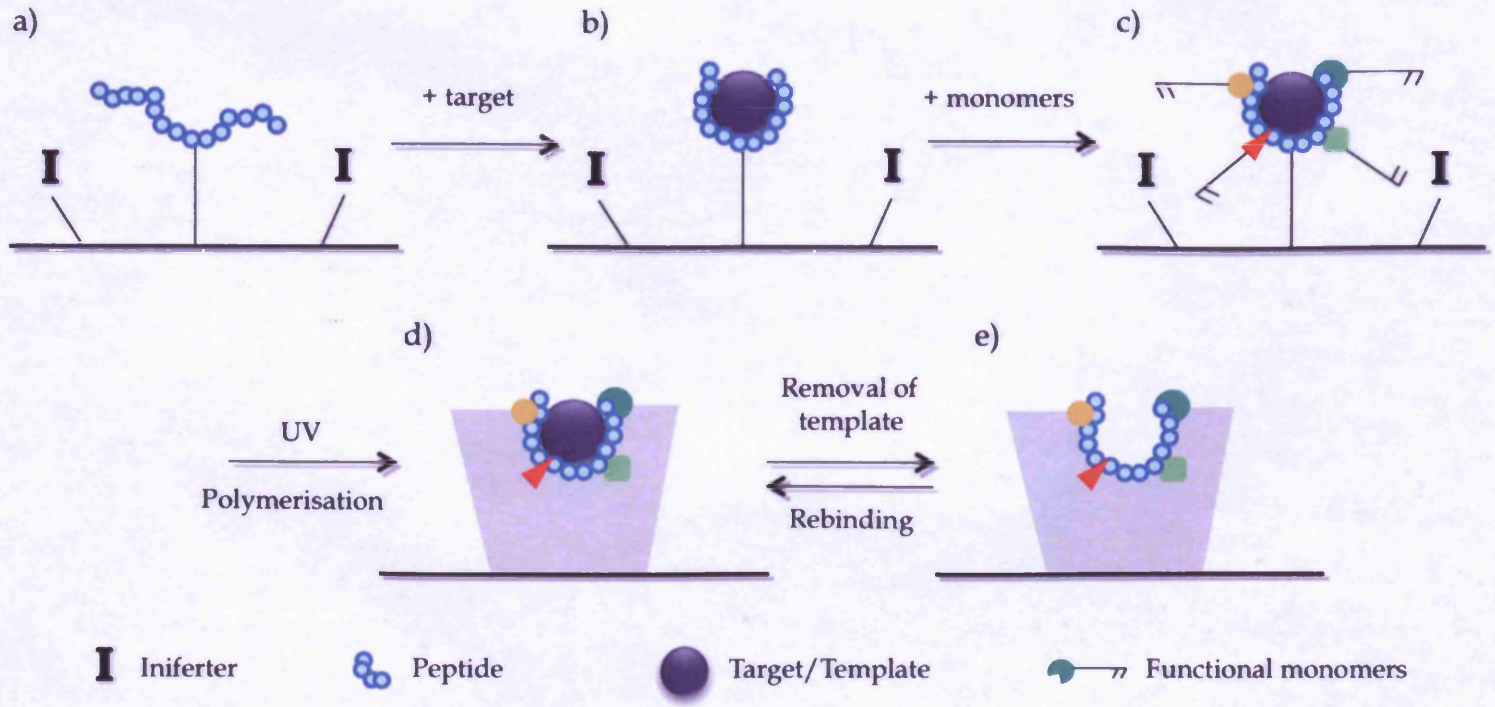

Figure 1.7 Schematic of the formation of the peptide-polymer hybrid system. The desired peptide is immobilised on to a solid support (a) and a solution phase complex with the target molecule is formed (b). Monomers are introduced and interactions form with the peptide-target complex (c). Polymerisation is initiated from surface-bound initiators via irradiation with UV light (d) forming a polymer matrix around the peptide-target complex that, on removal of the target molecule, leaves an imprinted site that is lined with a conformationally restricted peptide (e).

It is important to note that the schematic presented in Figure 1.7 illustrates the process for a target that is of similar size to the peptide species and therefore the imprinted site is entirely lined by the peptide. In the current study, it is possible that the template is considerably larger than the peptide; the length of rough LPS has been calculated to be 2.4 - 4.4 nm while those species possessing an O - antigen can be well in excess of 10nm depending on the number of repeating units present (26,134). It is therefore possible that the peptide only occupies a portion of the imprinted site, thus allowing further interactions between the monomer(s) and template to be established (Figure 1.8). The degree of interaction between the template and polymer is obviously dependent on the choice of monomer (presence of complementary functionality) but also on the height of polymer grafted from the surface of the solid support relative to the size of the target. In the case of a small target (as depicted in Figure 1.7), care must be taken to avoid growing the polymer beyond the peptide-template complex to ensure that the template does not become irreversibly entrapped with in the system. For larger targets, the polymerisation period may need to be extended to allow the polymer to grow around a portion of the molecule for template-polymer interactions to play a role (Figure 1.8).

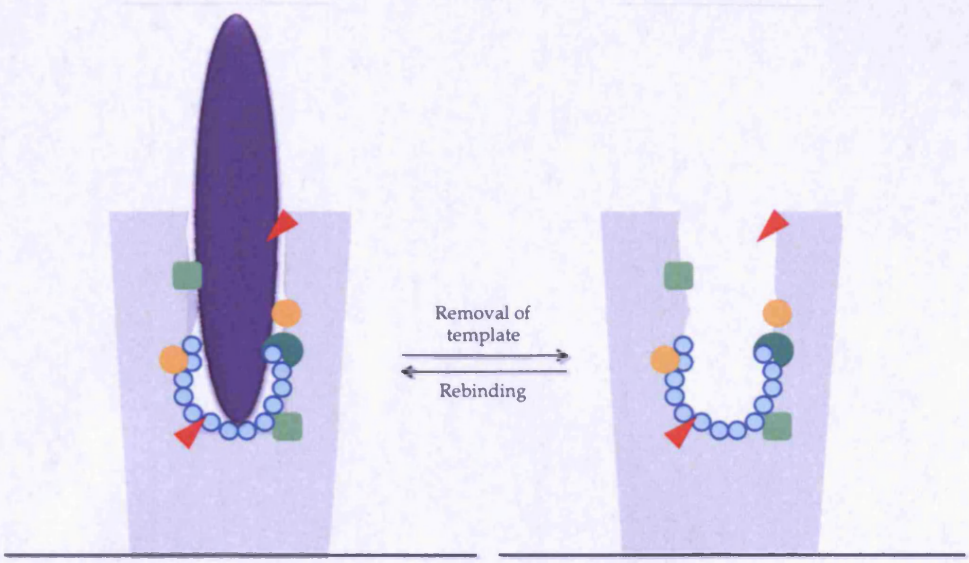

Figure 1.8: Schematic of the imprinted site when the template is larger than the peptide species. Figure key is same as in Figure 1.7.

The objective in Chapter Two was to develop an efficient and robust solid support to facilitate the co-immobilisation of a LPS specific peptide and an iniferter group capable of initiating controlled polymer growth. Standard Merrifield resin was chosen as the solid support as it was readily available and possessed a chloromethyl group to which an iniferter could readily be attached. It was also anticipated that the versatility of the chloromethyl functionality would additionally allow for further chemical modification with relative ease to generate bi-functionalised resins with pre-defined loadings of each tether.

Chapter Three investigated the use of the bacterial derived peptide polymyxin B, as a model peptide to provide evidence for the proposed polymer system. Polymyxin B has a high affinity for lipopolysaccharide and has therefore traditionally been used clinically as an anti-endotoxin. The peptide was immobilised onto the solid supports described in Chapter Two using a variety of attachment strategies and

binding assays conducted to determine affinities and binding capacities. Following full characterisation of the immobilised peptide, polymer growth was initiated from surface bound iniferter groups around the peptide when bound to LPS and the binding efficiency of the system evaluated.

The studies outlined in Chapter Four were undertaken to allow the transfer of the work described in Chapters Two and Three to a more biologically useful strategy for the detection and/or *in vivo* sequestration of lipopolysaccharide. Magnetic nanoparticles were synthesised and polymyxin immobilised to the surface. The ability of the nanoparticles to remove lipopolysaccharide from solution was then evaluated.

1.4 Reference List

1. Infectious Diseases Society of America. Bad Bugs, No Drugs. As Antibiotic Discovery Stagnates ...A Public Health Crisis Brews [Internet]. 2004 Jul;Available from: http://www.idsociety.org/10x20.htm

2. Arias CA, Murray BE. Antibiotic-resistant bugs in the 21st century--a clinical super-challenge. N. Engl. J. Med. 2009 Jan 29;360(5):439-443.

3. Boucher HW, Talbot GH, Bradley JS, Edwards JE, Gilbert D, Rice LB, et al. Bad bugs, no drugs: no ESKAPE! An update from the Infectious Diseases Society of America. Clin. Infect. Dis. 2009 Jan 1;48(1):1-12.

4. The Global Sepsis Alliance. Stamping Out Sepsis A Global Goal [Internet]. 2011 Feb 15 [cited 2011 Apr 25];Available from: http://www.infectioncontroltoday.com/articles/2011/02/stamping-out-sepsis-a-global-goal.aspx

5. Daniels R. NHS Evidence - Emergency and Urgent Care [Internet]. 2009 [cited 2010 Nov 1];Available from: http://www.library.nhs.uk/emergency/Page.aspx?pagename=SEPSIS

6. Marshall JC, Foster D, Vincent J-L, Cook DJ, Cohen J, Dellinger RP, et al. Diagnostic and Prognostic Implications of Endotoxemia in Critical Illness: Results of the MEDIC Study. Journal of Infectious Diseases. 2004;190(3):527 -534.

7. Opal SM, Scannon PJ, Vincent J-L, White M, Carroll SF, Palardy JE, et al. Relationship between Plasma Levels of Lipopolysaccharide

(LPS) and LPS-Binding Protein in Patients with Severe Sepsis and Septic Shock. Journal of Infectious Diseases. 1999 Nov 1;180(5):1584 -1589.

8. Marshall JC, Foster D, Vincent J-L, Cook DJ, Cohen J, Dellinger RP, et al. Diagnostic and Prognostic Implications of Endotoxemia in Critical Illness: Results of the MEDIC Study. The Journal of Infectious Diseases. 2004;190(3):527-534.

9. Rietschel ET, Cavaillon J-M. Richard Pfeiffer and Alexandre Besredka: creators of the concept of endotoxin and anti-endotoxin. Microbes and Infection. 2003 Dec;5(15):1407-1414.

10. Caroff M, Karibian D. Structure of bacterial lipopolysaccharides. Carbohydrate Research. 2003 Nov 14;338(23):2431-2447.

11. Rietschel E, Kirikae T, Schade F, Mamat U, Schmidt G, Loppnow H, et al. Bacterial endotoxin: molecular relationships of structure to activity and function. FASEB J. 1994 Feb 1;8(2):217-225.

12. Raetz CRH. Biochemistry of Endotoxins. Annu. Rev. Biochem. 1990 Jun;59(1):129-170.

13. Raetz CRH, Whitfield C. Lipopolysaccharide Endotoxins. Annu. Rev. Biochem. 2002 Jul;71(1):635-700.

14. Holst O, Ulmer AJ, Brade H, Flad HD, Rietschel ET. Biochemistry and cell biology of bacterial endotoxins. FEMS Immunology and Medical Microbiology. 1996;16(2):83-104.

15. Morrison DC, Ryan JL. Bacterial Endotoxic Lipopolysaccharides. 1st ed. CRC Press; 1992.

16. Lerouge I, Vanderleyden J. O-antigen structural variation: mechanisms and possible roles in animal/plant-microbe interactions. FEMS Microbiology Reviews. 2002 Mar;26(1):17-47.

17. Rietschel ET, Brade H, Brade L, Brandenburg K, Schade U, Seydel U, et al. Lipid A, the endotoxic center of bacterial lipopolysaccharides: relation of chemical structure to biological activity. Prog. Clin. Biol. Res. 1987;231:25-53.

18. Zähringer U, Lindner B, Rietschel ET. Molecular structure of lipid A, the endotoxic center of bacterial lipopolysaccharides. Adv Carbohydr Chem Biochem. 1994;50:211-276.

19. Seydel U, Schromm AB, Blunck R, Brandenburg K. Chemical structure, molecular conformation, and bioactivity of endotoxins. Chem. Immunol. 2000;74:5-24.

20. Netea MG, van Deuren M, Kullberg BJ, Cavaillon J-M, Van der Meer JWM. Does the shape of lipid A determine the interaction of LPS with Toll-like receptors? Trends Immunol. 2002 Mar;23(3):135-139.

21. Seydel U, Oikawa M, Fukase K, Kusumoto S, Brandenburg K. Intrinsic conformation of lipid A is responsible for agonistic and antagonistic activity. European Journal of Biochemistry. 2000 May 1;267(10):3032-3039.

22. Schromm AB, Brandenburg K, Loppnow H, Moran AP, Koch MHJ, Rietschel ET, et al. Biological activities of lipopolysaccharides are determined by the shape of their lipid A portion. European Journal of Biochemistry. 2000 Apr 1;267(7):2008-2013.

23. Whitfield C. Biosynthesis of lipopolysaccharide O antigens. Trends in Microbiology. 1995 May;3(5):178-185.

24. Van Leeuwen PA, Boermeester MA, Houdijk AP, Ferwerda CC, Cuesta MA, Meyer S, et al. Clinical significance of translocation. Gut. 1994 Jan;35(1 Suppl):S28-S34.

25. Licht TR, Krogfelt KA, Cohen PS, Poulsen LK, Urbance J, Molin S. Role of lipopolysaccharide in colonization of the mouse intestine by Salmonella typhimurium studied by in situ hybridization. Infection and immunity. 1996;64(9):3811-3817.

26. Murray GL, Attridge SR, Morona R. Altering the Length of the Lipopolysaccharide O Antigen Has an Impact on the Interaction of Salmonella enterica Serovar Typhimurium with Macrophages and Complement. J. Bacteriol. 2006 Apr 1;188(7):2735-2739.

27. Young RS. An investigation of the pulmonary effects of Escherichia coli Lipopolysaccharide. Thesis. University of Wales College, Cardiff; 1997.

28. Rosenfeld Y, Shai Y. Lipopolysaccharide (Endotoxin)-host defense antibacterial peptides interactions: Role in bacterial resistance and prevention of sepsis. BBA-Biomembranes. 2006;1758(9):1513-1522.

29. Chaby R. Strategies for the control of LPS-mediated pathophysiological disorders. Drug Discovery Today. 1999 May 1;4(5):209-221.

30. Tobias PS, Mathison J, Mintz D, Lee JD, Kravchenko V, Kato K, et al. Participation of lipopolysaccharide-binding protein in lipopolysaccharide-dependent macrophage activation. Am. J. Respir. Cell Mol. Biol. 1992 Sep;7(3):239-245.

31. Tobias PS, Soldau K, Ulevitch RJ. Identification of a lipid A binding site in the acute phase reactant lipopolysaccharide binding protein. Journal of Biological Chemistry. 1989 Jun 25;264(18):10867-10871.

32. Schumann R, Leong, Flaggs G, Gray P, Wright S, Mathison J, et al. Structure and function of lipopolysaccharide binding protein. Science. 1990 Sep 21;249(4975):1429-1431.

33. Beamer LJ, Carroll SF, Eisenberg D. The three-dimensional structure of human bactericidal/permeability-increasing protein Implications for understanding protein–lipopolysaccharide interactions. Biochemical Pharmacology. 1999;57(3):225-229.

34. Theofan G, Horwitz A, Williams R, Liu P, Chan I, Birr C, et al. An amino-terminal fragment of human lipopolysaccharide-binding protein retains lipid A binding but not CD14-stimulatory activity. The Journal of Immunology. 1994 Apr 1;152(7):3623 -3629.

35. Han J, Mathison JC, Ulevitch RJ, Tobias PS. Lipopolysaccharide (LPS) binding protein, truncated at Ile-197, binds LPS but does not transfer LPS to CD14. J. Biol. Chem. 1994 Mar 18;269(11):8172-8175.

36. Mathison J, Tobias P, Wolfson E, Ulevitch R. Plasma lipopolysaccharide (LPS)-binding protein. A key component in macrophage recognition of gram-negative LPS. The Journal of Immunology. 1992 Jul 1;149(1):200 -206.

37. Van Amersfoort ES, Van Berkel TJC, Kuiper J. Receptors, Mediators, and Mechanisms Involved in Bacterial Sepsis and Septic Shock. Clinical Microbiology Reviews. 2003;16(3):379-414.

38. Tobias PS, Soldau K, Iovine NM, Elsbach P, Weiss J. Lipopolysaccharide (LPS)-binding Proteins BPI and LBP Form Different Types of Complexes with LPS. Journal of Biological Chemistry. 1997 Jul 25;272(30):18682 -18685.

39. Elsbach P, Weiss J. Role of the bactericidal/permeability-increasing protein in host defence. Current Opinion in Immunology. 1998 Feb;10(1):45-49.

40. Playfair JHL, Chain BM. Immunology at a glance. Wiley-Blackwell; 2001.

41. Opal SM, Palardy JE, Marra MN, McKelligon BM, Scott RW, Fisher CJ. Relative concentrations of endotoxin-binding proteins in body fluids during infection. The Lancet. 1994 Aug;344(8920):429-431.

42. Beamer LJ, Carroll SF, Eisenberg D. Crystal Structure of Human BPI and Two Bound Phospholipids at 2.4 Angstrom Resolution. Science. 1997 Jun 20;276(5320):1861 -1864.

43. Gazzano-Santoro H, Parent JB, Grinna L, Horwitz A, Parsons T, Theofan G, et al. High-affinity binding of the bactericidal/permeability-increasing protein and a recombinant amino-terminal fragment to the lipid A region of lipopolysaccharide. Infect. Immun. 1992 Nov 1;60(11):4754-4761.

44. Wilde CG, Seilhamer JJ, McGrogan M, Ashton N, Snable JL, Lane JC, et al. Bactericidal/permeability-increasing protein and lipopolysaccharide (LPS)-binding protein. LPS binding properties and effects on LPS-mediated cell activation. J. Biol. Chem. 1994 Jul 1;269(26):17411-17416.

45. Beamer LJ, Carroll SF, Eisenberg D. The BPI/LBP family of proteins: a structural analysis of conserved regions. Protein Sci. 1998 Apr;7(4):906-914.

46. Elsbach P. The bactericidal/permeability-increasing protein (BPI) in antibacterial host defense. J. Leukoc. Biol. 1998 Jul;64(1):14-18.

47. Ooi CE, Weiss J, Doerfler ME, Elsbach P. Endotoxin-neutralizing properties of the 25 kD N-terminal fragment and a newly isolated 30 kD C-terminal fragment of the 55-60 kD bactericidal/permeability-increasing protein of human neutrophils. J. Exp. Med. 1991 Sep 1;174(3):649-655.

48. Bülow E, Gullberg U, Olsson I. Structural requirements for intracellular processing and sorting of bactericidal/permeability-

increasing protein (BPI): comparison with lipopolysaccharide-binding protein. J. Leukoc. Biol. 2000 Nov;68(5):669-678.

49. Iovine NM, Elsbach P, Weiss J. An opsonic function of the neutrophil bactericidal/permeability-increasing protein depends on both its N- and C-terminal domains. Proc Natl Acad Sci U S A. 1997 Sep 30;94(20):10973-10978.

50. Grunwald U, Krüger C, Westermann J, Lukowsky A, Ehlers M, Schütt C. An enzyme-linked immunosorbent assay for the quantification of solubilized CD14 in biological fluids. Journal of Immunological Methods. 1992 Nov 5;155(2):225-232.

51. Stelter F. Structure/function relationships of CD14. Chem. Immunol. 2000;74:25-41.

52. Kitchens RL. Role of CD14 in cellular recognition of bacterial lipopolysaccharides. Chem. Immunol. 2000;74:61-82.

53. Haziot A, Rong GW, Bazil V, Silver J, Goyert SM. Recombinant soluble CD14 inhibits LPS-induced tumor necrosis factor-alpha production by cells in whole blood. J. Immunol. 1994 Jun 15;152(12):5868-5876.

54. Haziot A, Rong G, Lin X, Silver J, Goyert S. Recombinant soluble CD14 prevents mortality in mice treated with endotoxin (lipopolysaccharide). The Journal of Immunology. 1995 Jun 15;154(12):6529 -6532.

55. Wurfel MM, Hailman E, Wright SD. Soluble CD14 acts as a shuttle in the neutralization of lipopolysaccharide (LPS) by LPS-binding protein and reconstituted high density lipoprotein. J. Exp. Med. 1995 May 1;181(5):1743-1754.

56. Kitchens RL, Thompson PA, Viriyakosol S, O'Keefe GE, Munford RS. Plasma CD14 decreases monocyte responses to LPS by transferring cell-bound LPS to plasma lipoproteins. J. Clin. Invest. 2001 Aug;108(3):485-493.

57. Pugin J, Schürer-Maly CC, Leturcq D, Moriarty A, Ulevitch RJ, Tobias PS. Lipopolysaccharide activation of human endothelial and epithelial cells is mediated by lipopolysaccharide-binding protein and soluble CD14. Proc Natl Acad Sci U S A. 1993 Apr 1;90(7):2744-2748.

58. Frey EA, Miller DS, Jahr TG, Sundan A, Bazil V, Espevik T, et al. Soluble CD14 participates in the response of cells to lipopolysaccharide. The Journal of Experimental Medicine. 1992 Dec 1;176(6):1665 -1671.

59. Wright S, Ramos R, Tobias P, Ulevitch R, Mathison J. CD14, a receptor for complexes of lipopolysaccharide (LPS) and LPS binding protein. Science. 1990;249(4975):1431 -1433.

60. Kielian TL, Blecha F. CD14 and other recognition molecules for lipopolysaccharide: A review. Immunopharmacology. 1995 Apr;29(3):187-205.

61. Takeda K, Kaisho T, Akira S. Toll-like receptors. Annu. Rev. Immunol. 2003;21:335-376.

62. Poltorak A, He X, Smirnova I, Liu MY, Van Huffel C, Du X, et al. Defective LPS signaling in C3H/HeJ and C57BL/10ScCr mice: mutations in Tlr4 gene. Science. 1998 Dec 11;282(5396):2085-2088.

63. Poltorak A, Smirnova I, He X, Liu MY, Van Huffel C, McNally O, et al. Genetic and physical mapping of the Lps locus: identification of the toll-4 receptor as a candidate gene in the critical region. Blood Cells Mol. Dis. 1998 Sep;24(3):340-355.

64. Qureshi ST, Larivière L, Leveque G, Clermont S, Moore KJ, Gros P, et al. Endotoxin-tolerant mice have mutations in Toll-like receptor 4 (Tlr4). J. Exp. Med. 1999 Feb 15;189(4):615-625.

65. Medzhitov R. Toll-like receptors and innate immunity. Nat Rev Immunol. 2001 Nov;1(2):135-145.

66. Jiang Z, Hong Z, Guo W, Xiaoyun G, Gengfa L, Yongning L, et al. A synthetic peptide derived from bactericidal/permeability-increasing protein neutralizes endotoxin in vitro and in vivo. International immunopharmacology. 2004;4(4):527-537.

67. Schromm AB, Lien E, Henneke P, Chow JC, Yoshimura A, Heine H, et al. Molecular genetic analysis of an endotoxin nonresponder mutant cell line: a point mutation in a conserved region of MD-2 abolishes endotoxin-induced signaling. J. Exp. Med. 2001 Jul 2;194(1):79-88.

68. Miyake K. Innate recognition of lipopolysaccharide by Toll-like receptor 4-MD-2. Trends in Microbiology. 2004 Apr;12(4):186-192.

69. Nagai Y, Akashi S, Nagafuku M, Ogata M, Iwakura Y, Akira S, et al. Essential role of MD-2 in LPS responsiveness and TLR4 distribution. Nat Immunol. 2002 Jul;3(7):667-672.

70. Akira S, Takeda K. Toll-like receptor signalling. Nat Rev Immunol. 2004 Jul;4(7):499-511.

71. Liew FY, Xu D, Brint EK, O'Neill LAJ. Negative regulation of Toll-like receptor-mediated immune responses. Nat Rev Immunol. 2005 Jun;5(6):446-458.

72. Chen G, Shaw MH, Kim Y-G, Nuñez G. NOD-Like Receptors: Role in Innate Immunity and Inflammatory Disease. Annu. Rev. Pathol. Mech. Dis. 2009 Feb;4(1):365-398.

73. Kanneganti T-D, Lamkanfi M, Núñez G. Intracellular NOD-like Receptors in Host Defense and Disease. Immunity. 2007 Oct;27(4):549-559.

74. Franchi L, Park J-H, Shaw MH, Marina-Garcia N, Chen G, Kim Y-G, et al. Intracellular NOD-like receptors in innate immunity, infection and disease. Cell. Microbiol. 2008 Jan;10(1):1-8.

75. Kumar A. Early Antimicrobial Therapy in Severe Sepsis and Septic Shock. Curr Infect Dis Rep. 2010 Jul;12(5):336-344.

76. Sjolin J, Goscinski G, Lundholm M, Bring J, Odenholt I. Endotoxin release from Escherichia coli after exposure to tobramycin: dose-dependency and reduction in cefuroxime-induced endotoxin release. Clinical Microbiology & Infection. 2000;6(2):74-81.

77. Simpson AJ, Opal SM, Angus BJ, Prins JM, Palardy JE, Parejo NA, et al. Differential antibiotic-induced endotoxin release in severe melioidosis. J. Infect. Dis. 2000 Mar;181(3):1014-1019.

78. Lolis E, Bucala R. Therapeutic approaches to innate immunity: severe sepsis and septic shock. Nat Rev Drug Discov. 2003;2(8):635-645.

79. Bernard GR, Vincent JL, Laterre PF, LaRosa SP, Dhainaut JF, Lopez-Rodriguez A, et al. Efficacy and safety of recombinant human activated protein C for severe sepsis. N. Engl. J. Med. 2001 Mar 8;344(10):699-709.

80. Martí-Carvajal AJ, Solà I, Lathyris D, Cardona AF. Human recombinant activated protein C for severe sepsis [Internet]. In: The Cochrane Collaboration, Martí-Carvajal AJ, editors. Cochrane Database of Systematic Reviews. Chichester, UK: John Wiley & Sons, Ltd; 2011 [cited 2011 Jun 21]. Available from: http://www2.cochrane.org/reviews/en/ab004388.html

81. Puttaswamy S, Lee BD, Sengupta S. Novel Electrical Method for Early Detection of Viable Bacteria in Blood Cultures. J. Clin. Microbiol. 2011 Apr 6;:JCM.00369-11.

82. Welch H, Calvery HO, McClosky WT, Price CW. Method of preparation and test for bacterial pyrogen. Journal of the American Pharmaceutical Association. 1943 Mar 1;32(3):65-69.

83. McClosky WT, Price CW, Van Winkle Jr. W, Welch H, Calvery HO. Results of first U. S. P. Collaborative study of pyrogens. Journal of the American Pharmaceutical Association. 1943 Mar 1;32(3):69-73.

84. Charles River Laboratories. EndosafeTimes: In vitro products and services newsletter. 2007;13(1):1-8.

85. Levin J, Bang FB. Clottable protein in Limulus; its localization and kinetics of its coagulation by endotoxin. Thromb Diath Haemorrh. 1968 Mar 31;19(1):186-197.

86. Levin J, Bang FB. The Role of Endotoxin in the Extracellular Coagulation of Limulus Blood. Bull Johns Hopkins Hosp. 1964 Sep;115:265-274.

87. Iwanaga S, Miyata T, Tokunaga F, Muta T. Molecular mechanism of hemolymph clotting system in Limulus. Thrombosis Research. 1992 Oct 1;68(1):1-32.

88. Brandenburg K, Howe J, Gutsman T, Garidel P. The expression of endotoxic activity in the Limulus test as compared to cytokine production in immune cells. Curr. Med. Chem. 2009;16(21):2653-2660.

89. Nachum R, Shanbrom E. Rapid detection of Gram-negative bacteriuria by Limulus amoebocyte lysate assay. Journal of Clinical Microbiology. 1981;13(1):158-162.

90. Hausmann MJ, Yulzari R, Lewis E, Saisky Y, Douvdevani A. Gel clot LAL assay in the initial management of peritoneal dialysis patients with peritonitis: a retrospective study. Nephrol. Dial. Transplant. 2000 May;15(5):680-683.

91. Cooper JF, Weary ME, Jordan FT. The impact of non-endotoxin LAL-reactive materials on Limulus amebocyte lysate analyses. PDA J Pharm Sci Technol. 1997 Feb;51(1):2-6.

92. Novitsky TJ. Limitations of the Limulus Amebocyte Lysate Test in Demonstrating Circulating Lipopolysaccharides. Annals of the New York Academy of Sciences. 1998 Jun 1;851(1):416-421.

93. Spectral's EAA Endotoxin Activity Assay [Internet]. [cited 2011 Jun 3];Available from: http://www.spectraldx.com/eaa.html

94. Romaschin AD, Harris DM, Ribeiro MB, Paice J, Foster DM, Walker PM, et al. A rapid assay of endotoxin in whole blood using autologous neutrophil dependent chemiluminescence. J. Immunol. Methods. 1998 Mar 15;212(2):169-185.

95. SC I C. Bacterial Endotoxin Testing in British Pharmacopoeia 2011. The Stationary Office;

96. Hirayama C, Sakata M. Chromatographic removal of endotoxin from protein solutions by polymer particles. Journal of Chromatography B. 2002 Dec 5;781(1-2):419-432.

97. Gorbet MB, Sefton MV. Endotoxin: The uninvited guest. Biomaterials. 2005 Dec;26(34):6811-6817.

98. Magalhães PO, Lopes AM, Mazzola PG, Rangel-Yagui C, Penna TCV, Pessoa A Jr. Methods of endotoxin removal from biological preparations: a review. J Pharm Pharm Sci. 2007;10(3):388-404.

99. Issekutz AC. Removal of gram-negative endotoxin from solutions by affinity chromatography. Journal of Immunological Methods. 1983 Jul 29;61(3):275-281.

100. Anspach FB. Endotoxin removal by affinity sorbents. J. Biochem. Biophys. Methods. 2001 Oct 30;49(1-3):665-681.

101. Aida Y, Pabst MJ. Removal of endotoxin from protein solutions by phase separation using triton X-114. Journal of Immunological Methods. 1990 Sep 14;132(2):191-195.

102. Petsch D, Anspach FB. Endotoxin removal from protein solutions. Journal of Biotechnology. 2000 Jan 21;76(2-3):97-119.

103. Li L, Luo RG. Use of Ca+2 to re-aggregate lipopolysaccharide (LPS) in hemoglobin solutions and the subsequent removal of endotoxin by ultrafiltration. Biotechnology Techniques. 1998 Feb;12(2):119-122.

104. Pauling L. A Theory of the Structure and Process of Formation of Antibodies*. Journal of the American Chemical Society. 1940 Oct 1;62(10):2643-2657.

105. Dickey FH. The Preparation of Specific Adsorbents. Proceedings of the National Academy of Sciences of the United States of America. 1949 May 15;35(5):227-229.

106. Wulff G, Sarhan A, Zabrocki K. Enzyme-analogue built polymers and their use for the resolution of racemates. Tetrahedron Letters. 1973;14(44):4329-4332.

107. Vlatakis G, Andersson LI, Muller R, Mosbach K. Drug assay using antibody mimics made by molecular imprinting. Nature. 1993 Feb 18;361(6413):645-647.

108. Alexander C, Andersson HS, Andersson LI, Ansell RJ, Kirsch N, Nicholls IA, et al. Molecular imprinting science and technology: a survey of the literature for the years up to and including 2003. Journal of Molecular Recognition. 2006;19(2):106.

109. Cormack PAG, Mosbach K. Molecular imprinting: recent developments and the road ahead. Reactive and Functional Polymers. 1999 Jul 15;41(1-3):115-124.

110. Ye L, Mosbach K. The Technique of Molecular Imprinting - Principle, State of the Art and Future Prospects. J. Inclusion Phenom. Macrocyclic Chem. 2001;41:107-113.

111. Piletsky SA, Alcock S, Turner APF. Molecular imprinting: at the edge of the third millennium. Trends in Biotechnology. 2001 Jan 1;19(1):9-12.

112. Chen L, Xu S, Li J. Recent advances in molecular imprinting technology: current status, challenges and highlighted applications. Chem. Soc. Rev. 2011;40(5):2922.

113. Komiyama M, Takeuchi T, Mukawa T, Asanuma H. Molecular Imprinting: From Fundamentals to Applications. Wiley VCH; 2003.

114. Yan M, Ramström O. Molecularly imprinted materials: science and technology. Marcel Dekker; 2005.

115. Sellergren B. Molecularly imprinted polymers: man-made mimics of antibodies and their applications in analytical chemistry. Elsevier; 2001.

116. Bartsch RA, Maeda M. Molecular and ionic recognition with imprinted polymers. American Chemical Society; 1998.

117. Sellergren B, Allender CJ. Molecularly imprinted polymers: A bridge to advanced drug delivery. Advanced Drug Delivery Reviews. 2005 Dec 6;57(12):1733-1741.

118. Sellergren B. Noncovalent molecular imprinting: antibody-like molecular recognition in polymeric network materials. TrAC Trends in Analytical Chemistry. June;16(6):310-320.

119. Turner NW, Jeans CW, Brain KR, Allender CJ, Hlady V, Britt DW. From 3D to 2D: A Review of the Molecular Imprinting of Proteins. Biotechnology Progress. 2006;22(6):1474-1489.

120. Janiak DS, Kofinas P. Molecular imprinting of peptides and proteins in aqueous media. Analytical and Bioanalytical Chemistry. 2007;389(2):399-404.

121. Nicholls IA, Andersson HS. Chapter 3 Thermodynamic principles underlying molecularly imprinted polymer formulation and ligand recognition [Internet]. In: Molecularly Imprinted Polymers - Man-made Mimics of Antibodies and their Aplications in Analytical Chemistry. Elsevier; 2000 [cited 2011 Jun 23]. p. 59-70.Available from: http://www.sciencedirect.com/science/article/pii/S0167924401800068

122. Bossi A, Bonini F, Turner APF, Piletsky SA. Molecularly imprinted polymers for the recognition of proteins: The state of the art. Biosensors and Bioelectronics. 2007 Jan 15;22(6):1131-1137.

123. Mallik S, Plunkett SD, Dhal PK, Johnson RD, Pack D, Shnek D, et al. Towards Materials for the Specific Recognition and Separation of Proteins. New J Chem. 1994 Jul 26;25(30):209-304.

124. Kempe M, Glad M, Mosbach K. An approach towards surface imprinting using the enzyme ribonuclease A. J. Mol. Recognit. 1995 Apr;8(1-2):35-39.

125. Hart BR, Shea KJ. Synthetic peptide receptors: molecularly imprinted polymers for the recognition of peptides using peptide-metal interactions. J. Am. Chem. Soc. 2001 Mar 7;123(9):2072-2073.

126. Titirici MM, Hall AJ, Sellergren B. Hierarchical Imprinting Using Crude Solid Phase Peptide Synthesis Products as Templates. Chemistry of Materials. 2003 Feb 1;15(4):822-824.

127. Titirici MM, Sellergren B. Peptide recognition via hierarchical imprinting. Analytical and Bioanalytical Chemistry. 2004;378(8):1913-1921.

128. Rachkov A, Minoura N. Towards molecularly imprinted polymers selective to peptides and proteins. The epitope approach. Biochimica et Biophysica Acta (BBA)/Protein Structure and Molecular Enzymology. 2001;1544(1-2):255-266.

129. Rachkov A, Minoura N. Recognition of oxytocin and oxytocin-related peptides in aqueous media using a molecularly imprinted polymer synthesized by the epitope approach. Journal of Chromatography A. 2000 Aug 11;889(1-2):111-118.

130. Nishino H, Huang C, Shea KJ. Selective Protein Capture by Epitope Imprinting. Angewandte Chemie International Edition. 2006 Apr 3;45(15):2392-2396.

131. Hoshino Y, Koide H, Urakami T, Kanazawa H, Kodama T, Oku N, et al. Recognition, Neutralization, and Clearance of Target Peptides in the Bloodstream of Living Mice by Molecularly Imprinted Polymer Nanoparticles: A Plastic Antibody. Journal of the American Chemical Society. 2010 May 19;132(19):6644-6645.

132. Hoshino Y, Urakami T, Kodama T, Koide H, Oku N, Okahata Y, et al. Design of synthetic polymer nanoparticles that capture and neutralize a toxic peptide. Small. 2009 Jul;5(13):1562-1568.

133. Hoshino Y, Kodama T, Okahata Y, Shea KJ. Peptide Imprinted Polymer Nanoparticles: A Plastic Antibody. Journal of the American Chemical Society. 2008 Nov 19;130(46):15242-15243.

134. Kastowsky M, Gutberlet T, Bradaczek H. Molecular modelling of the three-dimensional structure and conformational flexibility of bacterial lipopolysaccharide. Journal of Bacteriology. 1992;174(14):4798-4806.

Chapter Two : Merrifield Studies

2.1 Introduction

2.1.1 General Overview

Previous studies within our laboratory that attempted to develop the peptide-polymer hybrid recognition system described in Chapter One via conventional, bulk imprinting, techniques failed because the template became irreversibly trapped within the peptide-polymer system. It is imperative that access to the peptide is not unduly hindered by the polymer in order for the system to remain viable. We hypothesised that ligand access would be maintained if both peptide and polymerisation initiator were co-immobilised on a surface and polymer growth carefully controlled so as not to "overgrow" the peptide/target complex (shown schematically in Figure 1.7, Chapter One).

2.1.2 Merrifield Resin

Co-immobilisation of two different chemical species at a pre-defined molar ratio is extremely difficult to achieve using a homo-functional solid support. A sequential approach requires that the first attachment step is carried out with very precise control and that the chemistry involved does not affect the chemical tethers destined for immobilisation of the second moiety. Likewise, simultaneous strategies require extensive optimisation and are vulnerable to minor variations in reactant quality and reaction conditions.

Bifunctional resins have been prepared by co-polymerising monomers possessing more than one type of functional group but these require extensive optimisation of reaction conditions and careful consideration of monomer ratios and reactivities (1). Where multifunctional attachment or cleavage strategies are required, bifunctional non-

integral linkers or multiple non-integral linkers have more commonly been used to develop co-immobilisation strategies (2,3). However, it is not always desirable to significantly increase spacer length in order to bifunctionalise a resin and simultaneous or sequential modifications of a resin with multiple mono-functional linkers can again be vulnerable to minor variations in reactant quality and reaction conditions. Elegant enzymatic and optical approaches have led to spatially-resolved surface modifications giving rise to multifunctional resin surfaces, however these approaches involve serial protection/deprotection and rely on sophisticated microscopy for characterization (4,5).

Merrifield resin, a macroporous chloromethylated polystyrene, was developed by Robert Bruce Merrifield in 1969 as a platform for the solid-phase synthesis of peptides (6). As a support for the synthesis of small organic molecules, the resin (and the techniques developed from its use) has allowed a large number of reactions to move to solid-phase and has been critical in the development of powerful, modern, combinatorial chemistries (7). The usefulness of Merrifield resin is due in part, to the versatility of the chloromethyl functionality (Figure 2.1); a property that has been exploited in the current study. Furthermore, the resin has variable loading properties and is stable under a wide range of reaction conditions. One of the objectives of this study was to bifunctionalise Merrifield resin, in a controllable manner, in order to bring about the co-immobilisation of peptide and a surface bound initiator species at a pre-definable molar ratio.

The native chloromethyl group can be used to readily attach a polymerisation initiator species, however the immobilisation of a peptide requires an alternative functional group, for example a primary amine. It was hypothesised that controlled conversion of functional groups would allow a bifunctional support to be developed. Nucleophilic substitution of the chlorine group by an azide followed by

a Schmidt rearrangement using triflic (trifluromethanesulfonic) acid has been reported as an efficient method for the production of amino polystyrene resins from Merrifield resin (8). An alternative approach would be to use the Staudinger reaction; a mild technique that also reduces azide groups to amines in good yield with very few side products (9,10). Both mechanisms are outlined in Figure 2.1 and have been investigated in this study.

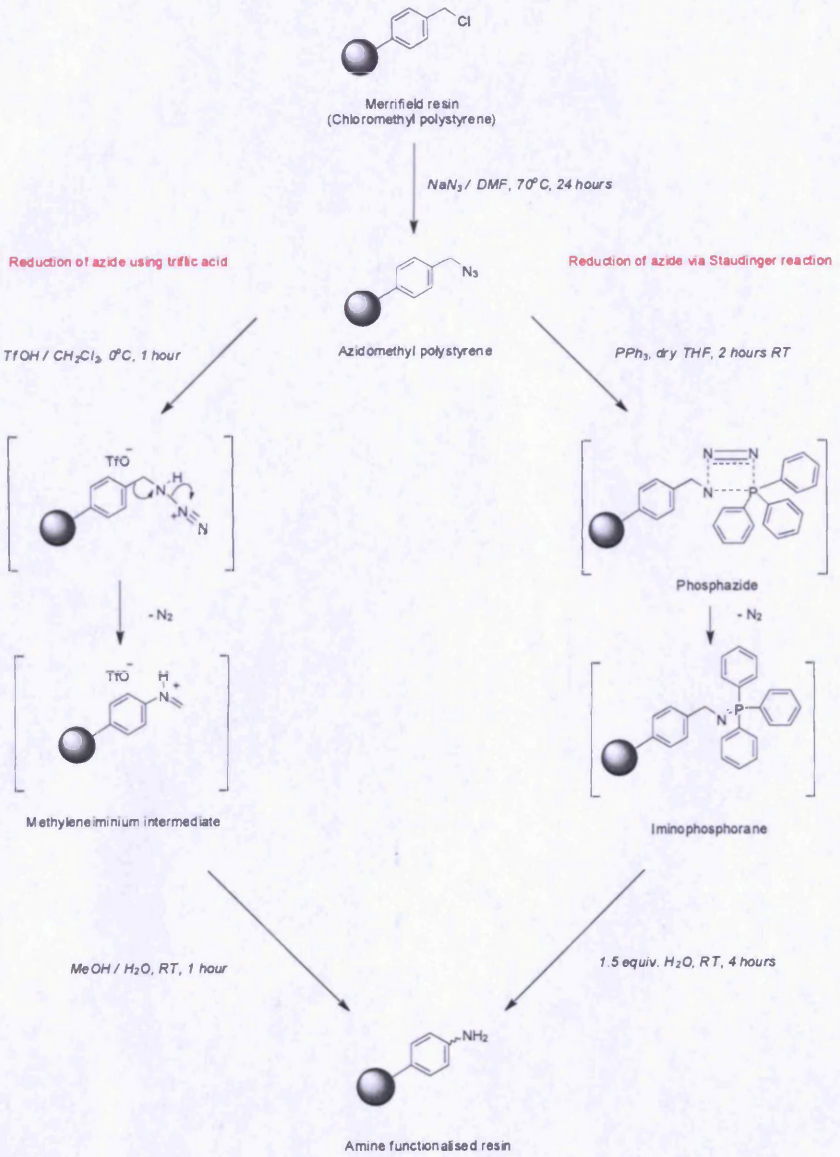

Figure 2.1: Mechanism of the formation of amine functionalised polystyrene resin via two different synthetic pathways. Greater experimental detail is provided in sections 2.2.2 to 2.2.4.

2.1.3 Living Radical Polymerisation

Conventional molecular imprinting methodologies typically rely on the use of an azo-type free radical initiator, commonly azobisisobutyronitrile (AIBN), to bring about and propagate polymerisation. These initiators are versatile, cost effective and efficient and, upon application of heat or UV radiation, undergo homolytic cleavage to generate two identical, short-lived, active cyanopropyl radicals and nitrogen gas (Figure 2.2). This type of polymerisation is a random process that generates the typical monolithic and bead polymer formats seen in bulk and precipitation polymerisation respectively.

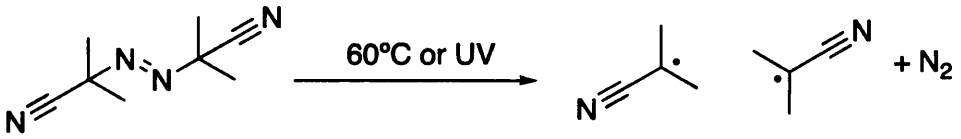

Figure 2.2: Homolytic cleavage of AIBN to generate two equally reactive cyanopropyl radicals and nitrogen gas.

In comparison, controlled/*living* radical polymerisation techniques can be used to control the polymerisation process to produce polymers with precise molecular weights and low poly-dispersity indices (11). By utilising such an approach in the current study, it was anticipated that polymer growth could be carefully controlled to allow for the formation of the peptide polymer receptor as described in section 1.2.2 of Chapter One.

Possible mechanisms to achieve such controlled polymer growth include atom-transfer radical polymerisation (ATRP) (12), nitroxide-mediated polymerisation (NMP) (13) and reversible addition-fragmentation transfer polymerisation (RAFT) (14). These techniques however typically require elevated temperatures, careful choice of monomers and the use of organic solvents (15); conditions not

conducive to the physicochemical properties of the target species and peptide moiety. Furthermore, RAFT agents generally require synthesis before polymerisation, as few are available commercially (16) and ATRP results in contamination of the polymer with the cuprous halide catalyst used in the reaction that often requires further clean-up procedures (15). An alternative method of achieving controlled polymer growth is through the use of an iniferter species (17,18). In 1982 Otsu and Yoshida coined the term *iniferter* (referring to the ability of their initiator species to function as an *ini*tiator, trans*fer* agent and *ter*minator) following studies investigating the polymerisation of styrene with tetraethylthiuram disulphide. They found that the polymers produced were end-capped with the radical group and were therefore capable of re-initiating polymerisation following the addition of another monomer (19). Further studies found that those molecules containing the *N,N*-diethyldithiocarbamyl group served as excellent iniferters (20). These dithiocarbamate-type species will readily react with the chloromethyl groups on the surface of Merrifield resin to produce the active initiator species. Following irradiation with UV light, the iniferter decomposes to form one surface-bound (active) and one solution-phase (inactive) radical species (Figure 2.3).

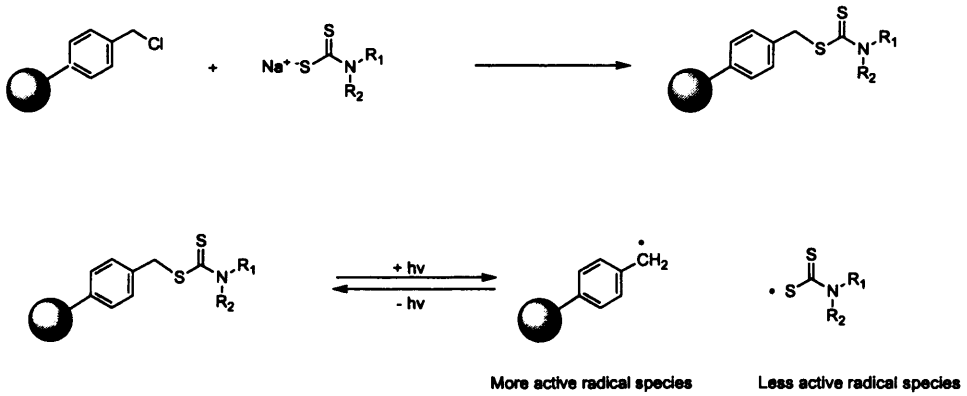

Figure 2.3: Synthesis of a surface immobilised iniferter and subsequent formation of the two radical species. Polymerisation proceeds from the surface bound, active radical species. R_1, R_2 : CH_2CH_3 (sodium diethyldithiocarbamate), R_1: CH_3 , R_2: CH_2COOH, (sodium dithiocarboxysarcosine)

The formation of two unequal radicals is important. The immobilised surface bound reactive radical initiates polymerisation, whilst the solution phase inactive radical provides a mechanism by which polymerisation can be controlled. During polymerisation, the dynamic recombination reaction of the two radicals means that polymer growth occurs in a stepwise, controlled manner. Additionally the less reactive radical species prevents solution phase polymerisation. The limited growth coupled with the absence of solution phase gelation, will ensure that the polymer will not occlude the peptide binding sites.

Iniferters have been successfully employed as radical sources in the polymerisation of a range of monomers, under a multitude of reaction conditions, to suit a variety of application needs (reviewed in (20,24)). Over the last decade iniferters (and the polymers derived from them) have been investigated as potential chemical sensors (22,23), used in the development of micropatterned surfaces for cell adhesion/encapsulation (24) and bioconjugation (25), as chromatographic stationary phases (26,27) and in the production of

telechelic polymers (28). More specifically, in the area of molecular imprinting, iniferters have found utilisation in the preparation of multi-functional nanoparticles (29-32) and in biomacromolecule recognition/separations (33,34). Studies investigating iniferter-derived polymers as imprinted chromatographic stationary phases have demonstrated several advantages over conventionally-prepared imprinted materials for this application (27,35,36).

2.1.4 Aims and objectives of Chapter Two

The overall aim of this section of work was to synthesise a bifunctional solid support to allow for the controlled immobilisation of iniferter and peptide species, from which the peptide-polymer hybrid system can be developed.*

The key objectives of this work were:

1. To investigate two synthetic pathways to generate a solid support capable of possessing two different chemical functionalities at a pre-defined molar ratio.
2. To immobilise an iniferter species on the surface of said support.
3. To demonstrate controlled growth of polymer from the surface of the support.

* The chemistries involved in the immobilisation of the peptide species will be discussed in Chapter Three.

2.2 Materials and Methods

2.2.1 Materials

All chemicals were purchased from Sigma-Aldrich, Poole, UK and were used as received unless otherwise stated. All organic solvents were of HPLC grade and were obtained from Fisher Scientific, Loughborough, UK unless otherwise stated.

2.2.2 Synthesis of azidomethyl polystyrene

The method outlined by Arseniyadis (8) was used, with some modifications, to generate the azidomethyl polystyrene intermediate. Merrifield resin (250 mg, ~2 mmol Cl g^{-1}, 1 % cross-linked with DVB, 200 - 400 mesh) was reacted with sodium azide in dry DMF (10 ml). The exact quantities of azide used depended on the degree of conversion required (0.1 molar equivalent to 4 fold excess). The resin was washed with DMF/water (50/50, 50 ml), DMF, water, ethanol, ether (50 ml volumes of each through two cycles) and dried under vacuum for 16 hours.

2.2.3 Azide reduction using triflic acid to produce amine functionalised resin

Azidomethyl polystyrene (250 mg, ~0.5 mmol azide) was dispersed in dichloromethane (2.5 ml) to which was added triflic acid (350 µl, 3.95 mmol). The reaction mixture was stirred at 0 °C for one hour. Methanol (2.5 ml) was added and the suspension stirred at room temperature for a further hour. The resin was washed with methanol/water (50/50, 100 ml), methanol/triethylamine (50/50, 100 ml) and dichloromethane (50 ml) and then dried under vacuum at 40 °C overnight (8).

2.2.4 Azide reduction via Staudinger reaction to produce amine functionalised resin

Azidomethyl polystyrene (250 mg, ~0.5 mmol azide) was dispersed in dry THF (4 ml) to which was added triphenylphosphine (131 mg, 0.5 mmol). The reaction mixture was stirred at room temperature for two hours. Approximately three equivalents of water (27 µl, 1.5 mmol) was added and the mixture left to stir for a further four hours before being filtered and washed with DMF, ethanol, ether, DMF, ether, ethanol and ether (10 ml of each). The resin was dried overnight at 40 °C under vacuum.

2.2.5 FTIR Analysis

All analysis was carried out on a Varian 3100 Excalibur FTIR (Agilent Technologies UK Limited, Cheshire, UK) using the Varian Resolutions Pro software. Samples were analysed as finely ground powders.

2.2.6 Elemental Analysis

Resin samples were sent for elemental analysis (Medac Ltd, Surrey) to determine carbon, hydrogen, nitrogen, sulphur and chlorine content.

2.2.7 Synthesis of benzyl diethyldithiocarbamate

The method outlined in Titirici (37) was used to produce the benzyl diethyldithiocarbamate iniferter species. Briefly, sodium diethyldithiocarbamate (4.1 g, 18 mmol) dissolved in ethanol (20 ml) was added to a two-neck round-bottomed flask under a nitrogen atmosphere at 0 °C. Benzyl chloride (2.55 g, 20 mmol) in 5 ml ethanol was added drop-wise over 30 minutes with stirring. The reaction mixture was allowed to gradually warm to room temperature and

stirred for a further 65 hours. Sodium chloride, formed as a precipitate during the reaction, was filtered off and the remaining solution was concentrated under vacuum. The final solution and all starting materials were confirmed using NMR before being used in subsequent polymerisation experiments.

2.2.8 Solution polymerisation studies

Solution polymerisation experiments were conducted to assess the efficacy of the iniferter species and to also provide further evidence of the successful formation of benzyl diethyldithiocarbamate. Studies were carried out using a 1 : 1 molar ratio of methacrylic acid to either benzyl diethyldithiocarbamate or benzyl chloride (Table 2.1). Methacrylic acid, benzyl chloride and benzyl diethyldithiocarbamate alone were also included as further controls. All reactions were carried out in HPLC autosampler vials, the mixtures purged with nitrogen for five minutes and then subjected to UV light (100 mw/cm^2, 325 nm at a distance of 8 inches) for ten minutes. The mixtures were observed at 0, 5 and 10 minutes and their physical characteristics recorded.

	MAA	*BDTC*	*BC*
1	84 µl (86 mg, 1 mmol)	240 µl (239 mg, 1 mmol)	-
2	84 µl	-	115 µl (126 mg, 1 mmol)
3	84 µl	-	-
4	-	-	115 µl
5	-	240 µl	-

Table 2.1: Compositions of the five different mixtures used in the solution polymerisation studies (MAA = methacrylic acid, BDTC = benzyl diethyldithiocarbamate and BC = benzyl chloride).

2.2.9 Attachment of sodium diethyl dithiocarbamate to Merrifield resin

A modified version of the method employed by Rückert *et al.* (38) was used in this study. Merrifield resin (1 g, ~2 mmol Cl) was dispersed in anhydrous ethanol (5 ml) in a 20 ml polymerisation vial. A solution of sodium diethyldithiocarbamate (1.8 g, 8 mmol) in dry ethanol (14 ml) was added and the reaction mixture stirred at 60 °C for 72 hours. Throughout the reaction, the polymerisation vial was covered in foil to protect the mixture from light. The resin was filtered and washed twice with water (100 ml), methanol (100 ml) and ethanol (100 ml), before being dried under vacuum at 40 °C overnight. The resins were analysed by FTIR.

2.2.10 Polymerisation studies with diethyl dithiocarbamate modified Merrifield

The method outlined in (34) was used in this study with minor modifications. Briefly, iniferter-modified Merrifield resin (200 mg), acrylamide (280 mg) and methylene bisacrylamide (30 mg) were dispersed in ethanol or deionised water (4 ml). All samples were stirred gently (~100 rpm) whilst irradiated with UV light (100 mw/cm^2, 325 nm at a distance of 8 inches) for various periods of time. The samples were then filtered and washed with ethanol (5 x 20 ml), before being re-incubated with ethanol (10 ml) and vortexed for 1 minute. The sample was then filtered again, washed with a further 20 ml ethanol and dried under vacuum at 40 °C overnight. The resins were analysed by FTIR.

2.2.11 Modification of Merrifield resin with the hydrophilic iniferter species, sodium N-(dithiocarboxy) sarcosine

A hydrophilic iniferter was synthesised (39) to allow for the polymerisation of the resin-polymer complex under aqueous

conditions. Sodium *N*-(dithiocarboxy)sarcosine was coupled to Merrifield resin by dispersing 836 mg (4 mmol) in 10 ml deionised water (or 10 ml methanol/10 ml DMF) and adding 500 mg resin (1 mmol Cl). The mixture was stirred at 40 °C for 72 hours, then filtered and washed with water and ethanol before being dried under vacuum at 40 °C overnight, protected from light. The resins were polymerised in the same manner as described in section 2.2.10 and subsequently analysed by FTIR and elemental analysis.

2.3 Results and Discussion.

2.3.1 Synthesis of azidomethyl polystyrene

FTIR analysis confirmed the successful synthesis of the azidomethyl intermediate (Figure 2.4b). Following incubation with a mole equivalent of sodium azide, an azidomethyl polystyrene intermediate was formed, indicated by the presence of a strong band at ~2100 cm^{-1} that was absent in the spectra of control Merrifield resin (Figure 2.4a).

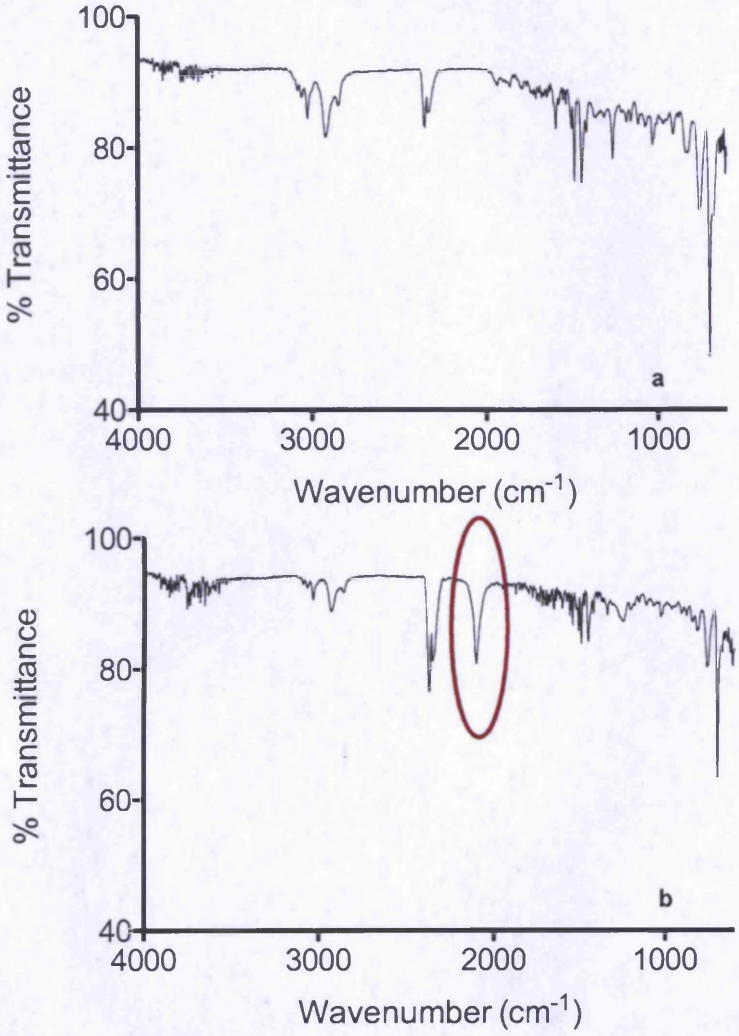

Figure 2.4: FTIR spectra for a) Merrifield resin and b) the azidomethyl polystyrene intermediate formed following reaction of Merrifield resin with 1 mole equivalent of sodium azide ($\upsilon_{N=N=N}$ ~2100cm^{-1}, circled in red in spectrum b)

Further investigation demonstrated that it was possible to control the conversion to azide groups by varying both concentration of sodium azide and reaction time. The results are shown in Figures 2.5 and 2.6 respectively. A total of thirteen different concentrations of sodium azide were reacted with the resin and the peak areas obtained from IR analysis recorded. The graph of azide concentration against peak area presented in Figure 2.5 suggest that a maximum conversion of chloromethyl groups to azide is achieved when Merrifield resin (500 mg, 2 mmol Cl g^{-1}) is reacted with > 2 mmol sodium azide, as demonstrated by attainment of a plateau in the plot. Increasing the molar ratio of Merrifield resin to sodium azide from 1 : 4 to 1 : 10 has no effect on azide peak area. Figure 2.6 demonstrates the effect of reaction time on the conversion to azidomethyl polystyrene. Two concentrations of sodium azide (4 mmol and 0.5 mmol) were taken forward into a time point study to assess the rate of conversion of chloro groups to azide. Both concentrations display the same time dependency, suggesting completion of the reaction within 6 hours regardless of concentration of sodium azide used. The plateau obtained for the reaction of 0.5 mmol sodium azide with Merrifield resin (1 mmol Cl) is obviously lower than that observed with 4 mmol azide (maximum conversion) as the reaction is also limited by the concentration of sodium azide available to react with.

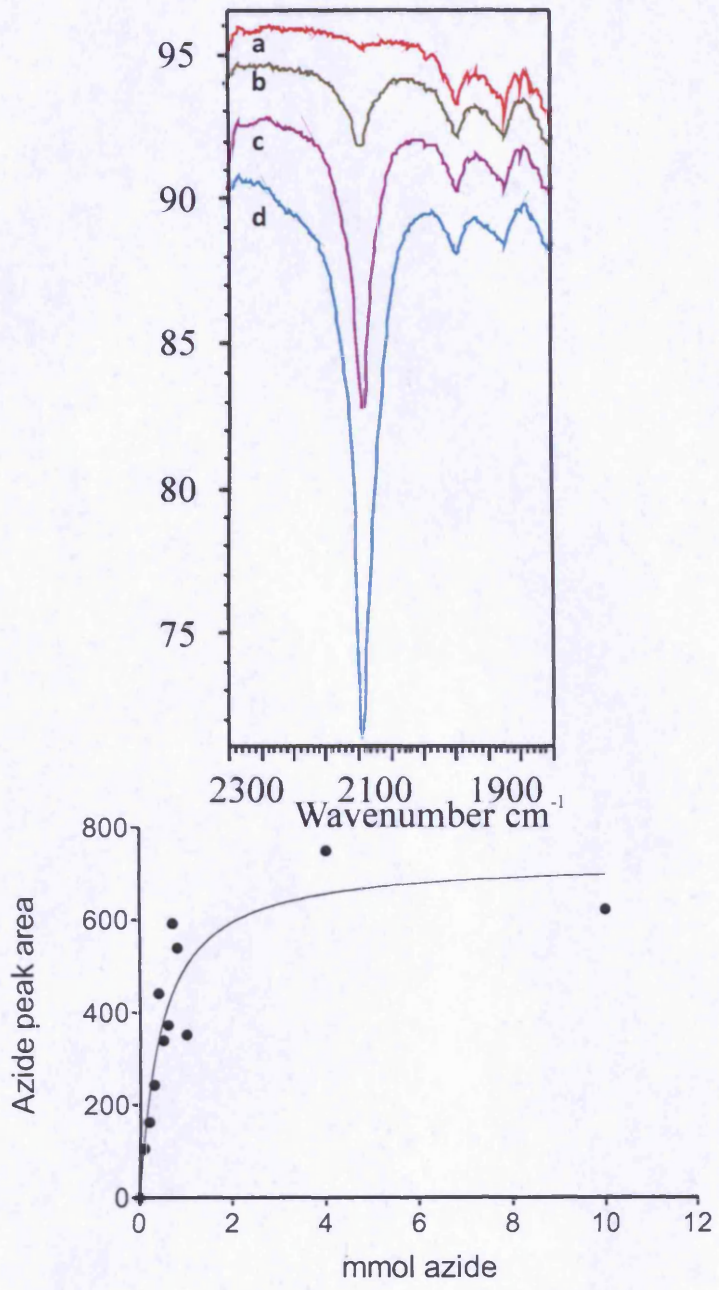

Figure 2.5: Azide peak area obtained from IR analysis of Merrifield resin following reaction with varying concentrations of sodium azide (NaN_3). In all cases concentration of resin was equivalent to 1 mmol chlorine while the concentration of azide ranged from 0.1 mmol to 10 mmol. Spectra (top) show the azide stretch at 2100 cm^{-1} for resin reacted with a) 0 mmol NaN_3, b) 0.1mmol NaN_3, c) 0.5 mmol NaN_3 and d) 1mmol NaN_3. Spectra are offset for clarity.

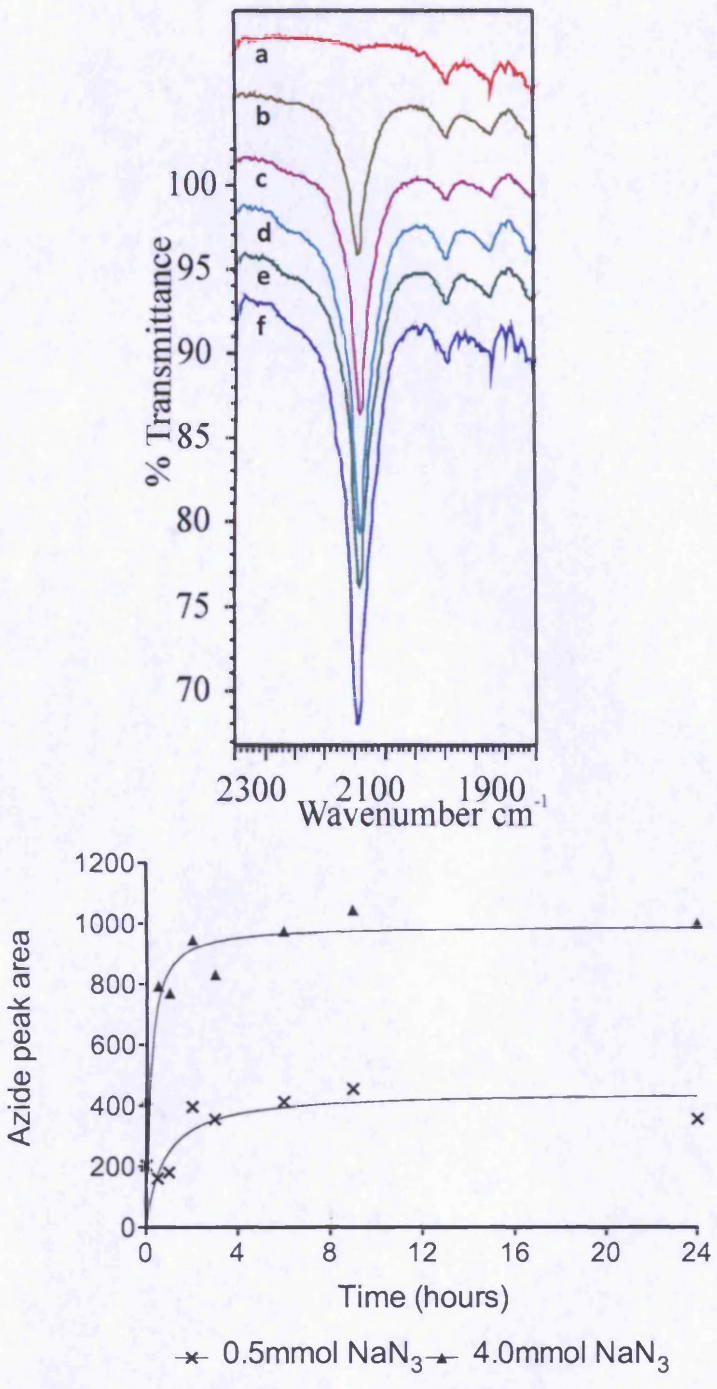

Figure 2.6: Conversion to azide as a function of both time and concentration. Two concentrations were investigated (1 mmol resin to 0.5 mmol and 4 mmol sodium azide) at eight time points over 24 hours. Spectra (top) show azide stretch for resin reacted with 4 mmol NaN_3 for a) 0 mins, b) 10 mins, c) 30 mins, d) 120 mins, e) 360 mins and f) 24 hours. Spectra are offset for clarity.

2.3.2 *Azide reduction using triflic acid to produce amine functionalised resin*

The addition of triflic acid to azidomethyl polystyrene successfully produced amine-modified resin as demonstrated by the spectra shown in Figure 2.7. Loss of the azide stretch was observed and new vibrational bands appeared in the region of 3300-3500 cm^{-1}, indicative of amine functionality (υ_{N-H} ~3400 cm^{-1}).

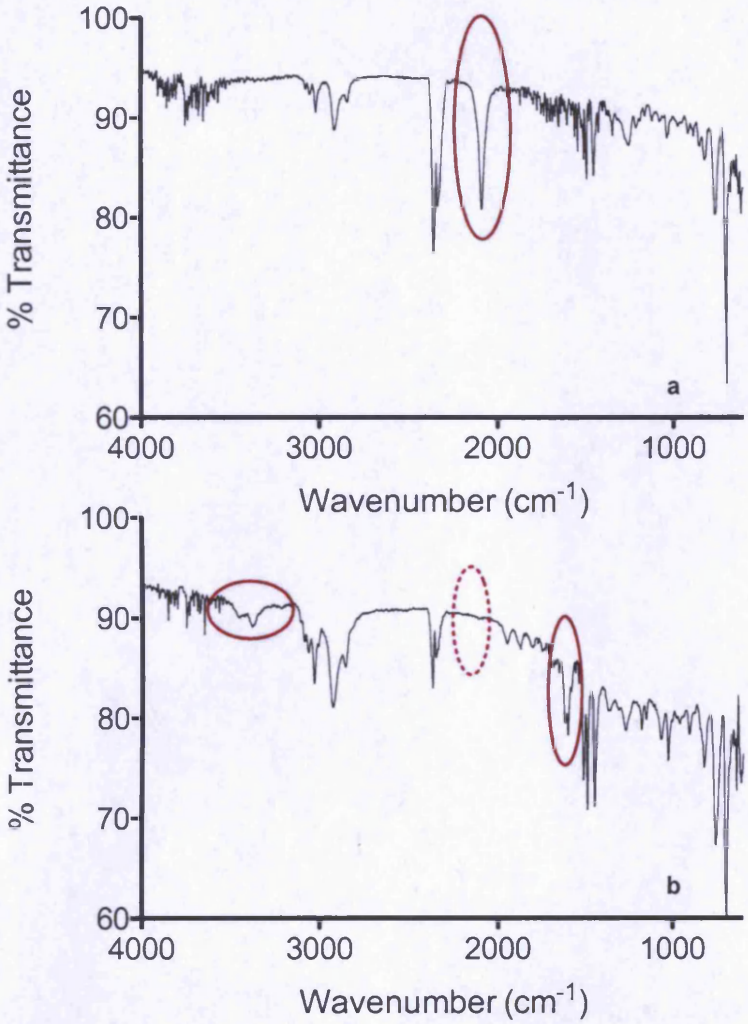

Figure 2.7: FTIR spectra demonstrating the reduction of azide to amine using triflic acid. The azide peak is clearly visible at ~ 2100 cm^{-1} in spectrum a (resin produced via the reaction with an excess of sodium azide). Following reaction with triflic acid, the azide is converted to an amine, demonstrated by the loss of the azide stretch (dashed circle in spectrum b) and the appearance of a vibrational nodes at ~3400 cm^{-1} (N-H stretch), ~1600 cm^{-1} (N-H bend) (circled in spectrum b).

A study was undertaken to assess the effect of triflic acid on the chlorine groups that had not been converted to azide. In order to successfully produce bifunctionalised resin it was imperative that the reaction conditions involved in creating the amine groups did not effect the remaining chloro functionality. These groups must be unmodified to allow for the attachment of the iniferter group. To investigate this, untreated Merrifield resin was subjected to the triflic acid reduction step and then subsequently treated with an excess of sodium azide. If the chlorine groups were unaffected by the triflic acid reaction, then the addition of azide would lead to the formation of azidomethyl polystyrene. The IR spectrum given in Figure 2.8 clearly demonstrates that following treatment with triflic acid, reaction of Merrifield resin with sodium azide does not give rise to the characteristic azide signal at 2100 cm^{-1} thus suggesting loss of chloro functionality.

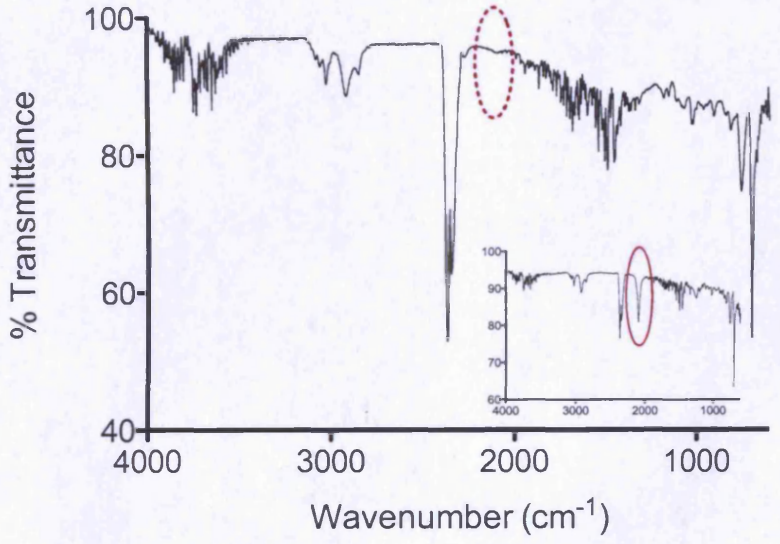

Figure 2.8: FTIR analysis of the resin clearly demonstrates the detrimental effect that triflic acid has on the unmodified chlorine groups. The main spectrum shows that following treatment with triflic acid and subsequent incubation with a ten-fold excess of sodium azide, no azide peak is visible (dashed circle, main spectrum). The inset spectra is Merrifield resin that has been reacted with an excess of sodium azide, the azide stretch is visible at ~2100cm $^{-1}$, circled.

Elemental analysis further confirmed the loss of chlorine functionality following reaction with triflic acid; resin treated with triflic acid showed a significant decrease in chlorine content (from 7.6 % in the Merrifield resin control to 0.21 %) while the carbon content of the resin increased from ~84.0 % to ~91 % (Table 2.2).

	MR	*TfOH MR*
	% (mmol/g)	*% (mmol/g)*
C	84.09 (70.08)	91.03 (75.86)
H	7.26 (72.60)	7.50 (75.00)
N	<0.10 (<0.07)	0.30 (0.21)
Cl	7.68 (2.19)	0.21 (0.06)

Table 2.2: Elemental analysis of untreated Merrifield resin (MR) and triflic acid treated resin (TfOH MR). Values are expressed as both percentage composition and as mmol/g of resin

A possible explanation for the loss of chlorine functionality following incubation of the resin with triflic acid is the formation of a benzyl methyl ether species via a benzyl triflate intermediate (Figure 2.9). The resin, when suspended in dichloromethane, is a creamy yellow colour that turns dark red on the addition of triflic acid. This colour is reversed when methanol is added suggesting the formation of two species.

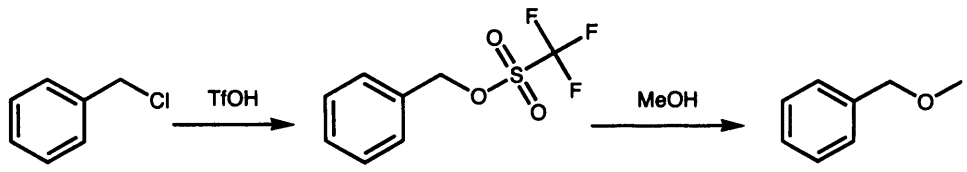

Figure 2.9: The proposed formation of a benzyl methyl ether species, via a triflate intermediate, that is hypothesised to form when Merrifield resin is exposed to triflic acid.

2.3.3 Azide reduction via Staudinger reaction to produce amine functionalised resin

As a consequence of the results obtained from the triflic acid studies i.e. the loss of viable chlorine groups following triflic acid treatment, an alternative method for the conversion of azide to amine was needed. The Staudinger reaction is reported to be the mildest method for the production of amines from azide groups (9) involving only reaction with triphenylphosphine using tetrahydrofuran and water. Experiments were undertaken to assess the efficiency of this reaction to convert azidomethyl polystyrene to amine functionalised resin and to determine its effect on any remaining, unmodified chlorine groups. Figure 2.10 shows that the Staudinger reaction was able to successfully reduce the azide groups to amines; the azide stretch at ~2100 cm^{-1} present in spectrum (a) is absent following reduction with triphenylphosphine and vibrational nodes indicative of amine functionality are apparent at ~ 3400 cm^{-1} and 1600 cm^{-1}.

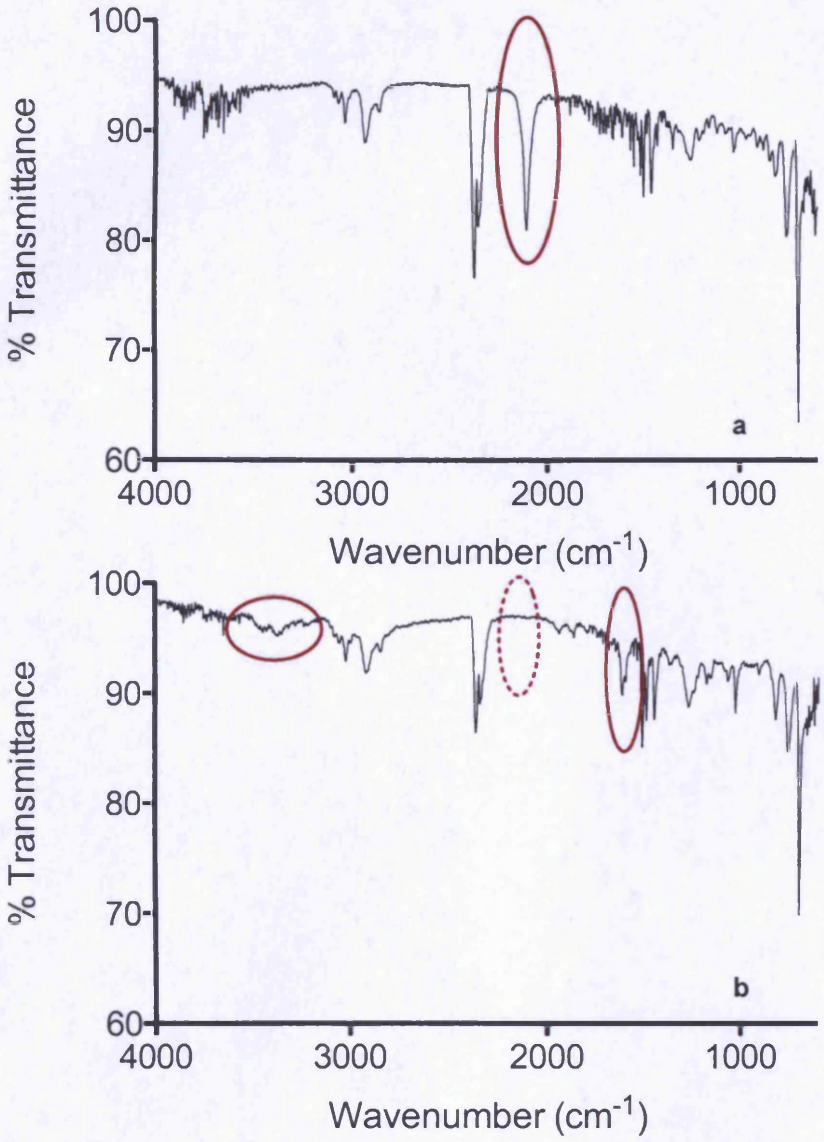

Figure 2.10: Conversion of azide groups to amines via the Staudinger reaction. The azide peak is clearly visible in the resin prior to Staudinger treatment at ~2100 cm^{-1} (circled in spectra (a)). Following reaction with triphenylphosphine the azide is converted to an amine, demonstrated by the loss of the azide stretch (dashed circle spectrum b) and the appearance of a vibrational nodes at ~3400 cm^{-1} (N-H stretch), ~1600 cm^{-1} (N-H bend) (circled in spectra b) (b).

Studies were undertaken to determine the effect of the Staudinger reaction on unmodified chloro groups. Unmodified resin was subjected to the Staudinger reaction conditions and then incubated with sodium azide. Not only did the Staudinger reaction not have an effect on the chloro functionality of the resin, concentration studies show that the conversion to azide was still concentration dependent. FTIR spectra of resin reacted with 0.2 mmol and 0.6 mmol sodium azide are given in Figure 2.11 as examples. The area of the peak between the spectra increases approximately three-fold. These peak areas are in line with those obtained for similar concentrations of sodium azide reacted with Merrifield resin unexposed to the Staudinger conditions.

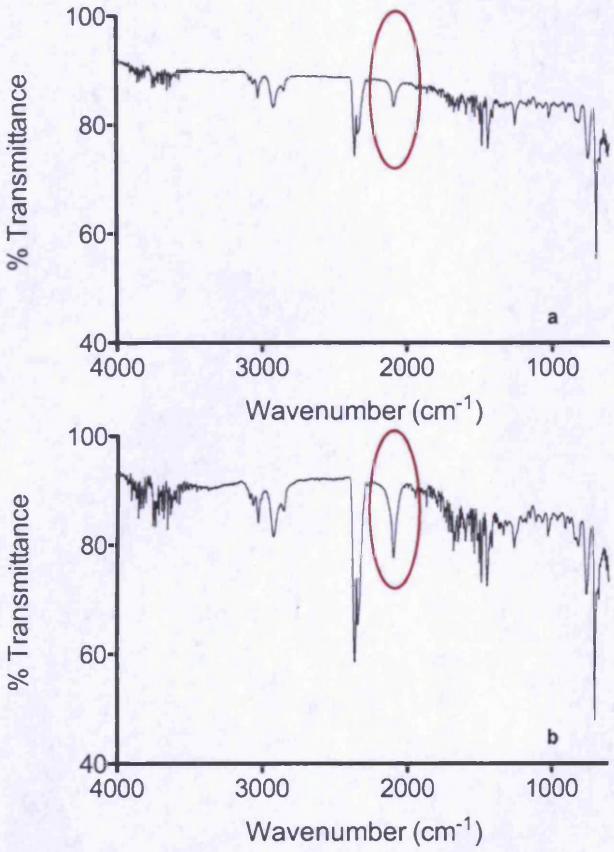

Figure 2.11: FTIR spectra of Merrifield resin which has undergone the Staudinger reaction and then subsequently been reacted with 0.2 mmol (a) and 0.6 mmol (b) sodium azide. The azide peak area (circled in spectra) is seen to be concentration dependent, suggesting no detrimental effect on chloro functionality by the reaction conditions.

Again elemental analysis was used to confirm these observations (Table 2.3). No significant change in chlorine content was observed following incubation of the resin under the conditions used in the Staudinger reaction. Additionally, elemental analysis was used to provide further evidence for the synthesis of a bifunctionalised resin and amino-polystyrene (Bifunc'MR and MR-NH_2 in Table 2.3 respectively). Nitrogen content in MR-NH_2 was attributed to the amine functionality since the presence of residual azide functionality was ruled out by the absence of the characteristic vibrational band at 2100 cm^{-1}.

	MR	*PPh_3 MR*	*Bifunc' MR*	*MR-NH_2*
	% (mmol/g)	*% (mmol/g)*	*% (mmol/g)*	*% (mmol/g)*
C	84.09 (70.08)	84.36 (70.30)	83.39 (69.49)	85.52 (71.27)
H	7.26 (72.60)	7.16 (71.6)	7.73 (77.30)	7.37 (73.70)
N	<0.10 (<0.07)	0.24 (0.17)	2.09 (1.49)	3.03 (2.16)
Cl	7.68 (2.19)	7.08 (2.02)	3.00 (0.86)	0.09 (0.03)

Table 2.3: Elemental analysis of untreated Merrifield resin (MR), resin that has been subjected to the conditions used in the Staudinger reaction (PPh_3 MR), resin displaying both chloro and amine functionality (Bifunc' MR) and amino-modified Merrifield (MR-NH_2). Values are expressed as both percentage composition and as mmol/g of resin.

2.3.4 Synthesis of benzyl diethyldithiocarbamate

The reaction between benzyl chloride and sodium diethyldithiocarbamate, outlined in Figure 2.3 and in section 2.2.7, succesfully produced the benzyl diethyldithiocarbamate iniferter species and was confirmed by NMR. [^{1}H NMR (500MHz, Toluene-d8) δ 7.10-7.00 (5H, m), 4.6 (2H, s), 3.5 (4H, m), 1.10 (6H, t)].

2.3.5 Solution polymerisation studies

Solution polymerisation studies were carried out as described in section 2.2.8. Figures 2.12 - 2.14 show the polymerisation process at three time points; 0, 5 and 10 minutes. Prior to polymerisation all samples were liquid. The methacrylic acid/benzyl dithiocarbmate (MAA/BDTC) solution had polymerised by 5 minutes, the methacrylic acid/benzyl chloride (MAA/BC) mixture had thickened while all controls remained liquid. At 10 minutes, the MAA/BC mix had completely polymerised whilst the other controls remained liquid.

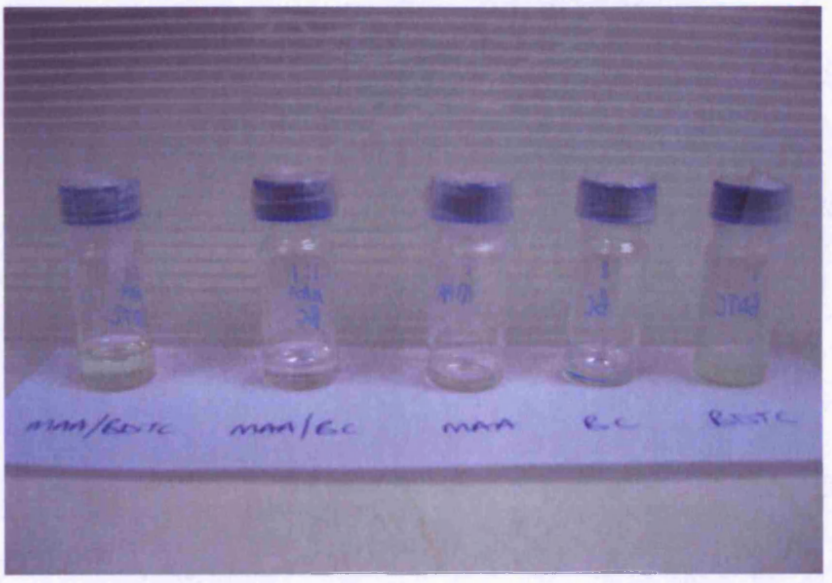

Figure 2.12: All samples are liquid prior to irradiation with UV light. (MAA/BDTC : methacrylic acid/benzyl diethyldithiocarbamate mixture, MAA/BC : methacrylic acid/benzyl chloride mixture, MAA : methacrylic acid, BC : benzyl chloride and BDTC : benzyl diethyldithiocarbamate).

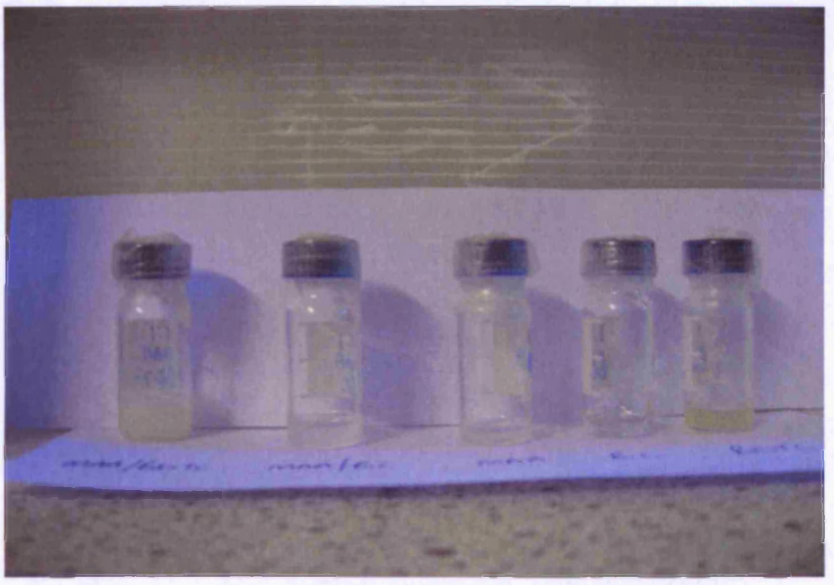

Figure 2.13: Following 5 minutes UV irradiation the MAA/BDTC mixture had polymerised (solid), the MAA/BC mixture had thickened, whilst the MAA, BC and BDTC controls remained liquid.

Figure 2.14: Following 10 minutes UV irradiation the MAA/BC mixture had polymerised (solid) whilst the MAA, BC and BDTC controls remained liquid.

It was probable that the polymerisation observed with the MAA/BC mixture was due to the formation of a benzyl radical upon irradiation with UV light and is discussed in more depth later (section 2.3.7) The process was however slower than when the iniferter species, BDTC, was used.

2.3.6 Coupling of the iniferter to Merrifield

Rückert *et al.* (38) used approximately 6 mmol iniferter to 10 mmol resin (expressed as chlorine concentration) and heated the reaction mixture at 60 °C for 50 hours. Elemental analysis of the product suggested that this resulted in only 0.1 mmol dithiocarbamate groups per gram of resin., however a time study included in the same work suggested that much higher conversions were possible. For the purposes of this study, a four-fold excess of iniferter was used and the reaction mixture was stirred at 60 °C for 72 hours to encourage maximal coupling of iniferter to resin. Figure 2.15 shows the IR spectra for untreated Merrifield resin and Merrifield resin to which the iniferter species has been coupled. Stretches in the region of 1275 - 1030cm^{-1} are indicative of the thiocarbonyl group, C=S of the iniferter species.

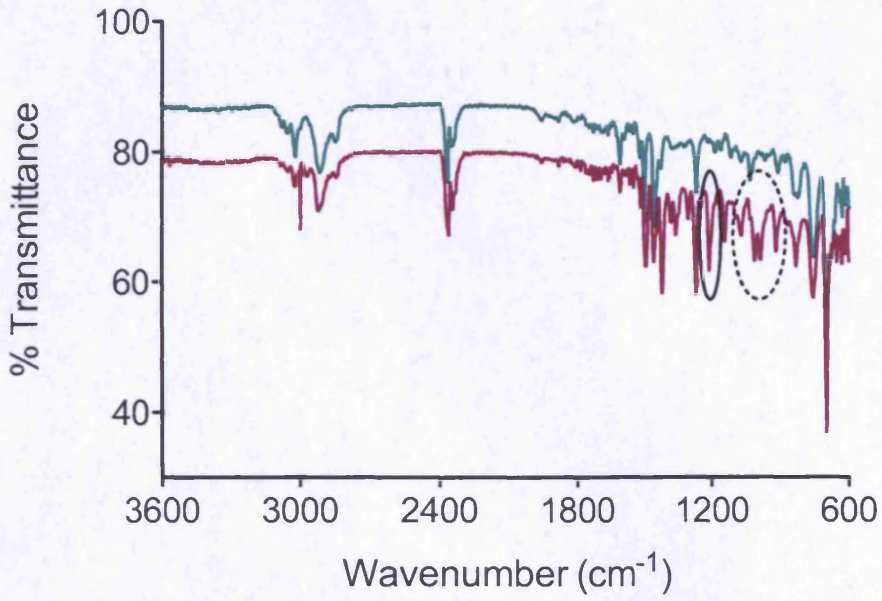

Figure 2.15: FTIR spectra of untreated Merrifield resin (green) and iniferter coupled resin (red). Stretches in the region of 1275-1030 cm-1 (dashed circle) are indicative of the thiocarbonyl group (C=S) of the iniferter species, the stretch observed at ~1210 cm-1 (solid circle) is attributable to the C-N bond. Spectra are offset for clarity.

Samples were again sent for elemental analysis to confirm the attachment of the iniferter group to the surface of the resin and to determine degree of functionality. The results, expressed as percentage composition and mmol/g of resin, are presented in Table 2.4 and suggest that approximately 1 mmol of iniferter was immobilised per gram of Merrifield resin. This is in good agreement with Qin *et al.* who report 1.70 % nitrogen content following a 48 hour reaction between Merrifield resin and sodium diethyl dithiocarbamate under the same conditions (34).

	MR	*MR-I*
	% (mmol/g)	*% (mmol/g)*
C	84.65 (70.54)	80.50 (67.08)
H	7.13 (71.30)	7.34 (73.40)
N	<0.10 (<0.07)	1.94 (1.39)
S	<0.10 (<0.03)	5.88 (0.92)
Cl	7.73 (2.21)	NA

Table 2.4: Elemental analysis of unmodified Merrifield resin (MR) and iniferter derivitised resin (MR-I). Values are expressed as both percentage composition and mmol/g of resin. NA = not analysed.

2.3.7 *Polymerisation experiments with iniferter coupled Merrifield resin*

Concurrently, preliminary experiments were being performed in our laboratory using the phage-display derived peptide TR401 that displays high affinity (K_d 0.27nM) for the fluorescent probe Texas Red (40). Stability studies and binding assays suggested that the peptide was stable and capable of recognising its target in both aqueous and ethanolic solutions (41). Using the method outlined in Qin *et al.* (34), polymerisation studies using iniferter-modified resin were undertaken. Initial experiments employed water as a solvent however due to poor dispersibility, the aggregation of the resin during polymerisation was problematic. Ethanol was therefore used in subsequent studies. Samples were polymerised for various periods of time and subsequently analysed by FTIR.

The spectra shown in Figures 2.16 - 2.18 clearly demonstrated the effect of polymerisation time on the growth of polymer from the surface of the resin. Following 15 minutes irradiation there was little evidence of

polymerisation (conferred from the lack of a carbonyl stretch at ~1675 cm^{-1} from acrylamide/methylene bisacrylamide); all three spectra were virtually identical (Figure 2.16). When the polymerisation time was increased to one hour (Figure 2.17), a carbonyl peak was observed in the acrylamide and acrylamide/methylene bisacrylamide samples but not in the control resin spectra suggesting polymer growth on the surface of the resin.

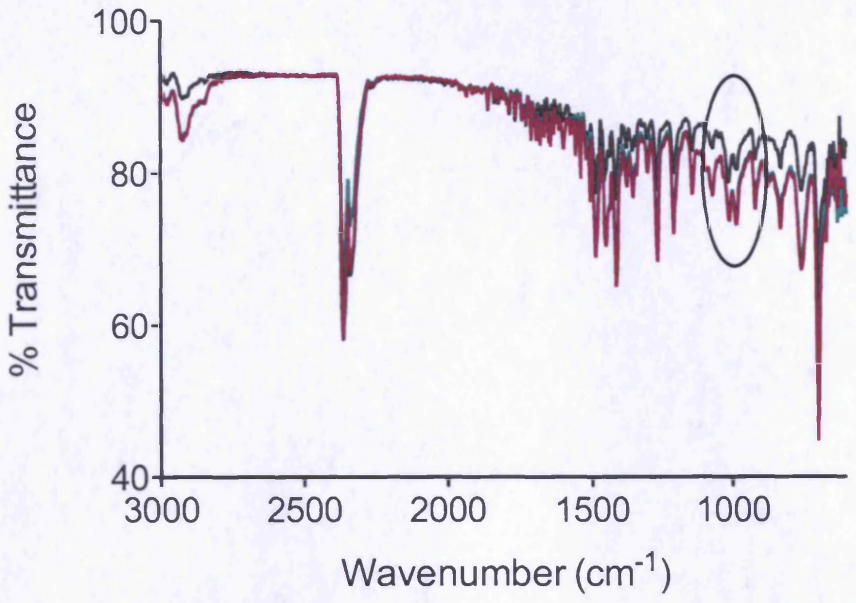

Figure 2.16: FTIR analysis of iniferter-modified resin following 15 mins UV irradiation in an ethanolic acrylamide (green) and acrylamide/methylene bisacrylamide (red) solution. There was no evidence of polymerisation (on the basis of the absence of a carbonyl stretch at ~1675 cm^{-1}); the spectra were the same as the control resin (iniferter-modified resin, no monomer/cross-linker, black). The characteristic thiocarbonyl stretch of the iniferter species (~1030 cm^{-1}) was present in all three spectra (circled).

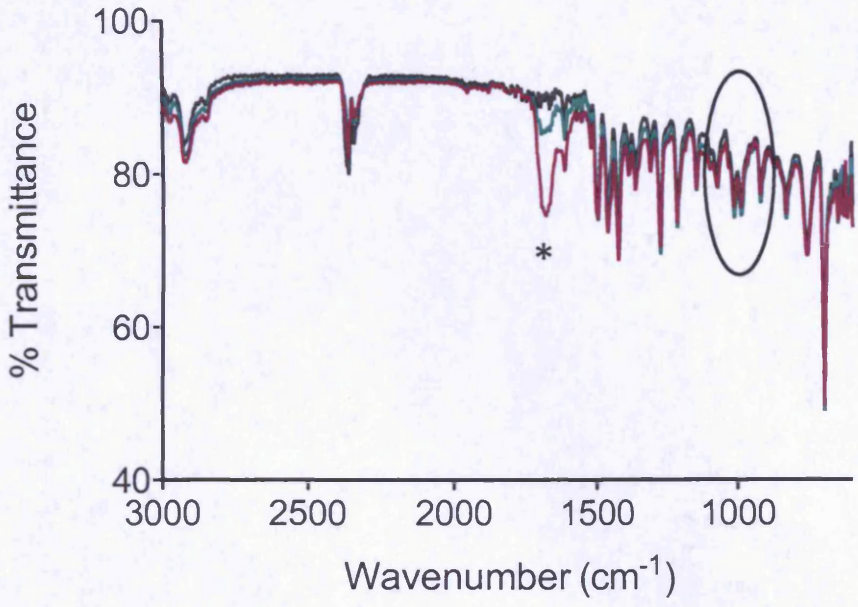

Figure 2.17: Polymerisation of iniferter derivitised Merrifield resin with acrylamide (green) and acrylamide/methylene bisacrylamide mixture (red) in ethanol after one hour. Polymerisation appeared to be more significant, based on relative carbonyl peak areas (*), when the mixture was used. In both polymer samples, the thiocarbonyl stretch of the iniferter species at ~1030 cm^{-1} (circled) remains suggesting successful endcapping of the polymer with the dithiocarbamyl radical (Black line : spectra obtained for the control iniferter-modified resin i.e resin irradiated in ethanol but in the absence of monomer).

The use of the monomer combination (acrylamide / methylene bisacrylamide) appeared to result in a greater carbonyl peak area being observed on the FTIR spectrum compared to the spectrum of acrylamide alone. Considering the molar ratio of acrylamide : methylene bisacrylamide used in this study (ca. 20 : 1), the increase in carbonyl peak area observed between the two samples appears somewhat disproportionate. Assuming an equal molar ratio, a possible explanation for the increase observed would be the increased rate of reactivity of methylene bisacrylamide compared to acrylamide; methylene bisacrylamide is likely to be incorporated at twice the rate of

acrylamide due to the presence of two polymerisable groups. Additionally, since methylene bisacrylamide contains two carbonyl groups it would have a greater contribution (peak area) to the IR signal observed at ~ 1675 cm^{-1} than acrylamide would. Therefore, on this basis and assuming equimolar incorporation in to the polymer, a four-fold increase may be envisaged. In this study however, this is complicated by the fact that the starting molar ratio of acrylamide to methylene bisacrylamide is approximately 20 : 1 and therefore one would expect the signal from the acrylamide carbonyl to be of more significance. This is not what was observed in Figure 2.17. The data suggests that the reactivity of the methylene bisacrylamide acrylamide groups is greater than that of acrylamide alone and therefore methylene bisacrylamide became incorporated into the polymer preferentially during the early stages of the polymerisation process. Following 24 hours the difference in carbonyl area is minimal (Figure 2.18) suggesting that whilst methylene bisacrylamide polymerisation predominates early in the reaction the large molar excess of acrylamide results in acrylamide rich polymer growth later in the process.

Importantly, the thiocarbonyl stretches (~1030cm^{-1}) were still apparent in the spectrum of resin polymerised for one hour suggesting successful endcapping of the polymer chains with the stable dithiocarbamyl species (Figure 2.17). On increasing the polymerisation period to 24 hours, FTIR analysis suggested significant growth of polymer on the surface of the resin (Figure 2.18), however there is no evidence of a dithiocarbamyl end group on the spectrum (loss of characteristic signal at ~ 1030 cm^{-1}). Chain transfer with solvent molecules or dimerization of the dithiocarbamyl species may have occurred leading to loss of the dithiocarbamyl radical during the washing and filtration process. Alternatively there is evidence to suggest that dithiocarbamate iniferter species can decompose via the loss of carbon disulphide to generate an

aminyl radical (42). If this radical species is formed and is capable of end-capping the polymer chains, a thiocarbonyl stretch would be absent from the spectra.

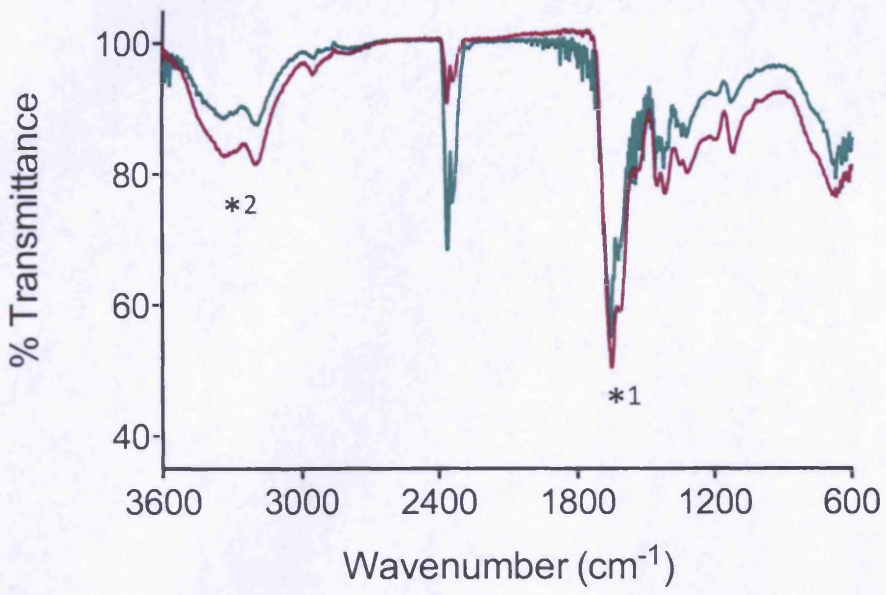

*Figure 2.18: FTIR spectra of iniferter coupled Merrifield following dispersion in an ethanolic solution of acrylamide (green) and acrylamide/methylene bisacrylamide mixture (red) and irradiation by UV light for 24 hours. The large peak seen at ~1650 cm^{-1} (*1) is indicative of the carbonyl group of the monomer while the stretch observed at 3400-3200 cm^{-1} (*2) represents the amide groups. The thiocarbonyl stretch of the iniferter (~1030 cm^{-1}) is absent from both spectra.*

Surprisingly, there was no discernible difference following polymerisation between the iniferter coupled resin and the control resin sample (unmodified Merrifield, Figure 2.19) used in the study. Benzyl chloride is known to form radicals upon exposure to UV radiation (43). Unlike the iniferter species, there is no stable radical species formed following photoolytic cleavage of the carbon-chlorine bond and therefore polymerisation proceeds in an uncontrolled fashion. Following 24 hours UV irradiation, significant solution phase

polymerisation was also evident and the resin had aggregated to form a disc-like structure on the surface of the solvent.

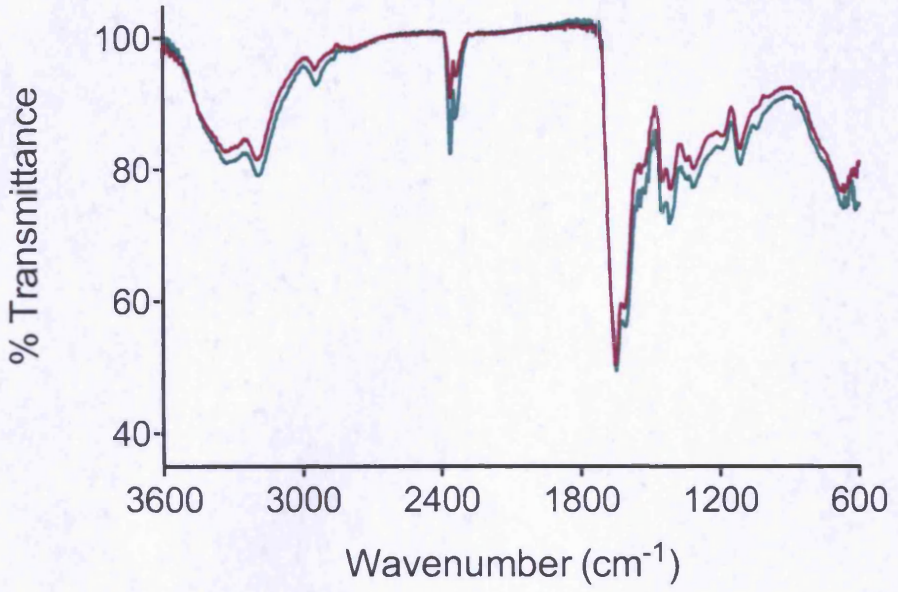

Figure 2.19: FTIR spectra of Merrifield resin control (green) and iniferter derivitised resin (red) following dispersion in an ethanolic solution of acrylamide and methylene bisacrylamide and irradiation by UV light for 24 hours. There is no discernible difference between the two spectra.

The control resin was also polymerised for 1 hour and compared to the iniferter modified species. The spectra demonstrated that even when the polymerisation period was reduced, the control resin continued to initiate polymerisation. In fact, Figure 2.20 suggested that the control resin may be more efficient at initiating the process than the iniferter, as the carbonyl and amide stretches observed were more significant.

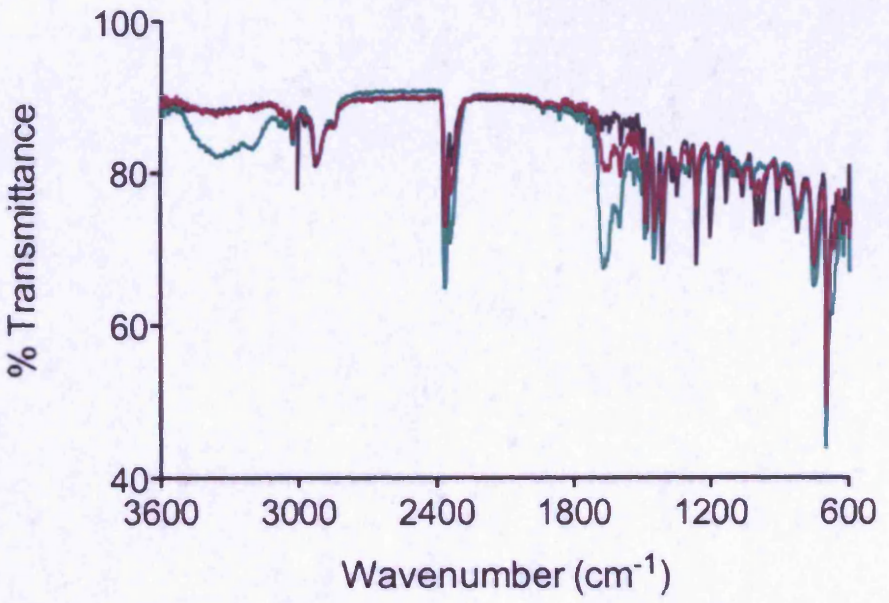

Figure 2.20: IR spectra of iniferter coupled (red) and un-modified Merrifield resin (green) following polymerisation of an ethanolic solution of acrylamide and methylene bisacrylamide for one hour. The spectra show that a greater degree of polymerisation was still observed with the Merrifield control compared to the iniferter-coupled resin even when the polymerisation time was reduced. Iniferter coupled Merrifield that had not been polymerised is shown on the spectra in black. The thiocarbonyl stretch at ~1030 cm^{-1} is present in the spectra of the iniferter coupled resin pre- and post-polymerisation (red and black) but is absent from the control polymerised resin (green).

Amine functionalised resin was investigated as a further control. Amino-polystyrene was irradiated with UV in the presence of acrylamide and methylene bisacrylamide (Figure 2.21). The FTIR spectrum shows no signs of polymerisation, therefore suggesting that the amine functionalisation successfully inhibited the formation of an active benzyl radical species

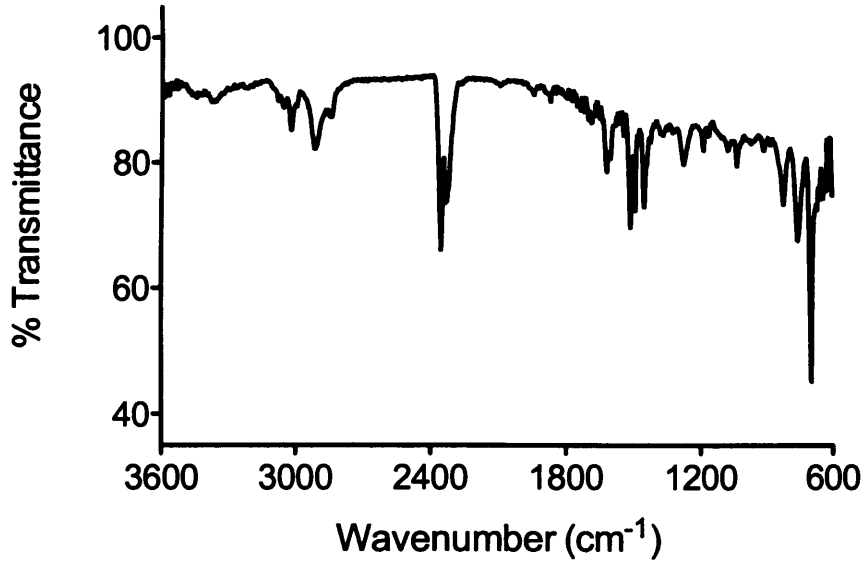

Figure 2.21: IR spectrum of amine functionalised Merrifield resin following dispersion in an ethanolic solution of acrylamide and methylene bisacrylamide and irradiation by UV light for 24 hours. Stretches in the region 3400 - 3200 cm^{-1} and at ~1600 cm^{-1} are attributable to the amine functionality of the resin.

The advantage of using an iniferter species, rather than just allowing the resin itself to initiate polymerisation, is the degree of control over polymer growth that can be attained. The presence of the less reactive radical species in solution following cleavage of benzyl diethyldithiocarbamate minimises solution phase polymerisation; the chloride radical produced when non-derivatised resin is used is much less stable than the diethyldithiocarbamate radical and therefore more reactive, leading to polymerisation of the monomer solution. This was evident when the resins were examined by microscopy (Figure 2.22). All iniferter derivitised resin remained as individual spheres following polymerisation, whilst the control resin had become aggregated due to the uncontrolled nature of the polymerisation. There was also evidence of solution phase polymerisation; small, irregular, polymer particles were observed.

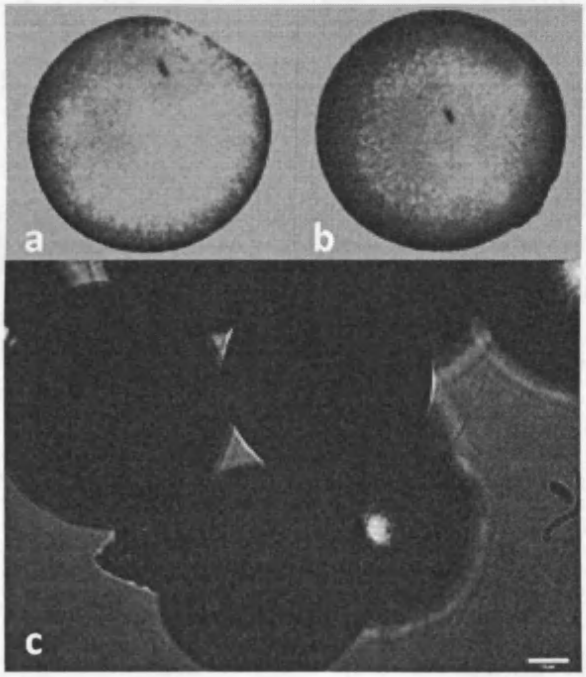

Figure 2.22: Epifluorescence microscopy images of iniferter derivitised Merrifield resin pre- (a) and post-polymerisation (b). Following polymerisation of the control resin the polystyrene spheres had aggregated (c) and there was evidence of solution phase polymerisation. (Scale bar = 15μm)

The aim of these studies was to better understand how iniferter initiated polymer growth might be utilised to bring about polymerisation around the co-immobilised peptide-template complex to give rise to our hypothesised synthetic receptor (Figure 1.7). A key consideration was therefore being able to control the depth of polymer growth so as not to hinder ligand access to the receptor. Data from within our laboratory (39) has shown that by varying irradiation times, polymer growth from iniferter modified silicon wafers can be tightly controlled. Using atomic force microscopy a gradual increase in polymer height, to a maximum of ~30 nm, over 60 minutes was observed. The polymer layer was shown to be homogenous over an area of 3 μm^2.

Since bifunctionalisation of the resin, to allow independent immobilisation of both peptide and iniferter, would give rise to a lower number of polymer initiation sites than had been present in earlier studies, experiments to confirm that the bifunctional resin would support polymer growth were also conducted. Bifunctionalised resin (azido- and chloromethyl) was produced and the iniferter moiety attached. The conversion of chloromethyl groups to amine was interrupted at the azide intermediate to allow for clear visualisation of the bifunctionalisation. Following polymerisation, FTIR was again used to confirm the presence of both polymer and azide on the surface of the resin (Figure 2.23). Small stretches at ~1650 $cm^{-1}$and 3200 - 3400 cm^{-1} are indicative of the presence of carbonyl and amide groups (i.e. polymer) and the distinctive azide signal at 2100 cm^{-1} demonstrated the bifunctionalisation.

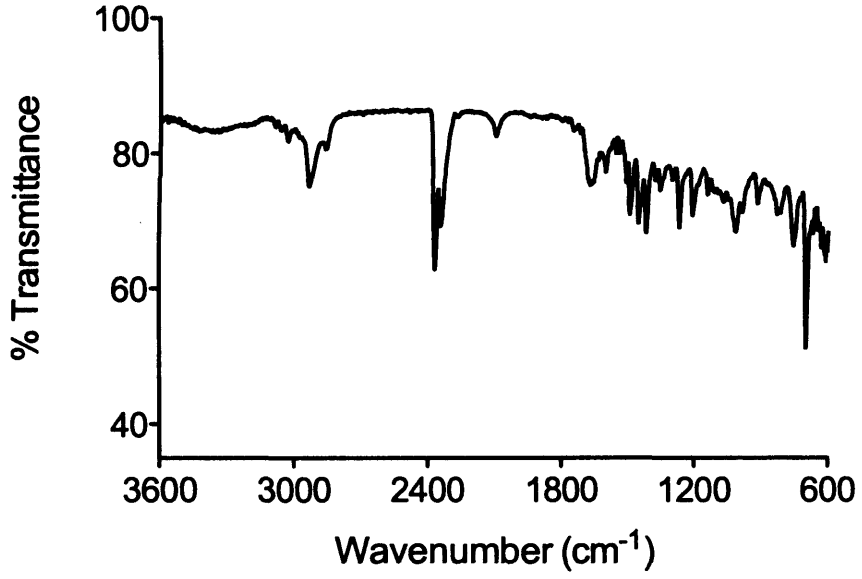

Figure 2.23: FTIR spectra of iniferter coupled bifunctionalised Merrifield resin following polymerisation of an ethanolic solution of acrylamide and methylene bisacrylamide for one hour. The azide peak is evident at ~2100 cm^{-1} indicative of bifunctionalisation, while the stretches at ~1600 cm^{-1} and 3200-3400 cm^{-1} demonstrate successful polymerisation of the sample.

For the strategy outlined in Chapter One to be successful it was imperative that the polymer did not interefere with the binding of the peptide to its target and therefore the choice of monomer was of paramount importance. Lipopolysaccharide (LPS) interacts via electrostatic and hydrophobic interactions with polymyxin B, the peptide species employed in this study (Chapter Three). At physiological pH, LPS is anionic by virtue of unique sugar residues and a degree of phosphorylation, therefore to reduce repulsion between the polymer surface and the target, monomers negatively charged at neural pH were disregarded. Furthermore, it was anticipated that such monomers might also interfere with the binding of LPS to polymyxin B, which carries a +5 charge at physiological pH, through direct interaction with the peptide. It was anticipated however that such

interactions would be minimised through the introduction of LPS to the system prior to the addition of the monomers. Conversely, basic monomers would possess positive charges at neutral pH and although this may increase interaction between LPS and the polymer, it is likely to do so in a non-specific fashion. Cationic monomers would also be less likely to form a protective polymeric "shell" around the peptide species due to electrostatic repulsion.

The choice of solvent is also important. In traditional imprinting systems organic solvents are often used; these conditions are not conducive to working with biological molecules. Lipopolysaccharide, due to its amphiphilic nature, forms micelles above certain concentrations (critical micelle concentration, CMC) in almost all solvent systems, however below the critical micelle concentration for a particular LPS species, homogenous aqueous solutions can be achieved. The monomers chosen must therefore be soluble in water. Based on these criteria and the earlier supporting data, it was decided that acrylamide and *N,N*-methylene bisacrylamide would be retained as the monomer combination.

As the work progressed it became obvious that the iniferter system that was effective in ethanol was less effective when water was used as the solvent. The resin dispersed very poorly in water and even with stirring a homogenous dispersion could not be achieved. FTIR analysis of resins showed little evidence of polymerisation when water was used as a solvent, even with prolonged periods of UV irradiation.

The hydrophobic nature of the dithiocarbamyl radical means that is likely to be poorly soluble in water. It is probable that this would have disfavoured initiator dissociation and retarded the polymerisation process when water was used as the solvent. Additionally, due to the non-swollen nature of Merrifield resin in water, the relative densities of

iniferter groups available to initiate polymerisation would likely have been significantly reduced. Insufficient deoxygenation of the system prior to polymerisation could also favour termination of polymerisation, however all water used was thoroughly degassed and sparged with nitrogen before use and each sample sparged with nitrogen for a second time prior to irradiation. These observations lead to the conclusion that a more hydrophilic iniferter species should be investigated.

2.3.8 Polymerisation experiments with dithiocarboxysarcosine coupled Merrifield resin

Matsuda and colleagues have previously used sodium *N*-(dithiocarboxy)sarcosine to successfully initiate the polymerisation of *N,N*-dimethylacrylamide and *N*-isopropylacrylamide in phosphate-buffered saline (44). One of the ethyl arms of sodium diethyldithiocarbamate is modified with a carboxylic acid group to increase the hydrophilicity of the less reactive radical species, thus encouraging polymerisation under aqueous conditions.

Sodium *N*-dithiocarboxysarcosine was synthesised from sarcosine and carbon disulfide (Figure 2.24) (39). The dithiocarboxysarcosine derivatised resin was prepared as described in section 2.2.11 and subsequently polymerised using the same combination of monomers as for the previous iniferter coupled resins (section 2.2.10). The FTIR spectra obtained are presented in Figure 2.25.

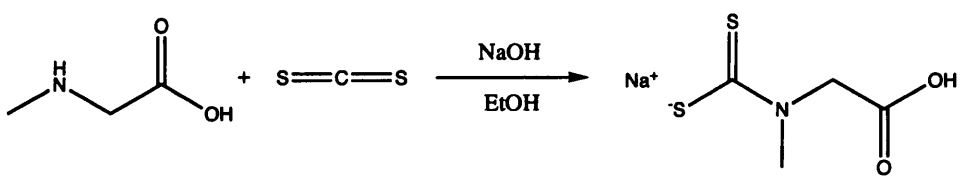

Figure 2.24: Synthesis of sodium N-dithiocarboxysarcosine

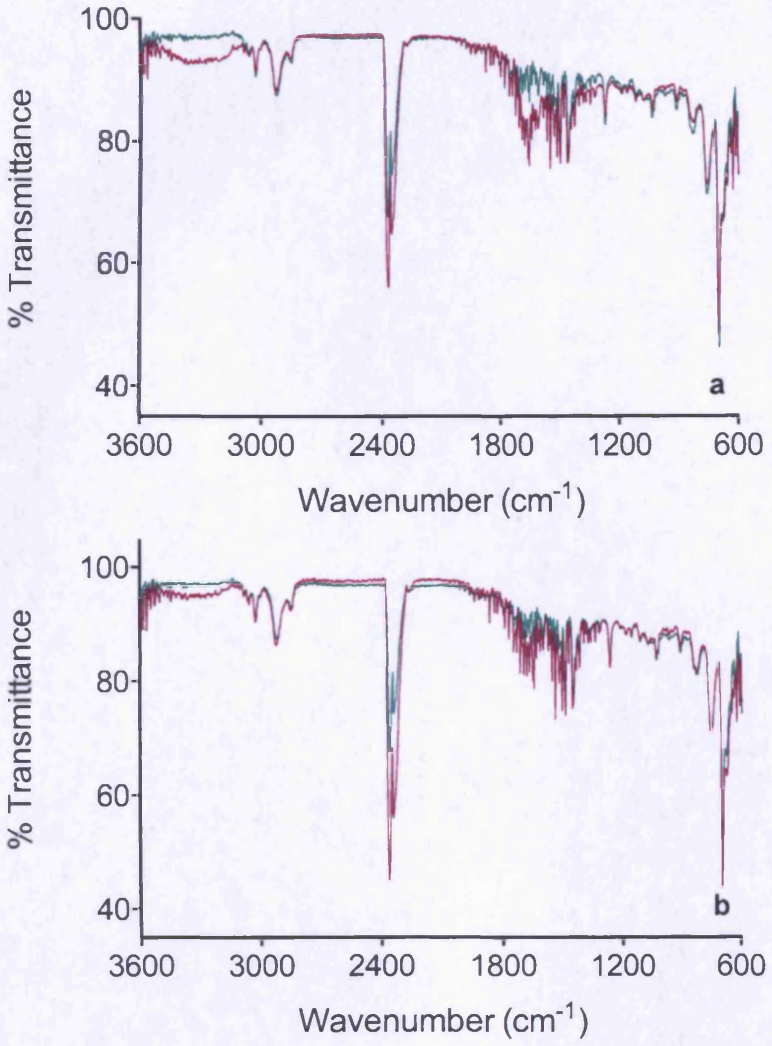

Figure 2.25: Spectra of the polymerisation of dithiocarboxysarcosine derivatised resin (a, red line) and unmodified Merrifield resin (b, red line) both overlaid with the spectra for dithiocarboxysarcosine derivitised Merrifield resin before prior to polymerisation (green).

The spectra for the water-soluble iniferter derivatised resin, pre-polymerisation (green in Figure 2.25), failed to show any discernible differences from the spectra obtained for control resin; the characteristic thiocarbonyl group from the iniferter was absent. Samples were sent for elemental analysis however the sulphur content of the iniferter functionalised resin before polymerisation was below limits of

detection (<0.1%). The apparent lack of an iniferter species is most likely due to the conditions employed in the attachment of the iniferter species. Water was used as a solvent for the reaction due to the high water solubility of *N*-dithiocarboxysarcosine, however Merrifield resin is hydrophobic and therefore under these conditions would have existed in a non-swollen/compacted form. This would mean that only the chloromethyl groups exposed on the very outer surface of the resin would be available for reaction with the iniferter species. *N*-dithiocarboxysarcosine is also soluble in methanol, however Merrifield resin swells relatively poorly in this solvent compared to aprotic solvents (1.8 ml/g in methanol compared to ~1 ml/g in water and >3.5 ml/g in solvents such as dichloromethane, dimethylformamide and tetrahydrofuran (45,46)). The attachment was therefore repeated in a 50 : 50 mix of methanol and DMF and the samples sent for elemental analysis and analysed by FTIR. The spectra obtained (Figure 2.26) demonstrates the successful attachment of the iniferter species; the thiocarbonyl stretch can be observed at ~1030 cm^{-1} (as is the case with diethyl dithiocarbamate) and a carbonyl peak is present at ~1650 cm^{-1}. Elemental analysis of the resin prepared under these reaction conditions suggest ~ 1.4 mmol of iniferter groups per gram of resin which is similar to values obtained with the diethyl dithiocarbamate iniferter species (Table 2.4).

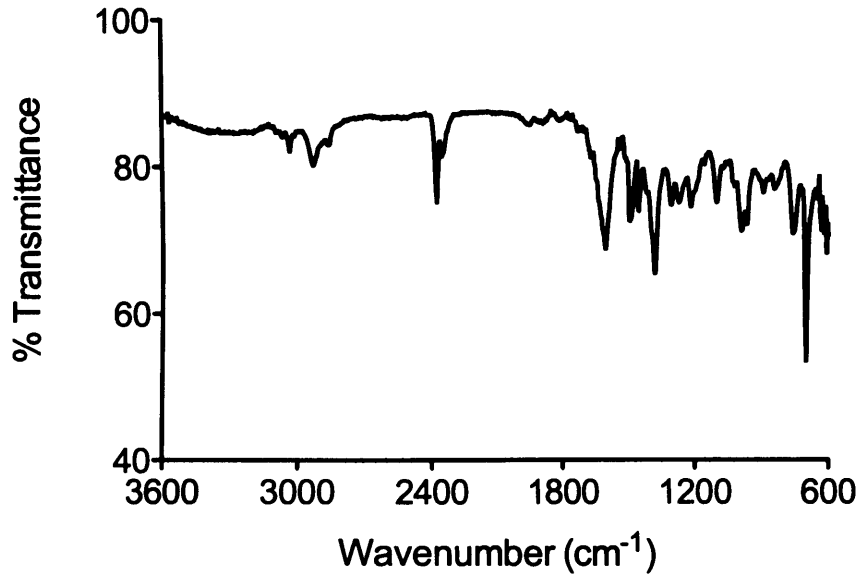

Figure 2.26: FTIR spectra of dithiocarboxysarcosine modified resin following attachment in DMF/MeOH 50/50 mix. A carbonyl peak at ~ 1650 cm^{-1} and a thiocarbonyl stretch at ~ 1030 cm^{-1} suggested successful immobilisation of the iniferter species.

Although this confirmed the attachment of the iniferter moiety, it does not necessarily represent the groups available for initiation of polymerisation. Due to the physicochemical properties of LPS, the polymerisation of the resin must take place in water. Under such conditions, Merrifield resin will exist in a non-swollen form and therefore the majority of iniferter groups will be trapped within the resin, unable to participate in the polymerisation reaction. It is therefore envisaged that only those iniferter groups on the outer surface of the resin will be capable of initiating polymerisation. The modification however does make the resin significantly more hydrophilic and this may influence its ability to swell in aqueous solvents.

The spectra in Figure 2.25 suggested however, that a greater degree of polymerisation was observed with the dithiocarboxysarcosine derivitised resin compared to the control Merrifield under aqueous

conditions. Additional time points were investigated and samples were analysed by FTIR and sent for elemental analysis to try and distinguish between the polymerisation observed with the two resins (i.e. iniferter modified and control, unmodified Merrifield resin). Elemental analysis demonstrated clear differences between the polymerisation of iniferter modified and control Merrifield resin, with the iniferter resin possessing 5.42% nitrogen following three hours polymerisation compared to 2.48% in the control resin. The FTIR spectra for these samples are given in Figure 2.28. These results suggested that dithiocarboxysarcosine had been successfully attached to the resin under aqueous conditions, however the analytical techniques used in this study were not capable of detecting such low densities of the iniferter species.

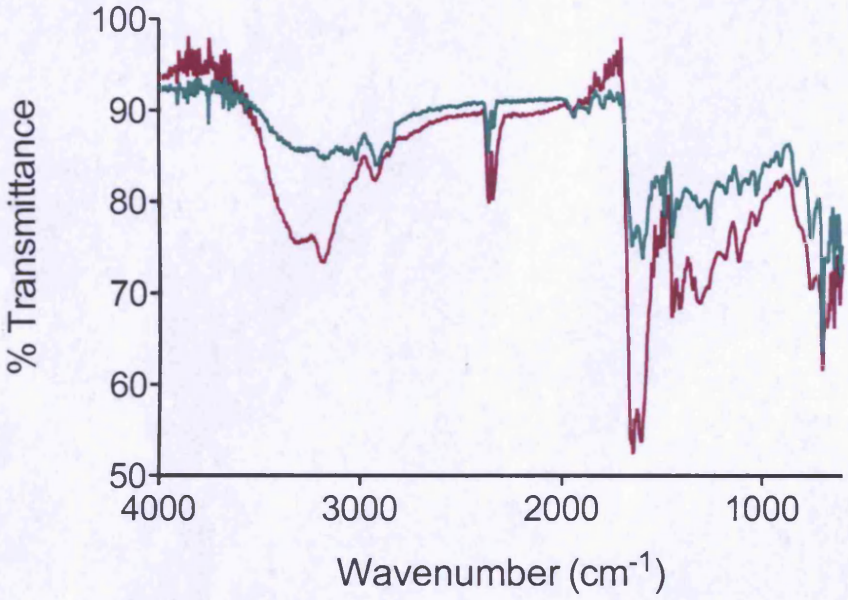

Figure 2.27: FTIR spectra of Merrifield control (green) and dithiocarboxysarcosine modified resin (red) following 3 hours polymerisation in an aqueous acrylamide/methylene bisacrylamide mixture. Both carbonyl and amide stretches are more significant in the iniferter modified resin, suggesting a greater degree of polymerisation.

2.4 Conclusion

The results outlined in this chapter have shown that it is possible to produce bifunctionalised resin i.e. resin displaying pre-defined molar ratios of chloromethyl and amino groups on its surface, via the generation of azidomethyl polystyrene and the subsequent reduction to amine using the Staudinger reaction. This will allow for the attachment of both the peptide moiety and the iniferter species. Two different dithiocarbamate-type iniferters have been immobilised on the surface of the resin and polymerisation successfully initiated under a variety of conditions. Chapter three will utilise the bifunctional resins developed herein to immobilise a peptide moiety and to provide proof-of-principle of the peptide-polymer hybrid system described in Chapter one.

2.5 Reference List

1. Kwong CK-W, Huang R, Zhang M, Shi M, Toy PH. Bifunctional Polymeric Organocatalysts and Their Application in the Cooperative Catalysis of Morita-Baylis-Hillman Reactions. Chem. Eur. J. 2007 Mar;13(8):2369-2376.

2. Cardno M, Bradley M. A simple multiple release system for combinatorial library and peptide analysis. Tetrahedron Letters. 1996 Jan 1;37(1):135-138.

3. Krattiger P, McCarthy C, Pfaltz A, Wennemers H. Catalyst-Substrate Coimmobilization: A Strategy for Catalysts Discovery in Split-and-Mix Libraries. Angew. Chem. Int. Ed. 2003 Apr;42(15):1722-1724.

4. Vágner J, Barany G, Lam KS, Krchnák V, Sepetov NF, Ostrem JA, et al. Enzyme-mediated spatial segregation on individual polymeric support beads: application to generation and screening of encoded combinatorial libraries. Proceedings of the National Academy of Sciences of the United States of America. 1996;93(16):8194 -8199.

5. Farrer RA, Copeland GT, Previte MJR, Okamoto MM, Miller SJ, Fourkas JT. Production, Analysis, and Application of Spatially Resolved Shells in Solid-Phase Polymer Spheres. Journal of the American Chemical Society. 2002 Mar 1;124(9):1994-2003.

6. Merrifield RB. Solid Phase Peptide Synthesis. I. The Synthesis of a Tetrapeptide. Journal of the American Chemical Society. 1963 Jul 1;85(14):2149-2154.

7. Chighine A, Sechi G, Bradley M. Tools for efficient high-throughput synthesis. Drug Discovery Today. 2007 Jun;12(11-12):459-464.

8. Arseniyadis S, Wagner A, Mioskowski C. A straightforward preparation of amino-polystyrene resin from Merrifield resin. Tetrahedron Letters. 2002 Dec 23;43(52):9717-9719.

9. Scriven EFV, Turnbull K. Azides: their preparation and synthetic uses. Chemical Reviews. 1988 Mar 1;88(2):297-368.

10. Köhn M, Breinbauer R. The Staudinger Ligation - A Gift to Chemical Biology. Angewandte Chemie International Edition. 2004;43(24):3106-3116.

11. Hawker CJ. Molecular Weight Control by a "Living" Free-Radical Polymerization Process. Journal of the American Chemical Society. 1994 Nov 1;116(24):11185-11186.

12. Wang J-S, Matyjaszewski K. Controlled/"living" radical polymerization. atom transfer radical polymerization in the presence of transition-metal complexes. Journal of the American Chemical Society. 1995 May 1;117(20):5614-5615.

13. Georges MK, Veregin RPN, Kazmaier PM, Hamer GK. Narrow molecular weight resins by a free-radical polymerization process. Macromolecules. 1993 May 1;26(11):2987-2988.

14. Chiefari J, Chong YK (Bill), Ercole F, Krstina J, Jeffery J, Le TPT, et al. Living Free-Radical Polymerization by Reversible Addition–Fragmentation Chain Transfer: The RAFT Process. Macromolecules. 1998;31(16):5559-5562.

15. Odian G. Principles of Polymerization. 4th ed. John Wiley Sons, Inc. 2004.

16. Barner-Kowollik C. Handbook of RAFT polymerization. Wiley-VCH; 2008.

17. Otsu T. Iniferter Concept and Living Radical Polymerization. J. Polym. Sci. A: Polym. Chem. 2000;38:2121.

18. Otsu T, Matsunaga T, Kuriyama A, Yoshioka M. Living radical polymerization through the use of iniferters: Controlled synthesis of polymers. European Polymer Journal. 1989;25(7-8):643-650.

19. Otsu T, Yoshida M. Role of initiator-transfer agent-terminator (iniferter) in radical polymerizations: Polymer design by organic disulfides as iniferters. Die Makromolekulare Chemie, Rapid Communications. 1982 Feb 16;3(2):127-132.

20. Otsu T, Matsumoto A. Controlled Synthesis of Polymers Using the Iniferter Technique: Developments in Living Radical Polymerization [Internet]. In: DiMari S, Funke W, Haralson MA, Hunkeler D, Joos-Müller B, Matsumoto A, et al., editors. Microencapsulation Microgels Iniferters. Berlin, Heidelberg: Springer Berlin Heidelberg; 1998 [cited 2011 May 6]. p. 75-137.Available from: http://www.springerlink.com/content/9qp22w0cflc8jhbb/

21. Deng J, Wang L, Liu L, Yang W. Developments and new applications of UV-induced surface graft polymerizations. Progress in Polymer Science. 2009 Feb;34(2):156-193.

22. Ivanova-Mitseva PK, Fragkou V, Lakshmi D, Whitcombe MJ, Davis F, Guerreiro A, et al. Conjugated Polymers with Pendant Iniferter Units: Versatile Materials for Grafting. Macromolecules. 2011 Apr 12;44(7):1856-1865.

23. Lee H-Y, S. Kim B. Grafting of molecularly imprinted polymers on iniferter-modified carbon nanotube. Biosensors and Bioelectronics. 2009 Nov 15;25(3):587-591.

24. Kwon IK, Matsuda T. Photo-iniferter-based thermoresponsive block copolymers composed of poly(ethylene glycol) and poly(N-

isopropylacrylamide) and chondrocyte immobilization. Biomaterials. 2006 Mar;27(7):986-995.

25. Watanabe J, Kano K, Akashi M. Bioconjugate polymer by photo-iniferter approach: Hydrophilic random or block copolymer-coated surface. Materials Science and Engineering: C. 2009 Aug 31;29(7):2287-2293.

26. Su S, Zhang M, Li B, Zhang H, Dong X. HPLC determination of sulfamethazine in milk using surface-imprinted silica synthesized with iniferter technique. Talanta. 2008 Sep;76(5):1141-1146.

27. Barahona F, Turiel E, Cormack PAG, Martín-Esteban A. Chromatographic performance of molecularly imprinted polymers: Core-shell microspheres by precipitation polymerization and grafted MIP films via iniferter-modified silica beads. J. Polym. Sci. A Polym. Chem. 2010 Mar;48(5):1058-1066.

28. Tasdelen MA, Kahveci MU, Yagci Y. Telechelic polymers by living and controlled/living polymerization methods. Progress in Polymer Science. 2011 Apr;36(4):455-567.

29. Sellergren B, Rückert B, Hall AJ. Layer-by-Layer Grafting of Molecularly Imprinted Polymers via Iniferter Modified Supports. Advanced Materials. 2002;14(17):1204-1208.

30. Poma A, Turner APF, Piletsky SA. Advances in the manufacture of MIP nanoparticles. Trends in Biotechnology. 2010 Dec;28(12):629-637.

31. Bossi A, Whitcombe MJ, Uludag Y, Fowler S, Chianella I, Subrahmanyam S, et al. Synthesis of controlled polymeric cross-linked coatings via iniferter polymerisation in the presence of tetraethyl thiuram disulphide chain terminator. Biosensors and Bioelectronics. 2010 May 15;25(9):2149-2155.

32. Pérez-Moral N, Mayes AG. Molecularly Imprinted Multi-Layer Core-Shell Nanoparticles - A Surface Grafting Approach. Macromolecular Rapid Communications. 2007 Nov 16;28(22):2170-2175.

33. Chen R-R, Qin L, Jia M, He X-W, Li W-Y. Novel surface-modified molecularly imprinted membrane prepared with iniferter for permselective separation of lysozyme. Journal of Membrane Science. 2010 Nov 1;363(1-2):212-220.

34. Qin L, He X-W, Zhang W, Li W-Y, Zhang Y-K. Surface-modified polystyrene beads as photografting imprinted polymer matrix for chromatographic separation of proteins. J Chromatogr A. 2009 Jan 30;1216(5):807-814.

35. Guerreiro AR, Chianella I, Piletska E, Whitcombe MJ, Piletsky SA. Selection of imprinted nanoparticles by affinity chromatography. Biosensors and Bioelectronics. 2009 Apr 15;24(8):2740-2743.

36. Oxelbark J, Legido-Quigley C, Aureliano CSA, Titirici M-M, Schillinger E, Sellergren B, et al. Chromatographic comparison of bupivacaine imprinted polymers prepared in crushed monolith, microsphere, silica-based composite and capillary monolith formats. J Chromatogr A. 2007 Aug 10;1160(1-2):215-226.

37. Titirici M-M. Synthesis and evaluation of novel formats in molecular imprinting [Internet]. 2005 [cited 2011 Feb 3];Available from: https://eldorado.tu-dortmund.de/handle/2003/20168

38. Rückert B, Hall AJ, Sellergren B. Molecularly imprinted composite materials via iniferter-modified supports. Journal of Materials Chemistry. 2002;12(8):2275-2280.

39. Kelly M. MIPs as Prion Biosensors. Cardiff University; 2011.

40. Rozinov MN, Nolan GP. Evolution of peptides that modulate the spectral qualities of bound, small-molecule fluorophores. Chemistry & Biology. 1998 Dec;5(12):713-728.

41. Jones JA. The Development of Functional Plastibodies. Thesis. Cardiff University; 2011.

42. Turner SR, Blevins RW. Photoinitiated block copolymer formation using dithiocarbamate free radical chemistry. Macromolecules. 1990 Mar 1;23(6):1856-1859.

43. Brocklehurst B, Porter G, Savadatti MI. Production of benzyl radicals by ionizing and ultra-violet radiation. Trans. Faraday Soc. 1964;60:2017.

44. Matsuda T, Ohya S. Photoiniferter-based thermoresponsive graft architecture with albumin covalently fixed at growing graft chain end. Langmuir. 2005 Oct 11;21(21):9660-9665.

45. Santini R, Griffith MC, Qi M. A measure of solvent effects on swelling of resins for solid phase organic synthesis. Tetrahedron Letters. 1998 Dec 3;39(49):8951-8954.

46. Wipf P. Handbook of Reagents for Organic Synthesis: Reagents for high-throughput solid-phase and solution-phase organic synthesis. John Wiley and Sons; 2005.

Chapter Three : Polymyxin Studies

3.1 Introduction

3.1.1 General Overview

Every year millions of people contract infections of bacterial, viral and/or fungal origin. The large majority of these will either be self-limiting requiring no pharmacological intervention or can be efficiently treated by empirical antimicrobial therapies. In recent years however, the incidence of multi-drug resistant infections, particularly nosocomial infections, has increased significantly. In 2004, the Infectious Diseases Society of America (IDSA) published a report that served to highlight the disparity between the dwindling number of new antimicrobial therapies and the increasing occurrence of bacteria resistant to multiple antibiotic classes (1). In the preceding seven years little has changed and the situation seems unlikely to improve in the near future. Despite multidrug resistant gram-positive bacterial infections such as MRSA being highlighted as a public health crisis, very little attention has been paid to the Gram-negative organisms that are rapidly developing resistance. As a consequence, for a growing number of Gram-negative infections there are no effective antimicrobial interventions currently available or in the advanced stages of clinical development (1,2). Antibiotics previously abandoned due to safety concerns are now being considered for those infections refractive to current treatment strategies (3,4).

The polymyxins are a family of cyclic polypeptides derived from the spore-forming soil-borne rod *Bacillus Polymyxa.* First discovered in the 1940's, the polymyxins consist of five structurally related decapeptides two of which, Polymyxin B and E (colistin), found extensive clinical use against infections of Gram-negative origin until the 1970's. Reported neuro and nephrotoxicity associated with their use saw them cast aside in favour of newer, less toxic antibiotics (5,6). However, the occurrence

of isolates of *Escherichia coli, Pseudomonas spp., Klebsiella spp., Acinetobacter spp.* and other Gram-negative pathogens displaying resistance to β-lactam antibiotics, aminoglycosides and fluoroquinolones, has initiated a resurgence in interest (4,5,7,8).

3.1.2 Structure

All members of the polymyxin family share a related pharmacophore consisting of a cyclic heptapeptide region and a linear tripeptide section to which a fatty acyl chain is attached. The general structure of polymyxin B is shown in Figure 3.1.

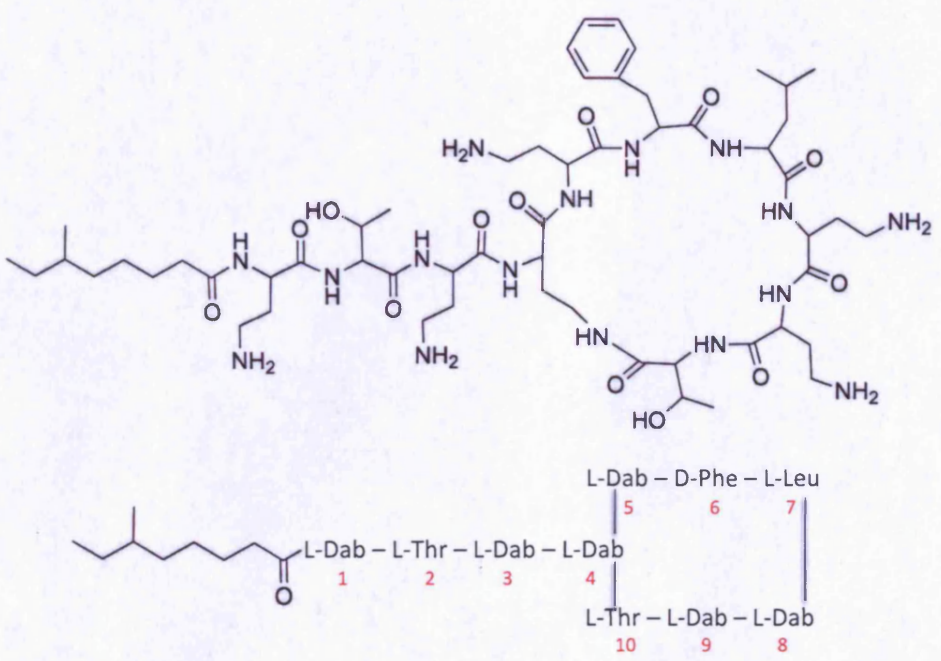

Figure 3.1: General chemical structure of polymyxin B. The cyclic decapeptide consists of six L-2,4-diaminobutyric acid residues (L-Dab), two threonine (L-Thr), one phenylalanine (D-Phe) and one leucine (L-Leu) residue attached to a 6-methyloctonic acid acyl chain.

Like most antimicrobial peptides, the polymyxins are amphipathic molecules, possessing distinct hydrophilic and hydrophobic domains. The presence of six L-diaminobutyric acid residues, five of which display free γ-NH_2 groups, give the molecule an overall positive charge and contributes to the hydrophilicity, while the acyl chain and the phenylalanine and leucine residues represent the hydrophobic region of the peptide (2).

Commercial polymyxin B sulfate is a mixture of several structurally related components and studies have sought to chemically separate and identify the individual molecular species (9,10). In total seven compounds have been isolated, all possessing the same amino acid structure, with the exception of Ile-polymyxin B1 that has isoleucine as the seventh residue. The length and degree of substitution of each of the acyl chains varies; Polymyxin B1 and B2 that constitute the majority of the mixture, have 6-methyloctanoic acid and 6-methylheptanoic acid as their acyl chains respectively. Another member of the polymyxin family, polymyxin E (colistin) is structurally identical to polymyxin B except for the substitiution of D-phenylalanine at position six with D-leucine (11).

3.1.3 Interaction with LPS and mechanism of action

The interaction of polymyxin with lipopolysaccharide and Gram-negative bacteria has been extensively studied over the past decades. Investigations have sought to discover the molecular basis of the interaction using fluorescent probes (12,13), nuclear magnetic resonance spectroscopy (14,15), surface plasmon resonance studies (16,17), isothermal calorimetry (18,19) and by monitoring the trans-membrane flux of various inorganic/organic ions (20). Results of these studies

suggest that the polymyxins exert their antimicrobial activity via a two-stage mechanism.

The initial interaction between the peptide and the surface of the bacterium is facilitated by electrostatic interactions between the positively charged primary amines of the L-2,4-diaminobutyric amino acid residues and the negatively charged KDO-Lipid A region of LPS. The peptide displaces the divalent magnesium and calcium cations that bridge the LPS molecules, thus destabilising the outer membrane of the Gram-negative bacteria. Additionally, this interaction serves to bring the fatty acyl chain of the peptide into close proximity with the Lipid A region of LPS to allow insertion of the hydrophobic tail into the outer leaflet of the outer membrane (21-23). The result is a loosening of the packing of lipid molecules and expansion of the outer leaflet of the membrane. Following this initial interaction and disruption of the immediate cellular barrier, polymyxin follows a self-promoted uptake pathway to permeate the inner leaflet of the outer membrane i.e. it facilitates its own entry into the cell as opposed to being actively taken up (24,25). Once in the periplasmic space, polymyxin can disrupt the inner membrane simply via direct insertion leading to cytoplasmic leakage and an increased permeability to lysozyme, proteins and hydrophobic antibiotics, ultimately leading to bacterial cell death (5,26,27). An alternative mechanism in which the peptide facilitates the exchange of lipids between the inner leaflet of the outer membrane and the outer leaflet of the cytoplasmic membrane has also been proposed. Such exchange would result in a loss of the osmotic balance of the cell and subsequent cell death (2,28-30) (Figure 3.2).

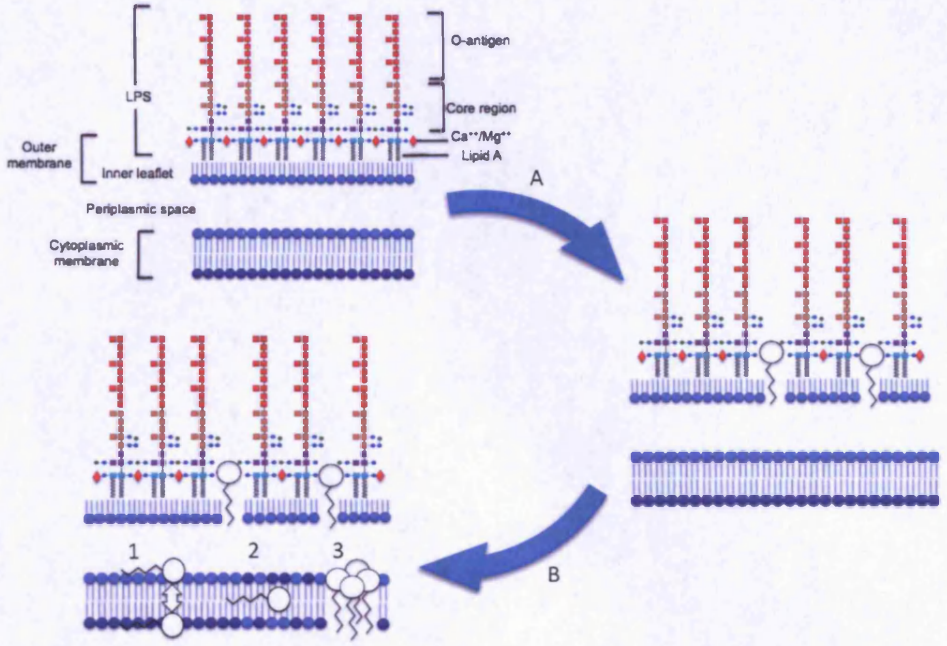

Figure 3.2: Mechanism of action of polymyxin B. Addition of polymyxin B (A) leads to displacement of divalent cations that bridge the LPS molecules in the outer membrane, thus destabilising the membrane and facilitating the self-promoted uptake of the peptide. Once it has traversed the outer membrane and entered the periplasmic space (B) the peptide disrupts the cytoplasmic membrane, enters the cell and brings about cell lysis either by 'flip-flopping' across the leaflets of the inner membrane (1), through facilitating lipid exchange between the two leaflets of the cytoplasmic membrane (2) or by direct insertion and aggregation into micelle type structures in the membrane (3). Adapted from (25).

The amphipathicity of the peptide, particularly the acyl chain, is vital for its antimicrobial activity; studies with polymyxin B nonapetide (i.e. polymyxin B that has undergone ficin/papain treatment to remove the final diaminobutyric acid residue and acyl chain), demonstrate little/no antimicrobial activity; the nonapetide has MIC ≥ 300μgml^{-1} against *E.coli* and *Salmonella spp.* compared to 1μgml^{-1} for the native peptide (31). This analogue however retains the ability to permeate the outer membrane of Gram-negative bacteria thus making them more susceptible to other

antibiotics and the effects of complement (23,31-36). The polymyxins are considered one of the strongest binders of LPS and therefore a potent anti-endotoxin, a property that is believed to be separate from its antimicrobial activity as nonapeptide analogues are capable of binding and neutralising the *in vivo* effects of LPS (27,35,37-41).

Although resistance to the polymyxins has rarely been reported, the number of resistant isolates is on the increase, particularly in Mediterranean areas and south-east Asia (6). This is leading to a generation of extremely drug resistant Gram-negative pathogens for which there is no known effective antibiotic treatment. It is via modification to the outer membrane, particularly the chemical structure of LPS, that Gram-negative bacterium develop resistance to the peptide antibiotic. The general mechanism for conferring resistance in *E.coli* and *Salmonella spp.*, is through a reduction in the net negative charge of the lipid A portion of LPS, thus interfering with/inhibiting the initial interactions between the peptide and the bacterium. This is achieved via the esterification of the phosphate groups with 4-amino-4-deoxy-L-arabinose and/or phosphoethanolamine, a process controlled by a two-component regulatory system (PhoP-PhoQ and PmrA-PmrB) that is activated under inappropriate cell culture conditions (for example, grown in Mg^{++} deficient media) or during exposure to sub-lethal concentrations of the peptide (2,4-6). Other bacteria such as *Neisseria spp., Providencia spp.* and *Proteus spp.* are intrinsically resistant to the actions of polymyxin as are Gram-positive organisms (6).

3.1.4 Clinical uses

Reports of neuro- and nephrotoxicity associated with the clinical administration of polymyxin intravenously severely limited its use after the mid 1970's (5,42). At that time however, many patients were also co-administered a plethora of other medications in an attempt to sustain

life, some of which may also have possessed nephrotoxic side effects. It is therefore difficult to retrospectively distinguish the effects caused by the administration of the antibiotic and other therapies and today, especially with the advent of superior intensive care medicine and support, the polymyxins are considered to be less toxic than was once believed (43,44). Indeed polymyxins, in the case of extreme antibiotic resistance, are finding their way into the clinic where associated toxicity can often be controlled through careful observation of the patient with subsequent modification of the dose and often spontaneously subside following withdrawal of treatment. Although still not widely used for the treatment of systemic infections in the UK, polymyxin B is found in a number of topical preparations for otic, ophthalmic and dermal infections of bacterial origin (e.g. Otosporin ear drops, Polyfax skin and eye ointments, Maxitrol eye drops/ointment (45)). Polymyxin E (colistin) has also continued to find use, particularly in inhalational therapy for cystic fibrosis patients. Administered via a nebuliser or intravenously as the inactive pro-drug colistimethate sodium, the antibiotic effectively treats *Ps. aeruginosa* and multi-drug resistant *Acinetobacter* infections with few adverse effects (4,11,46).

Use of polymyxin B immobilised on the surface of a solid support in extracorporeal apheresis has been investigated as a therapeutic intervention in sepsis, septic shock and associated multi organ failure (47-50). Toraymyxin (Spectral Diagnostics), a polymyxin haemoperfusion cartridge, has been used clinically in Japan since the early 1990's (51) with positive results and few adverse effects. It is currently the subject of a multi-centre, double-blind phase III clinical trial taking place in the USA (EUPHRATES: Evaluating the Use of Polymyxin B Hemoperfusion in a Randomized controlled trial of Adults Treated for Endotoxemia and Septic Shock (52)). In other studies, immobilised polymyxin has been found to mimic the outer

membrane permeabilisation effects of the free peptide resulting in inhibition of cell growth (53,54) in addition to acting as an endotoxin sequestrant.

3.1.5 Aims and objectives of Chapter Three

Polymyxin B is being used in this study as the high affinity peptide ligand for lipopolysaccharide to provide evidence for the proposed peptide-polymer system described in Chapter One.

The key objectives of this work were:

1. To successfully immobilise polymyxin on the surface of the resin.
2. To use the chemistries outlined in Chapter Two to bring about peptide-target capture within a polymer matrix.
3. To evaluate the binding efficiency of the peptide-resin and peptide-polymer hybrid system.

3.2 Materials and Methods

3.2.1 Materials

All chemicals were purchased from Sigma-Aldrich, Poole, UK and were used as received unless otherwise stated. All organic solvents were of HPLC grade and were obtained from Fisher Scientific, Loughborough, UK unless otherwise stated.

3.2.2 Synthesis of dansyl-polymyxin B

The method described by Schindler and Teuber (55) was used to synthesise the dansyl derivative of polymyxin B. Briefly, 40 mg (28.9 μmol) polymyxin B sulfate (Enzo Life Sciences, Exeter, UK) in 1.2 ml of 0.1 M sodium bicarbonate buffer (pH 8.4) was incubated with 10 mg (37.1 μmol) dansyl chloride in 0.8 ml acetone for 90 minutes at room temperature, protected from light. The mixture was subsequently loaded onto a Sephadex G50 column and the dansyl-polymyxin eluted with 10 mM sodium phosphate (pH 7.1)/0.145 M sodium chloride buffer. Fractions (20 x 5 ml) were collected and a handheld UV lamp used to detect the dansyl derivative (dansyl-polymyxin is yellow in colour whereas unreacted dansyl chloride is blue - green). All fractions containing dansyl-polymyxin were extracted into half a volume of butanol and dried under vacuum overnight prior to being resuspended in 3 ml HEPES buffer (5 mM, pH 7) and stored as 100 μl aliquots at -20 °C.

3.2.3 Dinitrophenylation assay

The method reported by Bader and Teuber (56) was used to determine concentrations of polymyxin with some modifications. A calibration

curve was prepared from a 1 $mgml^{-1}$ stock solution of polymyxin B in deionised water. To each sample, 200 µl of a 1 %w/v aqueous solution of sodium borate and 25 µl of 100 mM 1-fluoro-2,4-dinitrobenzene in ethanol was added and the solutions incubated at 37 ^{0}C for 1 hour. Hydrochloric acid (2 M, 1 ml) and 1 ml butanol was subsequently added and the samples vortexed. The butanol phase was analysed using a Perkin Elmer Lambda 5 UV/Vis Spectrophotometer, reading at 370 nm. A calibration curve was used to determine concentrations of polymyxin in unknown samples following the synthesis of dansyl-polymyxin.

3.2.4 Dansyl polymyxin binding assays

The dansyl-polymyxin synthesised was subsequently used to determine affinities of polymyxin for lipopolysaccharide. Lipopolysaccharide from *E. coli* 0111:B4 at concentrations of 1 and 100 μgml^{-1}, was incubated with a range of dansyl-polymyxin concentrations (0 - 1 µM, 0.1 µM increments) and the fluorescence intensity at 485 nm (λ_{Ex} 330 nm) recorded.

3.2.5 Immobilisation of polymyxin on Merrifield Resin

3.2.5.1 Imidoester linker

Dimethyl adipimidate dihydrochloride (490.3 mg, 2 mmol) was incubated with 100 mg amine-modified resin (~2 mmol NH_2/g, synthesised as described in Chapter 2) in 10 ml 0.2 M triethanolamine buffer, pH 8.0 for 1 hour at room temperature with gentle stirring. The resin was then filtered and washed with three 25 ml volumes of 0.2 M triethanolamine buffer, pH 8.0. Polymyxin B sulfate (207 mg, 0.15

mmol) was subsequently reacted with 50 mg (maximum 0.1 mmol) dimethyl adipimidate modified resin in 10 ml 0.2 M triethanolamine buffer, pH 8.0, for 1 hour at room temperature with gentle stirring. The resin was then filtered and washed with three 25ml volumes of 0.2 M triethanolamine buffer, pH 8.0. The filtrate plus all three washes were analysed by reverse phase HPLC (section 3.2.6) to allow the loading of polymyxin on the surface of the resin to be estimated.

a) Binding assays

Polymyxin-modified and control resins (10 mg) were incubated with various concentrations of FITC-labelled LPS from *E. coli* 0111:B4 in deionised water in 1 ml SPE cartridges fitted with 20 μm porosity polyethylene frits. The incubation was carried out at room temperature under non-equilibrium (less than 10 minutes) and equilibrium (16 hours) conditions. Fluorescence of the filtrates were analysed using a FLUOstar OPTIMA platereader (BMG Labtech GmbH, Ortenburg, Germany) at an excitation wavelength of 485 nm and emission wavelength of 520 nm. All samples were prepared in triplicate.

b) Effect of free polymyxin and dimethyl adipimidate on fluorescence of FITC-LPS

To investigate the effect of any free dimethyl adipimidate or polymyxin on the fluorescence of FITC-LPS, various concentrations of each were incubated with 1 μgml^{-1} FITC-LPS overnight in glass specimen tubes. The fluorescence of the solutions were measured and compared to a standard 1 μgml^{-1} FITC-LPS solution.

3.2.5.2 Click Chemistry

a) Synthesis of alkyne polymyxin

Polymyxin B sulfate (100 mg, 72 μmol) was reacted with glycidyl propargyl ether (7.76 μl, 72 μmol) in 10 ml methanol and stirred at 40 °C for 16 hours. The mixture was rota-evaporated to dryness and the resulting polymyxin residue re-suspended in de-ionised water.

b) Immobilisation of alkyne polymyxin on azide resin

Following the original Sharpless procedure (57), alkyne derivitised polymyxin (100 mg) and sodium ascorbate (59 mg, 0.3 mmol) were dissolved in 12 ml deionised water and copper (II) sulfate (4.78 mg, 0.03 mmol) added. Azide resin (200 mg) was subsequently added to the solution and stirred at room temperature for 16 hours. The resin was then filtered and washed with three 100 ml volumes of deionised water, 100 ml water/methanol (50/50) and 50 ml methanol and was then dried under vacuum at 40 °C for sixteen hours.

c) Standard binding assay

Polymyxin modified and control resins (10 mg) were incubated with various concentrations of FITC-labelled LPS from *E. coli* 0111:B4 in deionised water at room temperature for 16 hours. Samples were subsequently filtered through Whatman 1 paper and the fluorescence of the filtrate analysed. All samples were prepared in triplicate.

d) Hot-cold assay

Polymyxin-modified resin (5 mg) was incubated with various ratios of hot (FITC-labelled) and cold (unlabelled) LPS from *E. coli* 0111:B4

(Table 3.1) at room temperature for 16 hours. Samples were subsequently filtered through Whatman 1 paper, the fluorescence of the filtrates analysed (section 3.2.5.1 a) and the amount of FITC-LPS bound calculated from a calibration curve. All samples were prepared in triplicate.

Sample	[Hot] (μgml^{-1})	[Cold] (μgml^{-1})
1	5.00	0.00
2	4.00	1.00
3	3.00	2.00
4	2.00	3.00
5	1.00	4.00
6	0.5.0	4.50
7	0.25	4.75
8	0.05	4.95
9	0.00	5.00

Table 3.1: Various ratios of hot (FITC-labelled) and cold (unlabelled) E. coli 0111: B4 LPS used in the hot cold assay. At all ratios the mass of resin used was 5mg and the total volume of the system was 1ml.

e) Selectivity assay

FITC-LPS from *E. coli* 0111:B4 (2.5 μgml^{-1}) was incubated with polymyxin modified resin in the presence of a variety of other lipopolysaccharides (2.5 μgml^{-1}, *E. coli* 0111:B4 unlabelled, *Klebsiella pneumoniae, Pseudomonas aeruginosa* serotype 10, *Salmonella enterica* serotype Minnesota and *Serratia marcescens*) at room temperature for 16

hours. Samples were subsequently filtered through Whatman 1 paper and the fluorescence of the filtrate analysed. Binding of FITC-LPS and the competitors was determined relative to 2.5 μgml^{-1} and 5 μgml^{-1} FITC LPS (*E. coli* 0111:B4) standards.

3.2.6 HPLC analysis of polymyxin B sulfate

HPLC analysis was performed using an Thermo Scientific HPLC automated system fitted with a Gracesmart, 5 μm, C18, 25 mm x 4.6 mm i.d column (Alltech Associates Applied Science Ltd., Lancashire, UK) The mobile phase consisted of 22.25 % acetonitrile : 50 % sodium sulfate (0.7 %w/v) : 5 % phosphoric acid (6.8 %v/v) : 22.75 % deionised water, with UV detection at 215 nm (58). A 20 μl injection volume and a flow rate of 1 $mlmin^{-1}$ were used.

3.2.7 Linear polymyxin B

A linear analogue of polymyxin B (decapeptide without the acyl chain) was synthesised by collaborators at Tromsø University, Norway. The peptide was alkyne derivitised and attached to azide-modified resin in the same way as the cyclic form (see sections 3.2.5.2 a and b). Binding assays were performed as outlined in section 3.2.5.2 c.

3.2.8 Synthesis of polymyxin B-polymer hybrids

a) Immobilisation of polymyxin B on iniferter modified resin

Azide/sodium dithiocarboxy sarcosine (~ 50/50) modified resins (for attachment of iniferter species see section 2.2.11 in Chapter Two) were incubated with alkyne modified polymyxin B as described in 3.2.5.2 b).

b) Polymer growth assay

To assess the effect of polymer growth on the performance of the peptide, polymyxin B (cyclic)/sodium dithiocarboxysarcosine (~ 50/50) modified resin was polymerised for a variety of time periods and the binding properties of the hybrid systems evaluated. Resin (50 mg) was dispersed in an acrylamide (70 mg)/methylene bisacrylamide (7.5 mg) solution (4 ml deionised water). Polymerisation was initiated by UV and allowed to proceed for 30, 60 and 90 mins. Samples were filtered and washed with water (100 ml), methanol/water (50/50, 100 ml) and methanol (100 ml) before being dried under vacuum overnight at 40 °C. LPS binding was assessed via the overnight incubation of 5 mg of each resin with 1 $\mu g ml^{-1}$ FITC labelled *E. coli* 0111:B4 LPS. Samples were filtered through Whatman 1 paper and the fluorescence of the filtrate analysed. All samples were prepared in triplicate.

c) Equilibrium time point assay

An assay was conducted to determine the time necessary for the equilibrium in the binding of LPS by polymyxin modified Merrifield to be attained. Polymyxin resin (5mg) was incubated with 1 $\mu g ml^{-1}$ FITC labelled *E. coli* 0111:B4 LPS. The samples were filtered through Whatman 1 paper and the fluorescence of the filtrate analysed at various time points (10 minutes, 30 minutes, 1 hour, 3 hours, 6 hours and 24 hours). All samples were prepared in triplicate.

d) Polymerisation

Resins (polymyxin (cyclic and linear)/iniferter modified) were suspended in 10 ml deionised water. *E. coli* 0111:B4 LPS (200 μg) was added and the mixture stirred gently for 4 hours at room temperature. LPS was omitted from the control non-imprinted resin. Following

incubation with LPS, acrylamide (175 mg) and methylene bisacrylamide (18.75 mg) were added to all resin samples and the pre-polymerisation mixtures thoroughly sparged with nitrogen. All samples were stirred gently (~100 rpm) whilst irradiated with UV light (100 mw/cm^2, 325 nm at a distance of 8 inches) for 60 minutes. The samples were then filtered and washed with water (150 ml) before being incubated in each of the following mixtures for 1 hour; sodium deoxycholate (1 %w/v), water and 50/50 water/methanol. Between each of the incubation steps the resin was filtered and washed with 150 ml water. A final wash with methanol (no incubation) was performed before the resins were dried under vacuum at 40 °C overnight. The ability of the resins to bind LPS was assessed through the incubation of 5 mg of resin with 1 μg FITC labelled *E. coli* 0111:B4 LPS in 1 ml water overnight at room temperature. Samples were subsequently filtered through Whatman 1 paper and the fluorescence of the filtrate analysed. All samples were prepared in triplicate.

3.3 Results and Discussion.

3.3.1 Synthesis of dansyl-polymyxin B

Dansyl polymyxin B, first synthesised in 1955 (59), has been employed over the last six decades as a probe for determining the affinity of various peptide antibiotics for lipopolysaccharide (55,60,61). The reaction between dansyl chloride and a primary or secondary amine group, of which polymyxin B has five, generates a stable, fluorescent sulfonamide group (Figure 3.3) exhibiting an emission wavelength of ~530nm. When bound to lipopolysaccharide a characteristic blue shift and a disproportionate increase in fluorescence intensity occurs, allowing affinities to be estimated.

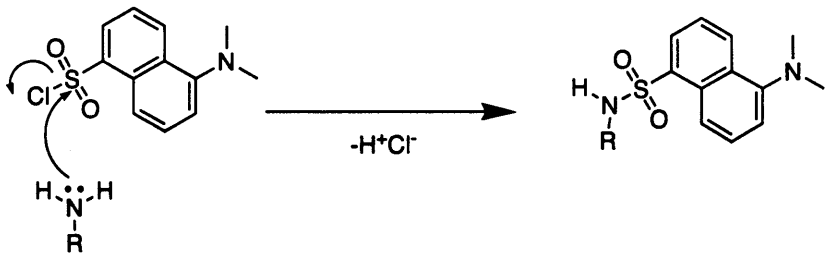

Figure 3.3: Reaction of dansyl chloride with a primary amine group. In this study the amine is provided by one of the five γ-amino groups of the L-diaminobutyric acid residues of polymyxin B

The conjugation of dansyl chloride to polymyxin B was successful using the method described in section 3.2.2. Figures 3.4 and 3.5 show the separation of the product (yellow) from the unreacted dansyl chloride (blue-green) on the Sephadex column and in the fractions collected.

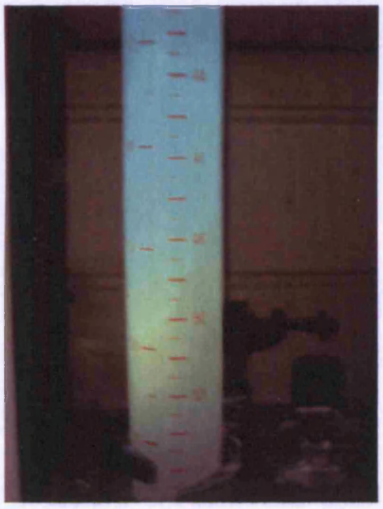

Figure 3.4: Column purification of dansyl – polymyxin B. As the reaction mixture elutes through the Sephadex column, dansyl-polymyxin B (yellow band) separates from the unreacted dansyl chloride (blue - green band)

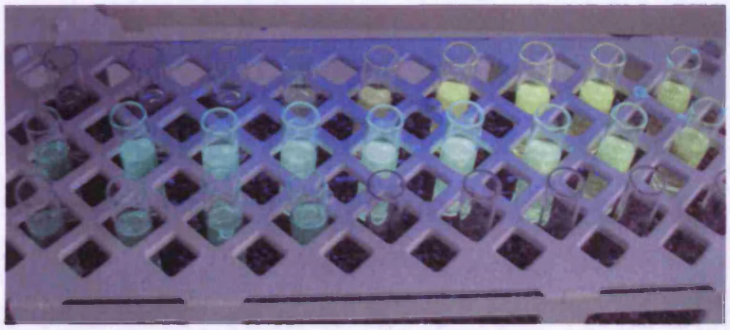

Figure 3.5: Fractions (~3ml volumes) are collected as they elute from the column. Illumination with a hand-held UV lamp allows the fractions to be separated into dansyl-polymyxin B and unreacted dansyl chloride.

Those fractions that contained dansyl-polymyxin B were subsequently extracted into half a volume of butanol to remove buffer salts and dried under vacuum at 40 °C. Following re-suspension in 5 mM, pH 7 HEPES buffer, the compound was analysed by fluorescence spectrometry (Figure 3.6) and NMR (Figure 3.7) to confirm structure.

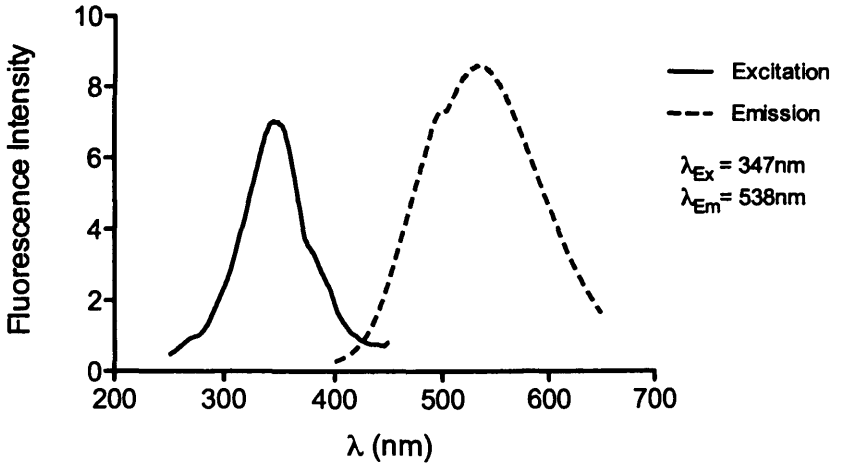

Figure 3.6: Fluorescence scan of dansyl-polymyxin B to determine excitation and emission wavelengths.

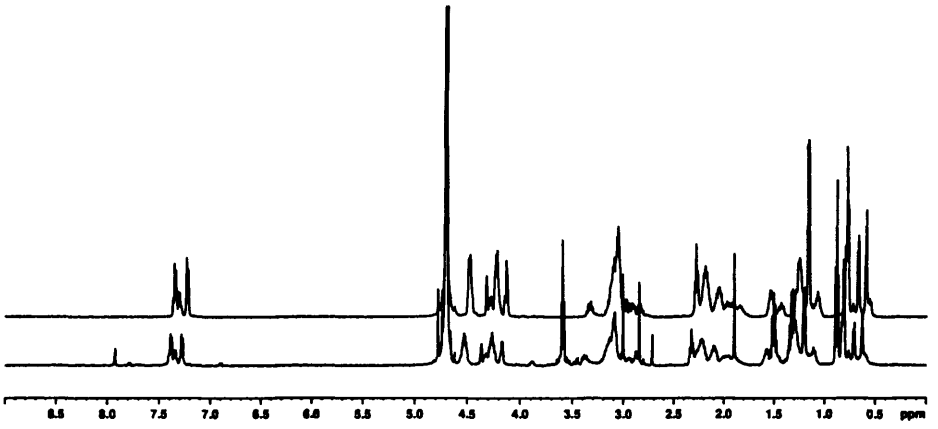

Figure 3.7: ^1H NMR spectra of polymyxin B (top) and dansyl-polymyxin B (bottom) in D_2O.

Several new signals are apparent in the dansyl polymyxin B sample (bottom) when compared to the underivitised polymyxin B (top) in the ^1H NMR spectra in Figure 3.7. The peaks observed between 3 and 4 ppm are indicative of the two methyl groups attached to the nitrogen

group of dansyl chloride, while those seen at ~8 ppm are due to the aromatic protons of the fluorophore.

A paper by Gmur *et al.* (62) used dansyl chloride to derivatise polymyxin B to allow analysis of the antibiotic in rat plasma samples by HPLC. They report the synthesis of the penta-dansyl derivative using a ten-fold excess of dansyl chloride in the reaction. In the reaction presented in this study, only a slight excess of the fluorophore is used (1 : 1.3 mol equivalents) and therefore one would expect the mono-dansyl product to predominate. It is important that not more than two of the free amine groups are derivitised since the number of amines/positive charges is important for efficient binding of LPS by polymyxin B (47,63).

3.3.2 *Quantification of dansyl-polymyxin B via dinitrophenylation assay*

Samples of the dansyl derivative of polymyxin B (5 µl and 20 µl) were analysed using the dinitrophenylation assay to determine the quantity of dansyl polymyxin synthesised. Dinitrophenylation of terminal amine groups of amino acids using 1-fluoro-2,4-dinitrobenzene was first suggested by Frederick Sanger in 1945 when he used the technique to determine the free amino groups in insulin (64) and although it has been largely superseded by other fluorescent molecules, peptidases and other amino acid sequencing techniques, it remains a useful tool for determining peptide structure. The basis of the assay relies on the dinitrophenylation of primary amine groups on peptides to form coloured *N*-substituted 2,4-dinitroanilines (Figure 3.8) that can be extracted into solvents such as cyclohexane and butanol, while the excess reagent is hydrolysed to 2,4-dinitrophenol (65).

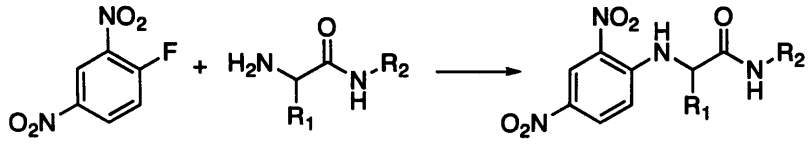

Figure 3.8: Schematic of the dinitrophenylation of amines to generate a N-substituted 2,4-dinitroaniline

A UV scan of dinitrophenylated polymyxin B (without dansyl tag) (Figure 3.9, left) was performed to determine the appropriate wavelength to measure the absorbance at and a standard curve was generated to ensure a linear response (Figure 3.9, right).

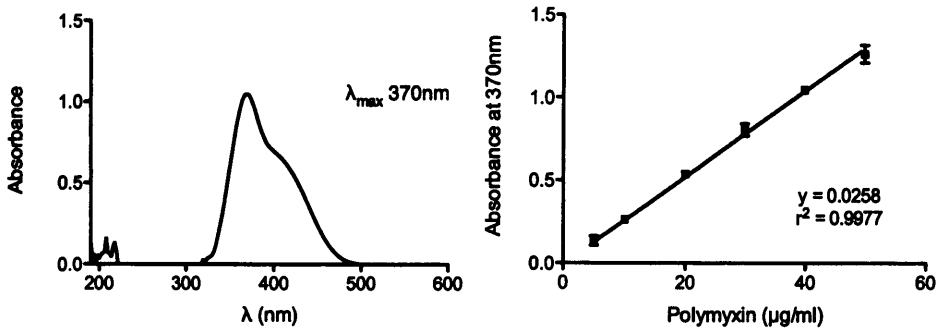

Figure 3.9: UV scan of dinitrophenylated polymyxin B (a) and example of calibration curve (b, dinitrophenylation of polymyxin without the dansyl tag) used to determine dansyl polymyxin concentrations following the reaction and column purification.

Since the calibration curve was produced using polymyxin B that had not been reacted with dansyl chloride, the response observed is based upon dinitrophenylation of five free amino groups. As dansyl polymyxin has one less free amine group (assuming the monodansyl species predominated), the value obtained for the samples of unknown concentration from the standard curve needed to be multiplied by 1.25 to obtain the true concentration of polymyxin. The results suggest a polymyxin concentration of ~ 3.3 $mgml^{-1}$, meaning that ~ 12 mg of

dansylated polymyxin is obtained following column purification of the reaction mixture.

3.3.3 Dansyl polymyxin binding assays

The method of Moore *et al.* (60) was used to determine the affinity of polymyxin B for *E. coli* 0111:B4 lipopolysaccharide in solution. Freshly synthesised dansyl polymyxin was incubated with a solution of lipopolysaccharide and an excitation/emission scan performed to determine the degree of shift in λ_{Em} upon binding of dansyl polymyxin to LPS. LPS alone did not display any fluorescence over the wavelength range used for the fluorescence scans. A shift in emission maxima from 538 nm to 490 nm when LPS is introduced to the dansyl polymyxin solution was observed, while the excitation wavelength (347 nm) remained constant. This blue shift in fluorescence is consistent with reported λ_{Em} (60) and is caused by the alteration of the immediate environment around the fluorophore upon binding of LPS to the labeled peptide.

The assay relies on determining the affinity of dansyl polymyxin B for LPS at sub-saturation concentrations through comparison with the fluorescence observed when all available binding sites on the peptide are saturated with LPS. To determine the appropriate concentrations for use in the assay, varying quantities of LPS were added to a 1 μM solution of dansyl polymyxin until the fluorescent response remained constant i.e. saturation of the peptide with LPS had been achieved. Figure 3.10 shows an initial disproportionate enhancement in fluorescence on the first addition of LPS (~3800 at 0 μgml^{-1} to ~10800 at 0.1 $ugml^{-1}$ LPS concentration) followed by a steady increase up to 10 μgml^{-1} LPS. Saturation is achieved between 10 and 100 μgml^{-1}. Assuming an average molecular weight of 10,000 for *E.coli* LPS (66), 10

μg is equivalent to 1 nmol thus suggesting an approximate 1:1 mole ratio of LPS to dansyl polymyxin.

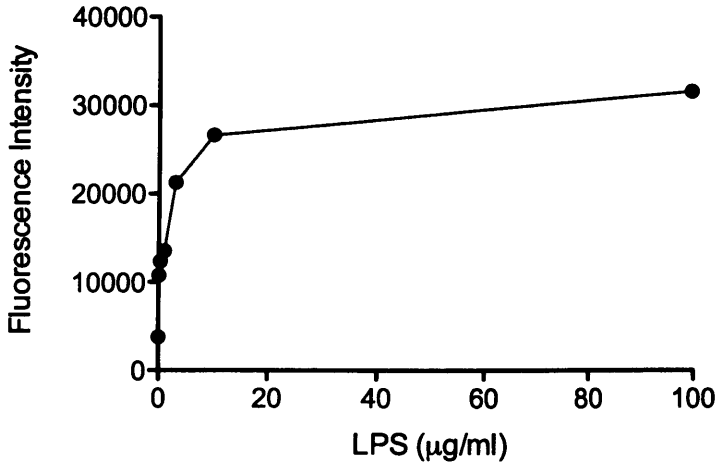

Figure 3.10 Saturation of dansyl polymyxin (1 μM) by E.coli 0111:B4 lipopolysaccharide. Saturation is achieved between 10 and 100 μg/ml LPS.

Based on the results of the saturation assay, 100 μgml^{-1} LPS was used as the 'super-saturated' concentration, to which the fluorescence response observed on addition of the 'sub-saturation' concentration (1 μgml^{-1}) was compared. A simple binding isotherm (Figure 3.11) and Scatchard plot (Figure 3.12) was generated for the interaction between LPS and dansyl polymyxin to allow for the calculation of K_d (0.21μM - 0.30μM). These affinities are in good agreement with those reported for polymyxin B sulfate and lipopolysaccharide (0.3 - 0.5μM (60)).

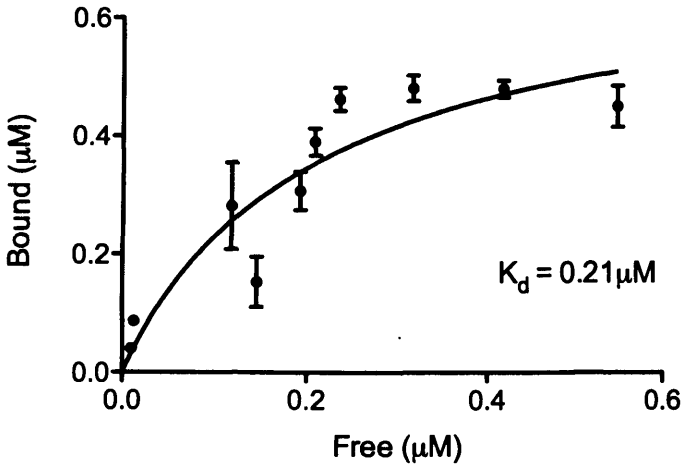

Figure 3.11: Binding isotherm of dansyl polymyxin and E. coli LPS. All samples were prepared in triplicate, error bars = +/- standard deviation.

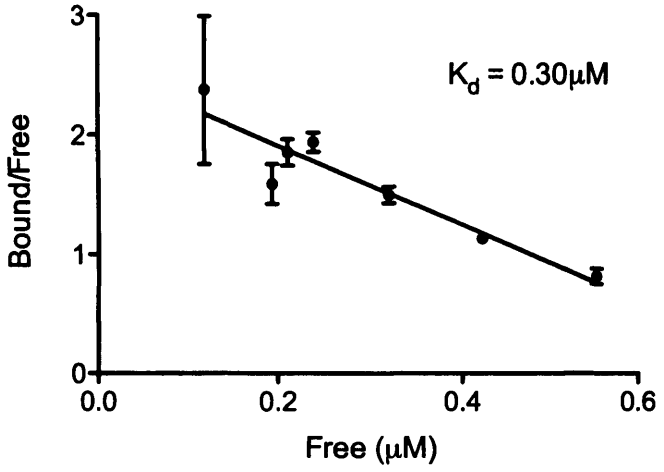

Figure 3.12: Scatchard plot of the above binding isotherm. All samples were prepared in triplicate, error bars = +/- standard deviation.

In the study conducted by Moore *et al.* (60), they report co-operativity in the binding of dansyl polymyxin B to LPS with approximately 4 moles of peptide bound per mole of LPS, an observation that was not evident

in the current study. It is important to note that the study by Moore *et al.* used lipopolysaccharide from *P. aeruginosa* and attributed the high ratio of dansyl polymyxin bound per mole of LPS to the relatively large degree of phosphorylation in this LPS strain (60). The LPS used in the current work was from the enterobacterial species *E. coli* 0111:B4 and although *P. aeruginosa* lipopolysaccharides have the same general molecular structure as enterobacterial LPS moieties, differences are observed in the composition of the acyl chains of lipid A and in the degree of phosphorylation (67). Other studies that have investigated the interaction of polymyxin with LPS from *Salmonella,* another species of the enterobacteriaceae family, have reported stoichiometric 1:1 binding of the peptide to the bacterial toxin (18,68-70). Lipopolysaccharides from *E.coli* and *Salmonella* species are structurally similar and therefore one would expect their interaction with antimicrobial peptides, such as polymyxin B, to also be similar. Given that the initial interaction between the peptide and the surface of the Gram-negative bacterium is facilitated by electrostatic interactions between the cationic *L*-2,4-diaminobutyric acid residues and the anionic core-lipid A region of LPS, it would seem unlikely that the binding of the peptide to LPS , thus altering the overall charge of the LPS moiety, would then positively influence the binding of an another peptide molecule.

3.3.4 Immobilisation of polymyxin on Merrifield resin

HPLC was used to estimate the amount of polymyxin attached to the surface of Merrifield resin through analysis of the filtrates and washes following reaction of polymyxin with the resins. A typical chromatogram is shown in Figure 3.13. As explained earlier, commercial polymyxin B sulfate is a mixture of several structurally related compounds, hence a number of peaks are observed in the chromatograph. For the purposes of determining an approximation of

the amount of peptide immobilised to the resin, the areas of two peaks (identified in Figure 3.13) were monitored. Based on a previous study by Orwa *et al.* (58) these peaks can most likely be attributed to polymyxin B_2 (peak 1, retention time: 22 minutes) and polymyxin B_1 (peak 2, retention time: 47 minutes). Typical calibrations for each peak are illustrated in Figure 3.14. Limits of quantitation were approximately 25 μM for peak 1 and 12.5 μM for peak 2, based on peak heights equal to 10 times the value of noise obtained from calibration curves.

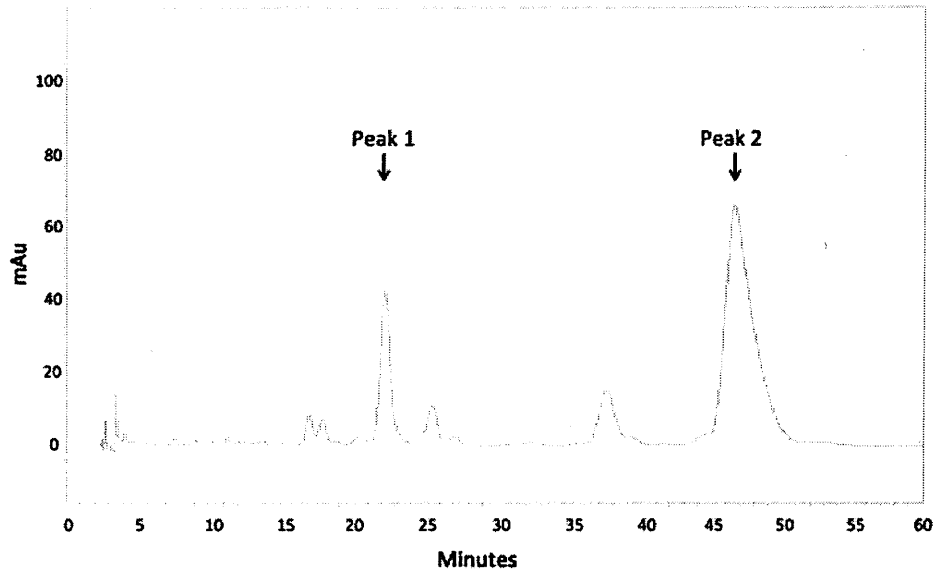

Figure 3.13: Typical chromatogram of polymyxin B sulfate (chromatography conditions: 22.25% acetonitrile : 50% sodium sulfate (0.7%w/v) : 5% phosphoric acid (6.8%v/v) : 22.75% deionised water mobile phase, 1mlmin^{-1} flow rate, UV detection at 215nm, 20μl injection volume).

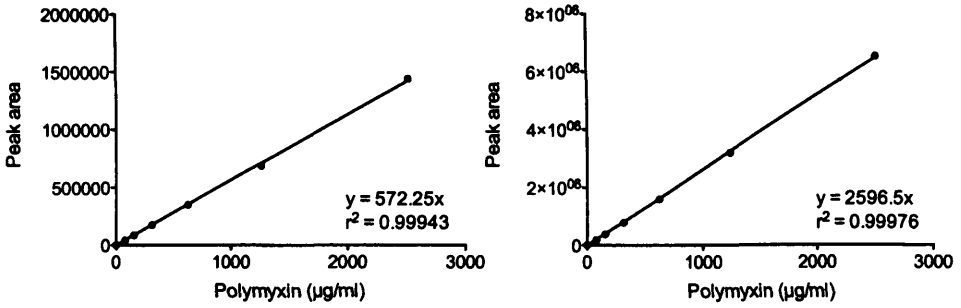

Figure 3.14: Typical calibrations obtained for peak 1 (polymyxin B2, left) and peak 2 (polymyxin B1, right)

The amounts immobilised on the surface of the resin are discussed in sections 3.3.4.1 and 3.3.4.2 b.

3.3.4.1 Immobilisation of polymyxin on Merrifield resin using an imidoester linker

Imidoesters, or imidates, are commonly employed as cross-linkers in the conjugation of biomacromolecules via amine groups. They display minimal cross-reactivity with other nucleophilic groups (71) but react efficiently with primary amines under mildly alkaline conditions (pH 8-9) to generate amidines (71,72). Dimethyl adipimidate (DMA), an example of a homobifunctional imidoester cross-linker, was employed in the current work to immobilise polymyxin B to the surface of amino-functionalised Merrifield resin. A schematic of the immobilisation process is provided in Figure 3.15.

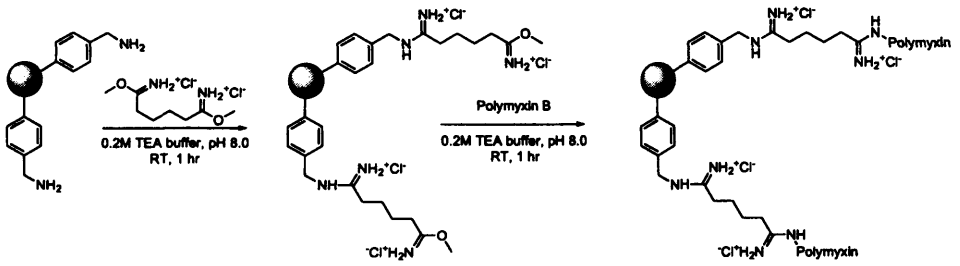

Figure 3.15: Immobilisation of polymyxin B on the surface of amino-functionalised Merrifield resin via dimethyl adipimidate.

The immobilisation of polymyxin was carried out in two steps as described in section 3.2.5.1 HPLC analysis of the filtrate plus the resin washes suggested approximately 54 μmoles (13.3 mg) of DMA was attached to the surface of 200 mg bifunctionalised Merrifield (ca. 0.2 mmol amine available for reaction) with approximately 16 μmoles (18.7 mg) of polymyxin being subsequently immobilised.

a) Binding assays

It was observed that the physicochemical characteristics of the resin were altered following immobilisation of the peptide. In particular the resin became dispersible in aqueous solvent systems, while the control resins (Merrifield and bi-functionalised resins) remained poorly wetable. As a consequence, the way in which binding assays were performed was optimised to allow efficient and complete separation of the bound and free fractions. Centrifugation was not feasible due to the hydrophobicity of the control resins, while filtration of the samples through nylon 0.2 μm membranes resulted in virtually complete loss of FITC-LPS from the calibration standards (<10% fluorescence remained following passage through the membrane) and variability between repeats was significant. As a result, resins were loaded into empty 1ml

SPE cartridges fitted with a 20 μm porosity polyethylene frit. A typical calibration curve for the assay is shown in Figure 3.16. In these experiments various concentrations of FITC-LPS were incubated in empty 1ml SPE cartridges overnight to account for adsorptive losses to the walls of the container. There was negligible loss of fluorescence following passage of the solution through the frit (< 10%) and variation between repeats was significantly reduced.

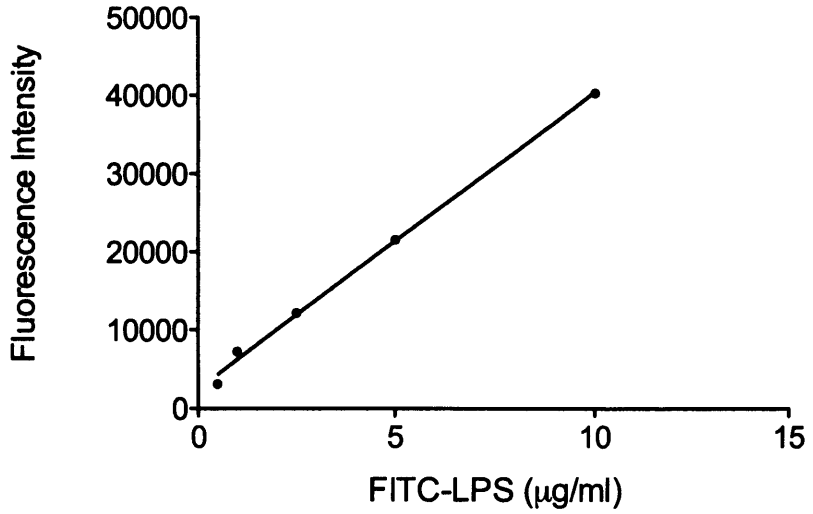

Figure 3.16: A typical calibration curve obtained following incubation of FITC-LPS in a 1ml SPE cartridge fitted with a 20 μm porosity polypropylene frit.

Polymyxin immobilised on solid supports has found use in the removal of LPS from formulations (Detoxi Gel, Thermo Scientific (73)) and in therapeutic apheresis of the septic patient (Toraymyxin, Spectral Diagnostics Ltd. (51)). In both applications, the LPS contaminated fluid is simply filtered through the polymyxin supports and therefore initial experiments with polymyxin modified Merrifield resin were performed under non-equilibrium conditions i.e. incubation time of less than 10

minutes. The results from these preliminary assays are illustrated in Figure 3.17.

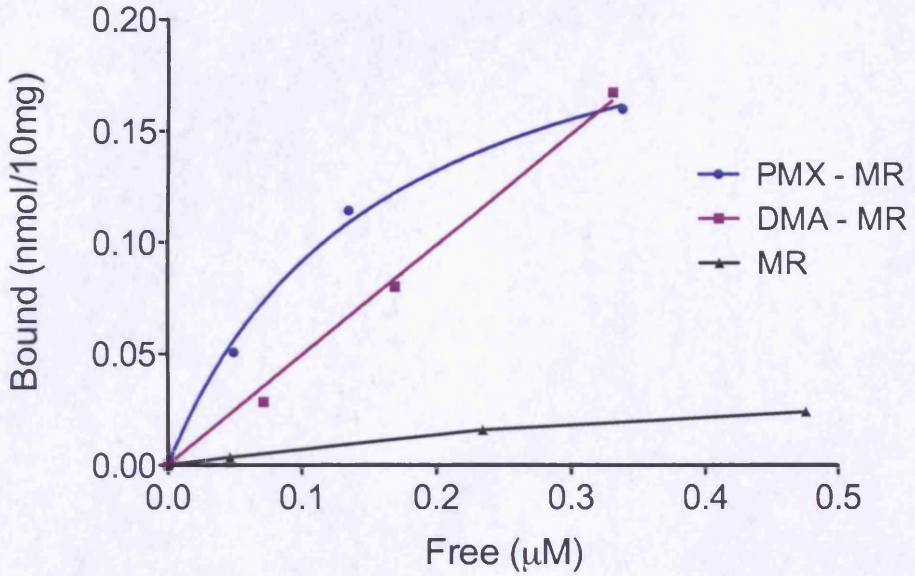

Figure 3.17: Amount of FITC labelled E.coli 0111:B4 LPS (nmol) bound to 10 mg of polymyxin modified resin (blue, PMX-MR), dimethyl adipimidate modified resin (purple, DMA-MR) and unmodified Merrifield resin (black, MR) under non-equilibrium conditions.

The immobilised polymyxin was shown to possess a K_d value similar to that observed with the dansyl polymyxin experiments (0.18μM (calculated from the binding isotherm in Figure 3.17) compared to 0.21μM, Figure 3.11), Non-specific binding to the control, dimethyl adipimidate modified resin was however high, whilst minimal binding to the original, unmodified, chloromethyl Merrifield resin was observed.

One of the advantages of dimethyl adipimidate as a homobifunctional linker in bioconjugation reactions is that it retains the overall charge of the macromolecule, as it possesses two positive charges (74). The

loading of the linker onto amine-modified Merrifield resin was estimated to be approximately 3.5 fold higher (mole per mole) than that of polymyxin, most likely as a consequence of the relative sizes of the two molecules and/or an increasing inefficiency of the reaction with time. Based on this estimated molar ratio, coupled with the fact that each molecule of dimethyl adipimidate posseses two positive charges and polymyxin has an overall charge of + 4 (assuming four of the five L-2,4-diaminobutyric acid amines remain unmodified), the relative density of charge on the surface of the resins would be approximately 7 : 4 (dimethyl adipimidate resin : polymyxin resin). It is therefore unsurprising that such high non-specific binding is observed with the dimethyl adipimidate modified resin, given that the initial interaction between the peptide and lipopolysaccharide is electrostatic in nature.

The performance of the resins was subsequently evaluated under equilibrium conditions, following the same conditions for the non-equilibrium binding assay except with an overnight (16 hour) incubation. Again non-specific binding to the dimethyl adipimidate resin was significant, however of more concern was the considerable variation in results between experiments. Analysis of fluorescence following overnight incubation on occasions suggested that the polymyxin-modified resin was performing as expected, while at other times an increase in fluorescence intensity in the polymyxin and dimethyl adipimidate resin samples was observed relative to the LPS standards and control Merrifield resin. An example of the raw data is given in Table 3.2.

Sample	Average fluorescence (n = 3)
Blank water	3290
FITC-LPS from E. coli 0111:B4 (1 μgml^{-1} standard)	24060
FITC-LPS from E. coli 0111:B4 (1 μgml^{-1}) plus Merrifield resin	22330
FITC-LPS from E. coli 0111:B4 (1 μgml^{-1}) plus dimethyl adipimidate modified Merrifield resin	51150
FITC-LPS from E. coli 0111:B4 (1 μgml^{-1}) plus polymyxin modified Merrifield resin	51420

Table 3.2: Raw fluorescence readings following overnight incubation of 10mg of resin with 1μgml^{-1} FITC LPS from E.coli 0111:B4. In the presence of dimethyl adipimidate and polymyxin modified resins, the fluorescence doubles compared to the LPS standard.

It was hypothesised that the linker and/or peptide was being desorbed from the surface of the resin and bringing about the change in results. Although the amidine bond formed via the reaction of an imidoester and an amine is stable in acidic and neutral environments, at alkaline pHs (> 10) it is susceptible to cleavage (71). As the incubation of the resin with LPS was carried out in an unbuffered system, it is possible that the pH of the system was changing during the course of the incubation, resulting in cleavage of the amidine bond with subsequent release of polymyxin and dimethyl adipimidate. Incubation of the resin in 0.2 M triethanolamine buffer (pH 8.2) however, yielded similar results.

b) Effect of free polymyxin and dimethyl adipimidate on the fluorescence of FITC-LPS

To further investigate the reason behind the increase in fluorescence, several studies were undertaken to assess the effect of dimethyl adipimidate and polymyxin on FITC-LPS in solution. Various concentrations of polymyxin and dimethyl adipimidate were incubated overnight with 1 μgml^{-1} FITC-LPS and the fluorescence of the solutions analysed the following day. The results presented in Figure 3.18 show a gradual increase in fluorescence relative to the control FITC-LPS solution (i.e. 0 μgml^{-1} polymyxin) as the peptide concentration increases. At 2.5 $mgml^{-1}$, the fluorescence of the solution is double that of the FITC-LPS standard. Polymyxin alone exhibited no significant fluorescence at the excitation and emission wavelengths employed in the study. It is possible that the increase in fluorescence was due to the formation of LPS micelles at higher polymyxin concentrations but this is highly speculative.

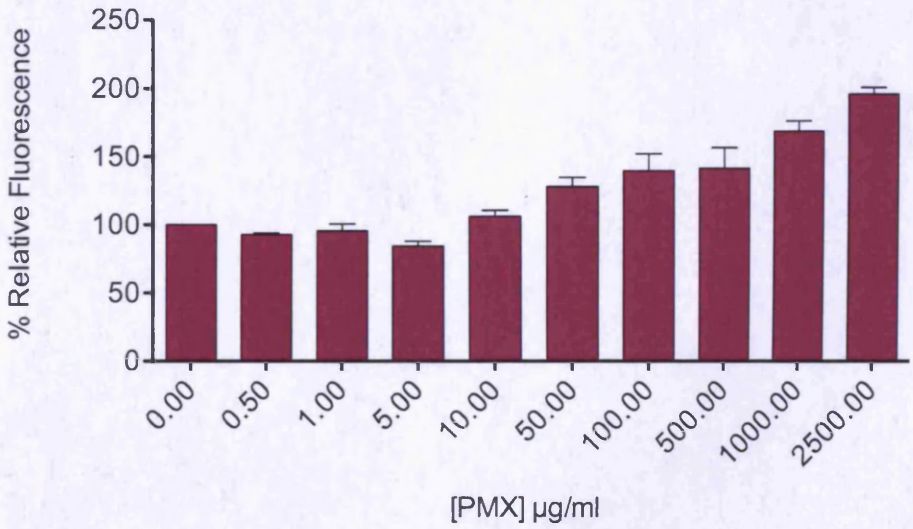

Figure 3.18: Effect of various concentrations of polymyxin (PMX) on the fluorescence of a 1 μgml^{-1} solution of FITC LPS. Fluorescence is plotted as percentage fluorescence relative to a FITC-LPS control solution (0 μgml^{-1} PMX).

A similar pattern was observed following the addition of dimethyl adipimidate up to a concentration of 7.5 μgml^{-1} (Figure 3.19). At concentrations greater than 10 μgml^{-1}, the fluorescence of the FITC-LPS solution returned to 85-105% of the standard solution before dropping to around 50% of the standard at concentrations above 1 $mgml^{-1}$. This reduction in fluorescence at higher concentrations was surprising and is not obviously explainable. As a consequence of these experiments, the reliability of previously performed binding assays was reconsidered; even when a decrease in fluorescence was observed with resin treated samples, it would be difficult to distinguish between a real 'binding event' and an artifactual decrease precipitated by the release of increased amounts of dimethyl adipimidate from the resin. In the light of these studies an alternative attachment strategy was sought.

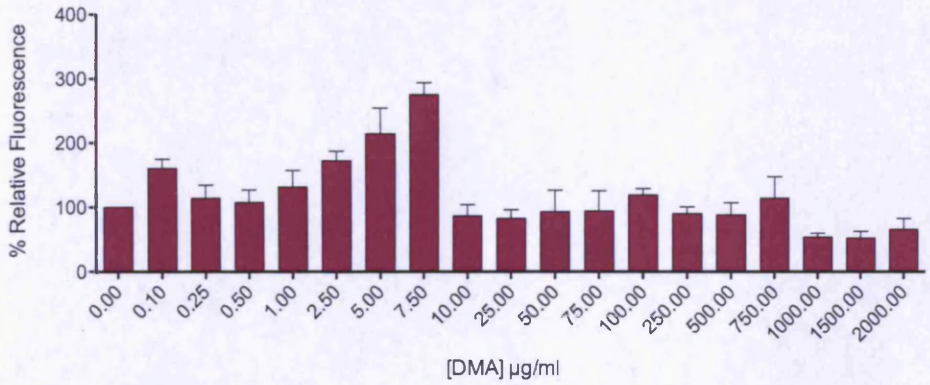

Figure 3.19: Effect of various concentration of dimethyl adipimidate (DMA) on the fluorescence of a 1 μgml^{-1} solution of FITC LPS. Fluorescence is plotted as percentage fluorescence relative to a FITC-LPS control solution (0 μgml^{-1} DMA). All samples were prepared in triplicate, error bars = +/- standard deviation.

It was anticipated that using a neutral cross-linker would help to reduce non-specific binding, as LPS, being anionic, relies on charge interactions as its initial mode of binding. Disuccinimidyl suberate (DSS, Figure 3.20) was investigated as an alternative homobifunctional

linker, however binding assays suggested no significant immobilisation of polymyxin on the surface of DSS-modified resin, with the resin performing similarly to controls. It is possible that the reaction conditions employed in attaching the linker resulted in hydrolysis of the NHS ester, regenerating the free carboxylate group, before polymyxin was introduced to the system. The DSS-resin did however display less non-specific binding than the DMA resin.

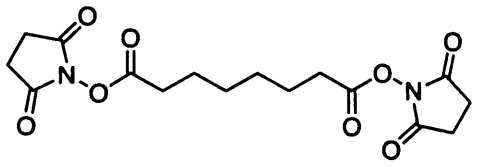

Figure 3.20: Disuccinimidyl suberate

3.3.4.2 Immobilisation of polymyxin on Merrifield resin using click chemistry

The synthesis of amino- and bi-functionalised Merrifield resins described in Chapter Two proceeds via an azide intermediate. The resin is therefore amenable to reaction with terminal alkyne groups in a Huisgen cycloaddition reaction ("click" chemistry) to generate a 1,4-disubstituted 1,2,3-triazole. Advantages of this approach are that the linking reaction proceeds efficiently at room temperatures in a range of solvents and without the need for pH control. Additionally, due to an absence of azide and alkyne groups in many biological systems the reaction proceeds with few side reactions and with high regio-selectivity when catalyzed with copper (57,75,76).

a) Synthesis of alkyne polymyxin

Glycidyl propargyl ether (Figure 3.21) was used to introduce alkyne functionality to polymyxin B. Glycidyl ethers are know to react efficiently with amines under a variety of conditions, however reactions occur at a greater rate when polar protic solvents are used (77,78). Glycidyl propargyl ether is not miscible in water and therefore the reaction was performed in methanol using a 1:1 molar ratio of glycidyl propargyl ether to polymyxin B. Carbon NMR was used to confirm formation of the product. Figure 3.22 compares the carbon NMR spectra of the product with polymyxin B. The three new signals at ~ 58 and 72 ppm (up) and at 76 ppm (down) in the top spectra represent the C, CH_2 and terminal CH groups of glycidyl propargyl ether respectively. Glycidyl propargyl ether is a liquid and therefore any excess is removed during the evaporation process; a clean carbon NMR was achieved following the rotary-evaporation of glycidyl propargyl ether in methanol.

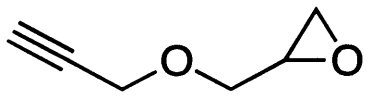

Figure 3.21: Glycidyl propargyl ether

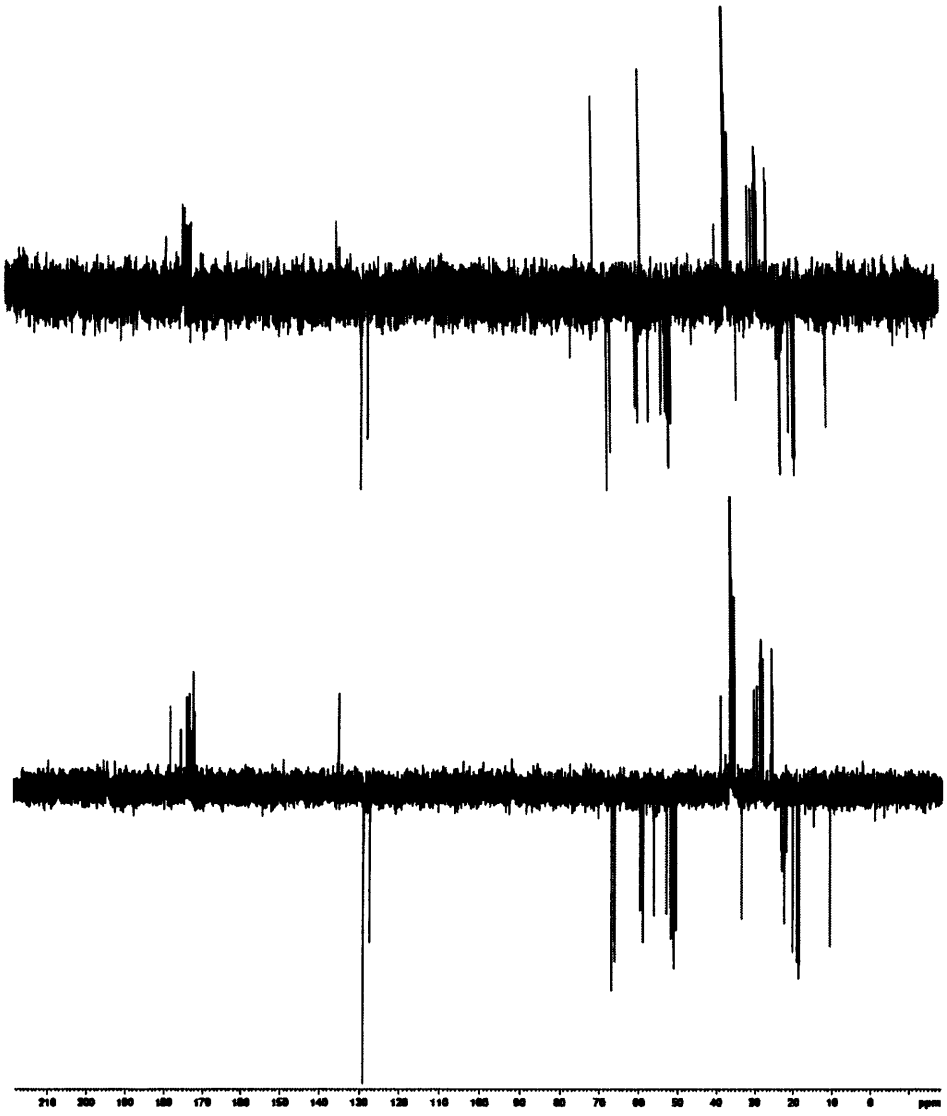

Figure 3.22: Carbon NMR of alkyne derivitised polymyxin (top) and polymyxin B (bottom) in D_2O. Extra signals at ~ 58 and 72 ppm (up) and at 76 ppm (down) in the top spectrum demonstrated the successful derivitisation of the peptide with an alkyne group.

b) Immobilisation of alkyne polymyxin on azide modified resin.

The original method of Sharpless was used to attach the alkyne derivitised peptide to the azido-polystyrene resin (57). Copper (II)

sulfate was employed as the copper catalyst and sodium ascorbate as the reducing agent to ensure a continuous supply of Cu(I) ions throughout the course of the reaction. A schematic illustrating the immobilisation of the peptide on the surface of azide/chloro bifunctionalised resin via click chemistry is given in Figure 3.23. A disadvantage of the "click" reaction is the use of copper as the catalyst that has the potential to contaminate the final product. Copper has been shown to be toxic to cells and it is therefore important that complete removal of any remaining copper is ensured if the system is to be used in any biological approaches.

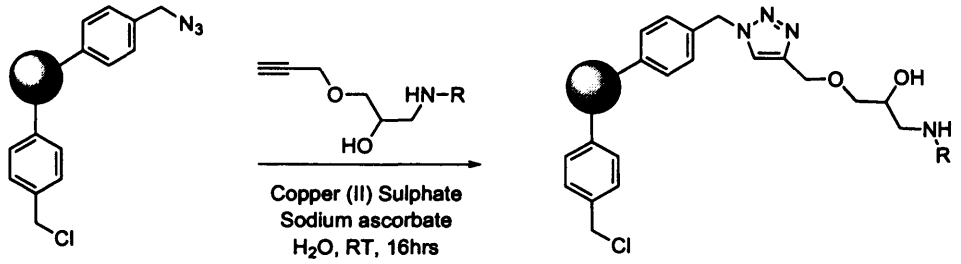

Figure 3.23: Generation of polymyxin modified resin via the attachment of alkyne derivitised polymyxin to azide/chloro bifunctional Merrifield resin. The NH group is donated by one of the L-2,4-diaminobutyric acid residues of polymyxin B while the R group represents the rest of the peptide moiety.

Following an overnight incubation at room temperature the resin again become dispersible in aqueous solvents, just as the imidoester linked polymyxin resin had done. HPLC analysis of the supernatant plus washes of the resin (4 x 20 ml deionised water) suggested that approximately 10 mg of polymyxin B was successfully immobilised per 100 mg of azide-modified (100%) Merrifield resin. The resin was also

analysed by FTIR. The spectrum given in Figure 3.24 demonstrates the presence of azide groups (characteristic signal at ~ 2100 cm^{-1}) and peptide (carbonyl stretch and amino stretch apparent at ~ 1650 cm^{-1} and 3200 - 3400 cm^{-1} respectively).

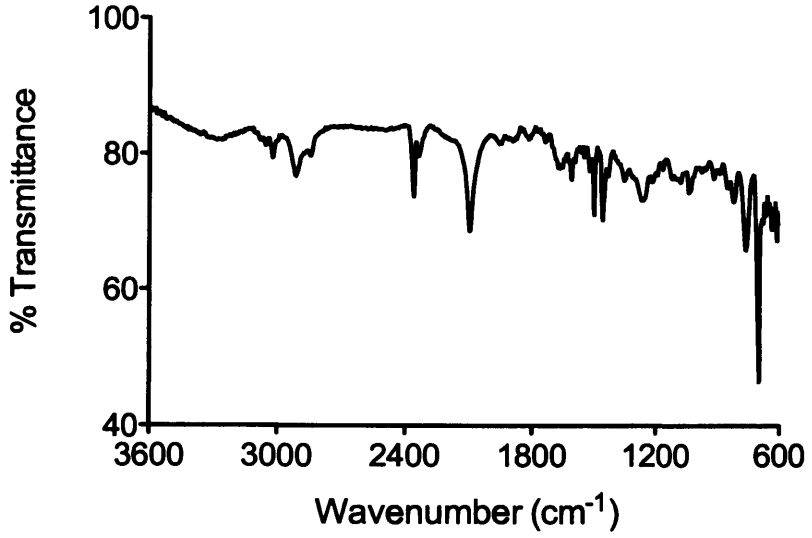

Figure 3.24: FTIR spectra of bifunctionalised azide/polymyxin Merrifield resin. The azide stretch is evident at ~2100cm^{-1} while small carbonyl and amino stretches from the peptide are also apparent at ~1650cm^{-1} and ~3200-3400cm^{-1} respectively.

An azide signal remains on the spectra due to the reaction conditions employed in the conversion of Merrifield resin to azidomethyl polystyrene and the subsequent attachment of polymyxin B. The synthesis of azide functionalised resin was performed in DMF (section 2.2.2) to swell the resin to ensure maximal conversion of chloro groups to azides, therefore the estimated loading of azide groups per gram of resin is ~ 2 mmol. The immobilisation of the peptide to azide modified resin was performed in water due to solubility constraints and therefore the large majority of the azide groups would not have been available for interaction due to the compacted nature of the resin in aqueous conditions. Only those azide groups exposed on the surface of the resin

would have been able to react with the alkyne group of the peptide. Additionally due to size of polymyxin B it was envisaged that not all of the surface confined azides would have participated in the reaction due to steric hindrance, therefore the decrease in azide number is most likely insignificant relative to the total loading of the resin.

c) Standard binding assay.

Using polymyxin-modified resins (generated from 100 % azide and bifunctionalised (i.e. ~ 50 % azide, 50 % chloro) resins) (section 3.2.5.2 b), standard binding assays were conducted to assess LPS binding performance. Figure 3.25 illustrates the binding isotherm obtained. K_d values for the two polymyxin-modified resins were calculated as 0.277μM (100% resin) and 0.220μM (50% resin) while the B_{max} values were 0.070 nmol/mg (700 ng/mg based on average molecular weight of 10,000 for *E. coli* 0111:B4) for the 100 % polymyxin modified resin and 0.055 nmol/mg (550 ng/mg) for the 50 % resin. The derivitisation of the peptide with alkyne functionality and the subsequent immobilisation on the resin's surface appear to have had little affect on the affinity of polymyxin for LPS. Importantly the problem of high non-specific binding, as observed with the dimethyl adipimidate resins, was not significant for the azide-alkyne click resin system.

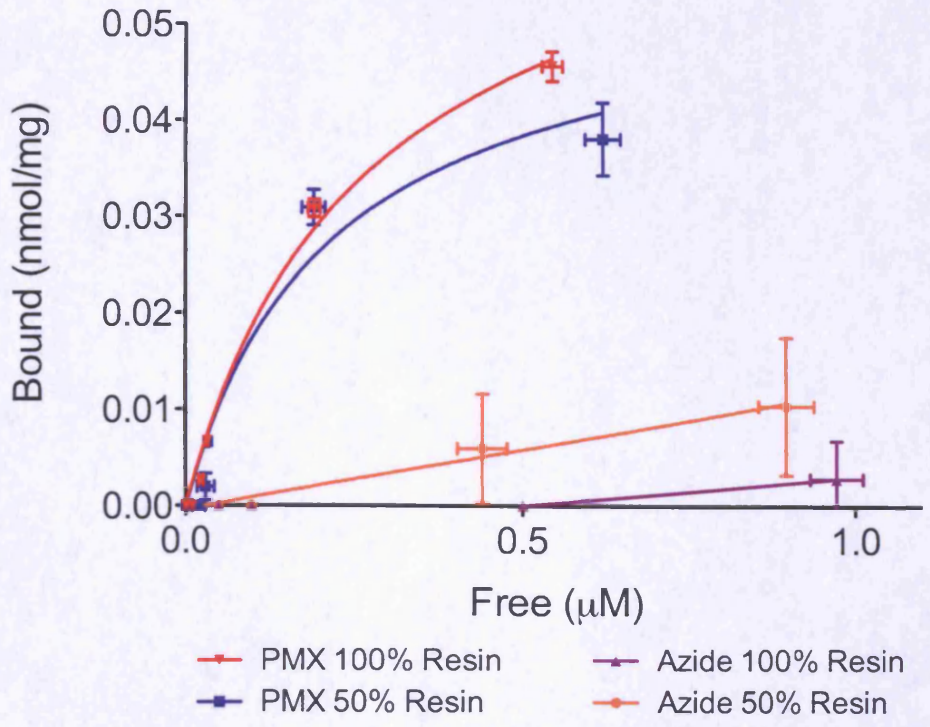

Figure 3.25: Standard binding isotherm for polymyxin modified resins, generated from 100% azide resin (red) and 50% azide/chloro bifunctional resin (blue). Azide resins (100% - purple and 50% - orange) were used as controls in the experiment. All samples were prepared in triplicate, error bars = +/- standard deviation.

d) Hot cold assay.

An assay was undertaken to determine the relative affinities of polymyxin for the unlabelled and labelled versions of *E. coli* 0111:B4 LPS. Assuming the labelling of LPS does not influence the binding of the molecule to the peptide, then a linear relationship should be observed as the ratio of hot (labelled) to cold (unlabelled) LPS is varied ("Line of equivalence" in Figure 3.26). The various ratios of hot : cold LPS are defined in Table 3.1. A minor deviation from the line of equivalence is observed in Figure 3.26 suggesting that polymyxin displays a slightly higher affinity for the FITC labelled LPS species.

Fluorescein isothiocyanate possesses a carboxylic acid group that would be deprotonated at physiological pH. Although the loading of FITC per milligram of LPS is relatively low (3.80 μg/mg) it is possible that the negative charge conferred by the deprotonated acid could influence the affinity of polymyxin for the LPS, given that electrostatic interactions play a significant role in the binding event.

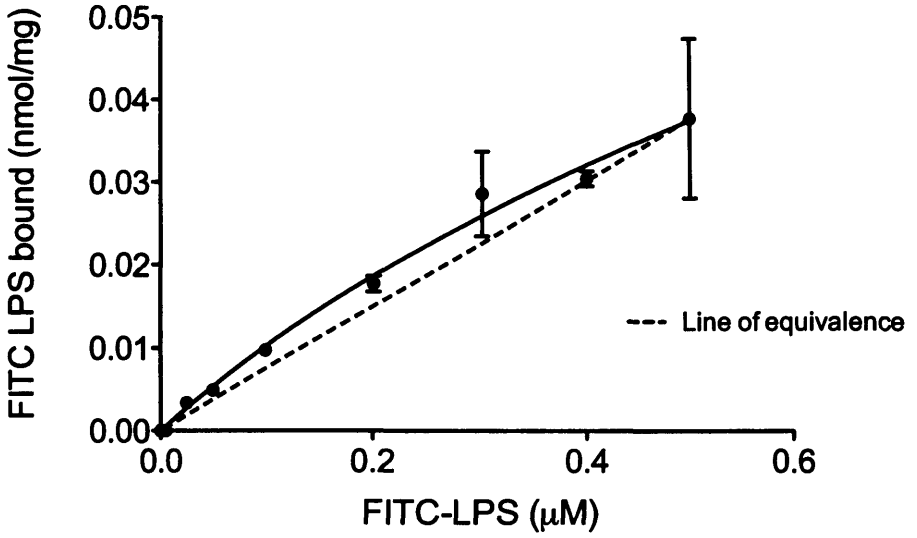

Figure 3.26: Amount of FITC-LPS bound by 1 mg of polymyxin modified resin at various ratios of labelled : unlabelled LPS from E. coli 0111: B4. The corresponding unlabelled LPS concentration for each FITC-LPS concentration is given in Table 3.1. All samples were prepared in triplicate, error bars = +/- standard deviation.

e) Selectivity assay.

To assess whether polymyxin B displays any selectivity between different bacterial LPS species, the system was challenged with a variety of competitors at a single concentration. The resin was incubated with 5 $\mu g ml^{-1}$ (0.5 μM) and 2.5 $\mu g ml^{-1}$ (2.5 μM) of FITC-LPS in the absence of any competitors to evaluate the resins binding capacity . Subsequently, polymyxin modified resin was incubated in a 1 ml solution containing 2.5 μg of FITC-LPS from *E. coli* 0111:B4 plus 2.5 μg

of a non-labelled LPS competitor overnight. Following filtration and analysis, the relative binding of the fluorescent analogue was determined. Binding of the competitor was estimated based on the assumption that 1 mg of the resin is capable of binding roughly 0.038 nmol of LPS from a 5 μgml^{-1} (0.5 μM) input; the amount of FITC-LPS bound in the presence of each competitor was deducted from this value to give an approximation of the amount of competitor LPS bound. The values obtained are presented in Figure 3.27.

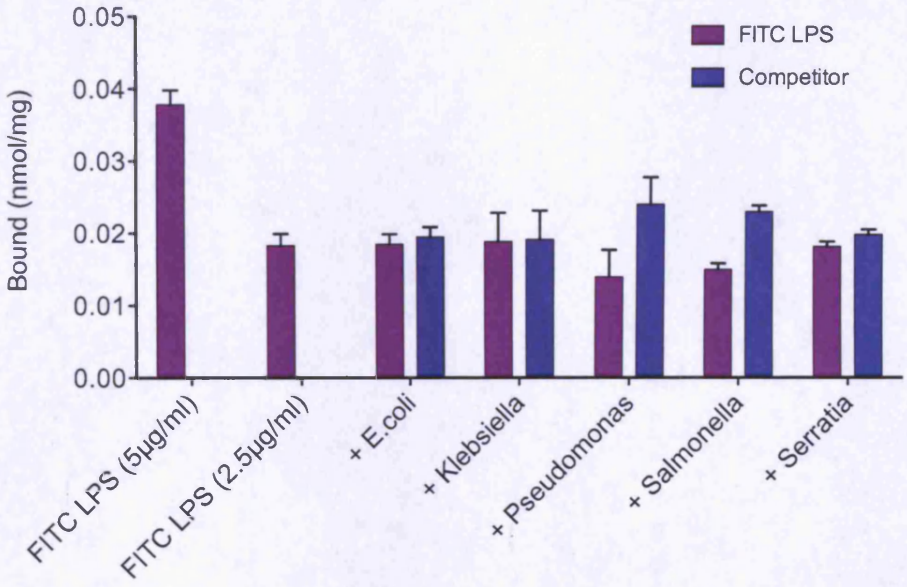

Figure 3.27: Amount of LPS bound by 5mg of resin over a range of competitor species. Uness otherwise stated, the total concentration of the system was 5μgml^{-1} (0.5μM) made up of 2.5μg of FITC-LPS from E. coli 0111:B4 and 2.5μg of an unlabelled competitor species. All samples were prepared in triplicate, error bars = +/- standard deviation.

It was assumed that all LPS species were equal in terms of molecular weight (thus assuming an equal mole ratio of FITC-LPS : competitor LPS) when this assay was performed. However, the molecular weight varies considerably not only between bacterial species but also at an

intra-species level depending on the stage of biosynthesis when LPS was extracted from the outer membrane. MALDI-MS analysis would enable an average molecular weight for each species to be determined, therefore allowing equal mole ratios to be employed in the assay giving a more realistic perspective of relative affinities for the different LPS species. This assay does however, serve as a comparator for later assays utilising the peptide-polymer system.

3.3.5 Linear analogue of polymyxin B.

When developing the original hypothesis presented in Chapter One, it was always envisaged that a linear peptide would be more amenable to our imprinting process than a cyclised species due to the difference in conformational flexibility. A cyclic peptide is already conformationally restrained and therefore our imprinting process is likely to have little effect on its overall structure. A linear peptide on the other hand, has a much greater degree of flexibility and it was anticipated that through interaction with its target during the polymerisation process, the peptide could be "locked" into a position that is more favourable for binding. Cyclic polymyxin B was simply used as a cost-effective and readily available peptide to provide proof-of-principle for our hypothesised system.

Over the past two to three decades, many groups have investigated ways in which to reduce the toxicity associated with polymyxin B, with studies focussed on removing the hydrophobic tail and final *L*-2,4-diaminobutyric acid residue to generate polymyxin B nonapeptide. Indeed, reduced toxicity is observed but antimicrobial activity is also severely compromised. The nonapeptide does however retain the anti-endotoxin properties of the parent peptide (39). Polymyxin B nonapeptide is also cyclised and therefore offers little to the current

study except for the observation that the fatty acid chain is not a prerequisite for efficient LPS binding. A linear, decapeptide, analogue of polymyxin B with an N-terminal alkyne group (4-pentynoic acid) was synthesised by colleagues at Tromsø University, Norway (sequence given in Figure 3.28).

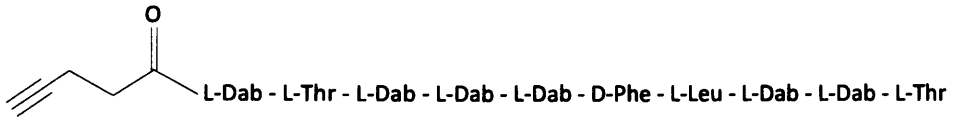

Figure 3.28: Sequence of the alkyne derivitised, linear analogue of polymyxin B.

The peptide was attached to bifunctionalised resin (~ 50/50 azide/chloro) as described in section 3.2.5.2 b and assays performed to assess its binding efficiency (3.2.5.2 c). The results obtained are presented in Figure 3.29 (blue line). The graph compares the linear polymyxin resin to the cyclic peptide modified resin (red line) and demonstrated a decrease in apparent K_d for the linear species (1.53 μM compared to ~ 0.22 μM (Figure 3.25)). There was a concomitant increase in B_{max} (approximately 2.5 fold) from 0.055 nmol/mg (cyclic) to 0.129 nmol/mg (linear) which was thought to be due to less steric hindrance conferred by the linear analogue compared to the cyclic species. The K_d value obtained for the linear decapeptide was not dissimilar to that reported for polymyxin nonapeptide (1.3 μM (33)).

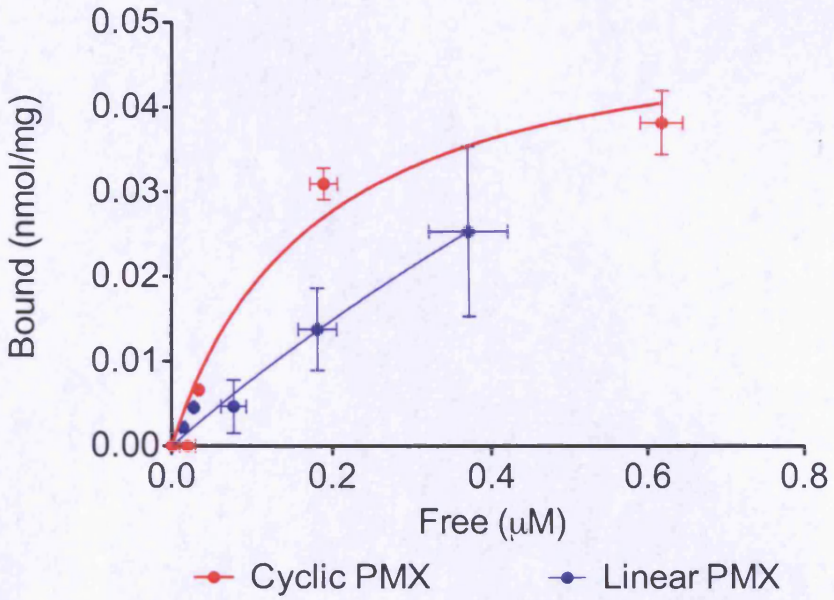

Figure 3.29: Binding isotherm for the linear analogue of polymyxin B (blue) and the natural peptide (red) immobilised on bifunctionalised (i.e. ~ 50/50 azide/chloro) resin. All samples were prepared in triplicate, error bars = +/- standard deviation.

3.3.6 Synthesis of the peptide-polymer hybrid.

a) Polymer growth assay

Using the hydrophilic iniferter modified resins developed through the work described in Chapter Two, a series of experiments were undertaken to determine the effect of polymerisation time on peptide performance. Polymyxin B (cyclic) was immobilised on resin to which the iniferter species, sodium dithiocarboxysarcosine, had previously been attached. Polymerisation was initiated and allowed to proceed for various periods of time. At each time point the binding efficiency of the resin was evaluated. The results are presented in Figure 3.30 and demonstrate a reduction in the ability of the peptide resin to bind LPS as the polymerisation time increased. A linear decrease in amount bound was observed between 0 and 60 minutes, after which a plateau is

achieved. This suggested that following polymerisation for 60 minutes the polymer had overgrown the peptide, thus hindering the access of LPS to the binding sites. As a result of this assay, all imprinted resins (and non-imprinted controls) were polymerised for 60 minutes.

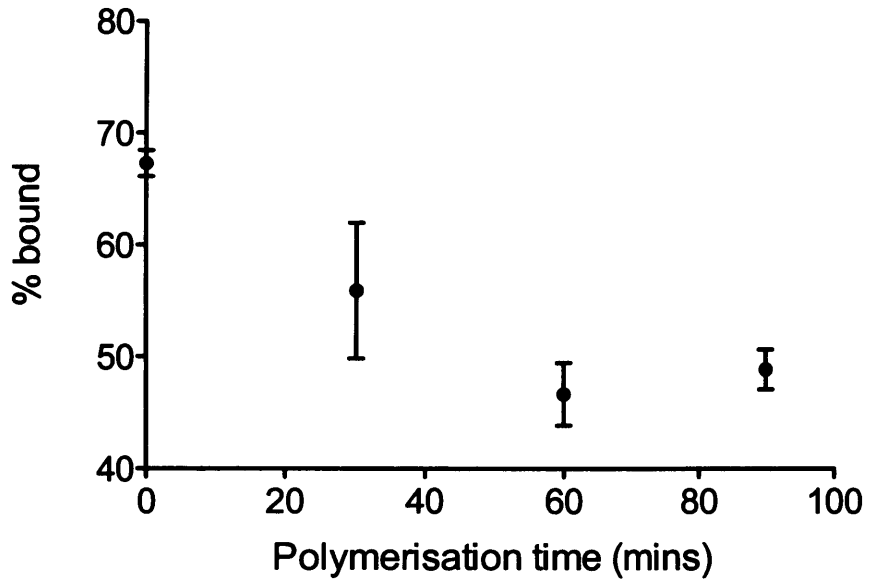

Figure 3.30: Percentage of FITC-LPS bound from a 1μgml^{-1} input by 5mg of PMX/iniferter resin following various polymerisation periods in acrylamide/methylene bisacrylamide solution. All samples were prepared in triplicate, error bars = +/- standard deviation.

b) Determining saturation concentration of LPS for imprinting experiments.

During the imprinting process it is vital that sufficient LPS is added to the system to ensure that a high proportion of the surface immobilised polymyxin is complexed with template, so that the access is not hindered through the growth of polymer over the peptide. The concentration of LPS required to saturate the resin was calculated from extrapolation of the isotherm for 100% polymyxin resin (red line, Figure 3.25) using the equation of the curve ($Y = B_{max}*X/(K_d + X)$) and the

generation of a line of conservation of ligand (dashed line in Figure 3.31). The line of conservation of ligand was generated based on a hypothetical experiment where 10 ml of a 2 μM LPS solution was incubated with 1 mg (Figure 3.31 a) or 50 mg (Figure 3.31 b) of polymyxin modified resin. The *x* intercept is a theoretical point where *all* ligand is free and therefore equals the starting ligand concentration. The *y* intercept is a theoretical point when *all* ligand is bound and is therefore equal to the total amount of ligand in the system divided by the mass (mg) of polymer used in the experiment. The equilibrium point is where the line of ligand conservation intercepts the binding isotherm. This intercept should be through the plateau region of the isotherm to ensure maximum occupancy of the binding sites.

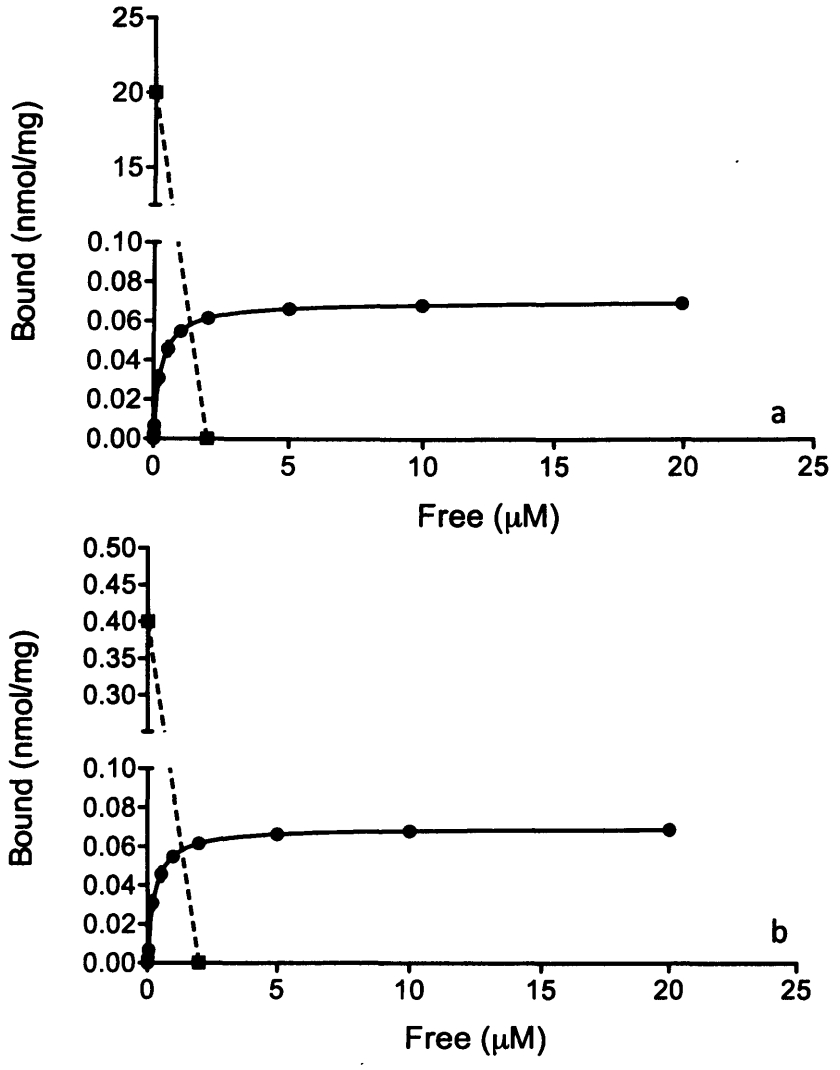

Figure 3.31: Binding isotherm used to calculate the amount of LPS to incubate with polymyxin/iniferter resin prior to polymerisation to ensure complete saturation of binding sites. The line of conservation of ligand (dashed line) intercepts the binding isotherm near the B_{max} and was calculated based on an input concentration of 10 ml of a 2.0 μM solution of E.coli 0111:B4 LPS with 1mg (a) or 50 mg (b) of polymyxin modified resin.

As is evident from Figure 3.31 b, incubation of 50 mg of resin with a 2 μM solution of LPS results in the line of conservation of ligand intercepting the isotherm near to the plateau/B_{max} region. A

concentration of 2 μM (20 μgml^{-1} LPS) and a mass of resin of 50mg was a compromise to ensure sufficient resin to conduct the relevant assays while trying to maintain the concentration at or below the critical micelle concentration (CMC). The CMC value will vary depending on the species of LPS but an estimated value for *E coli* 0111:B4 LPS is 22 μgml^{-1} (79). Above this concentration, LPS will mainly exist in an aggregated form. Although polymyxin B is able to recognise and bind to LPS aggregates and whole bacterial cells, the previous experiments in the current study, including the equilibrium time point assay (section 3.3.6 c), have investigated binding activity up to a concentration of 10 μgml^{-1}. At and below this concentration, LPS would most likely have existed in a mainly monomeric form, which may impact on time taken to reach equilibrium. At a concentration of 20 μgml^{-1}, it is likely that some of the LPS moieties will have aggregated, however it is also likely that a proportion of monomeric LPS will remain. It may be important for future applications of the synthetic receptor that it is capable of recognising LPS in a variety of aggregated forms. From a clinical perspective typical systemic concentrations of LPS are in the high picogram/low microgram per millilitre but a multitude of forms exist including free LPS, intact bacterial cells and membrane blebs.

c) Equilibrium time point assay.

An assay was performed to allow estimation of the time needed for the binding of LPS to polymyxin-modified resin to reach equilibrium. The results presented in Figure 3.32 suggested that equilibrium was attained between 3 and 6 hours; continuing the incubation of LPS with peptide resin for more than 6 hours showed little increase in the overall amount bound. Based on this assay, all resins to be used in the imprinting strategy were pre-incubated with LPS for 4 hours to ensure maximal occupancy of binding sites prior to polymerisation.

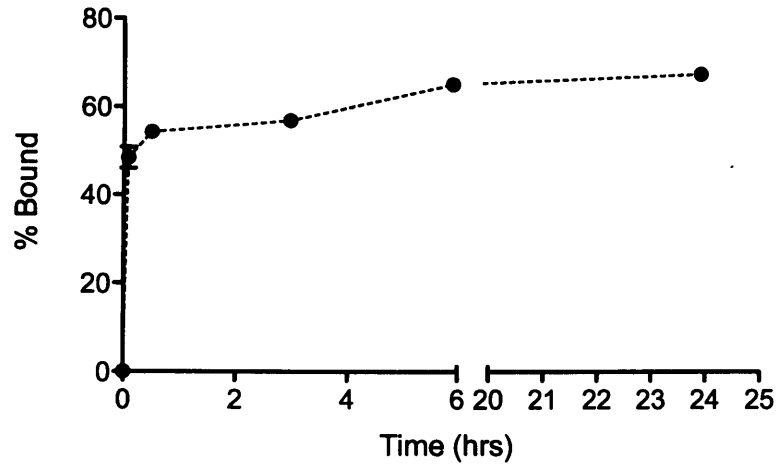

Figure 3.32: Percentage of a 1μgml^{-1} FITC LPS input bound as a function of time. All samples consisted of 5mg 100% polymyxin modified resin and were prepared in triplicate, error bars = +/- standard deviation.

d) Evaluation of the peptide-polymer hybrid system.

Following polymerisation of the cyclic and linear peptide/iniferter resins, binding assays were performed to evaluate the effect of imprinting on the peptide - polymer hybrid systems. The results are presented in Figure 3.33. The peptide modified resins prior to polymerisation bound ~ 70 % and 50% (cyclic (PMX resin) and linear (Linear resin) polymyxin) of a 1 μgml^{-1} FITC LPS solution. Following polymerisation however, binding efficiency was reduced to ~ 45 % (PMX MIP) and 24 % (Linear MIP). A small imprinting effect was observed, with the non-imprinted counterparts binding ~ 36 % (PMX NIP) and 19 % (Linear NIP). It is important to note that although the amount bound to the peptide resins prior to polymerisation was greater than that observed for their polymerised counterparts, this does not necessarily indicate reduced affinity of the hybrid systems compared to the simple peptide resins. Following polymerisation it would be expected that the number of sites containing accessible peptides would be lower than the number of accessible peptides available for binding

pre-polymerisation. This would manifest itself as a reduction in B_{max}. The observed variations in amount of ligand bound in the current assay are therefore likely to be a function of changes in B_{max} and/or K_d. The reasons for the apparent altered binding efficiencies could be deconvoluted through the construction of a full isotherm.

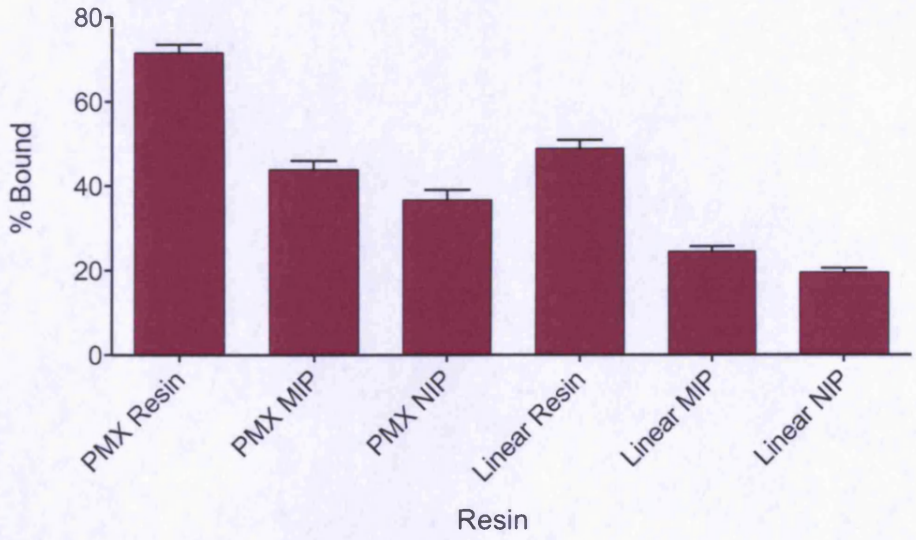

Figure 3.33: Evaluation of the binding efficiency of cyclic and linear polymyxin imprinted resins prepared from "click" immobilised resins. All samples contained 5 mg of the respective resin plus 1 μg of FITC – labelled E. coli 0111:B4 LPS in 1 ml of water. All samples were prepared in triplicate, error bars = +/- standard deviation. (PMX resin = polymyxin modified resin prior to polymerisation, PMX MIP = PMX resin that has been polymerised in the presence of E. coli 0111:B4 LPS, PMX NIP = PMX resin that has been polymerised without LPS, Linear resin = resin modified with the linear decapeptide form of polymyxin B, Linear MIP and Linear NIP are the same as PMX MIP and PMX NIP but with the linear analogue of polymyxin).

The results in Figure 3.33 were somewhat disappointing compared to those obtained during the first attempt at imprinting using the resins employing dimethyl adipimidate as the linker. In that assay, a clear imprinting result was evident (Figure 3.34). The amount of LPS bound

to the polymyxin MIP (~ 42 %, PMX MIP) was significantly greater than that bound to its non-imprinted antipode (~ 18 %, PMX NIP). Encouragingly, the polymyxin MIP also appeared to bind slightly more LPS (~ 6 %) than the conventional polymyxin resin (MR - PMX). The polymyxin resin appears to bind less than in the current assay due to different resin masses and incubation concentration of FITC LPS (10 mg resin and 10 $\mu g ml^{-1}$ LPS compared to 5 mg and 1 $\mu g ml^{-1}$ in the current assay).

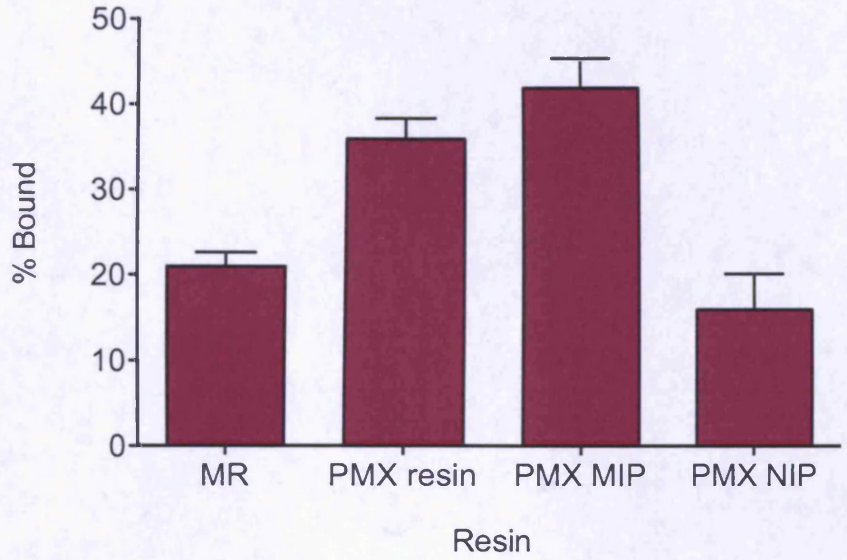

Figure 3.34 : Evaluation of the binding efficiency of cyclic polymyxin imprinted resins prepared from dimethyl adipimidate linked resins. All samples contained 10 mg of the respective resin plus 10 μg of FITC – labelled E. coli 0111:B4 LPS in 1 ml of water. All samples were prepared in triplicate, error bars = +/- standard deviation. (MR = standard Merrifield resin, PMX resin = polymyxin modified resin prior to polymerisation, PMX MIP = PMX resin that has been polymerised in the presence of E. coli 0111:B4 LPS, PMX NIP = PMX resin that has been polymerised without LPS).

The main difference between these two systems, other than the attachment chemistry, is the way in which the iniferter species were

introduced. The iniferter was attached to resin used in the click approach in a swollen state and therefore the relative densities of iniferter to peptide most likely differ considerably to that displayed by the dimethyl adipimidate linked resin. Additionally, since the resin possessing more iniferter groups is likely to be more hydrophilic, the degree of swelling observed in aqueous solutions may also be greater. This could possibly allow greater access of monomers to the interior of the resin resulting in more significant polymerisation observed over the same time period. Whether this is the reason for the difference in behaviour between the two assays remains to be elucidated.

3.4 Conclusion

Polymyxin resins, produced via the immobilisation of alkyne derivitised polymyxin B on the surface of azidomethyl polystyrene via "click" chemistry, were able to efficiently bind LPS from aqueous solutions with an apparent K_d of ~ 0.2 μM. Although the development of the peptide - polymer hybrid system using these resins appeared somewhat unsuccessful, whether the reduction of binding observed is due to changes in the B_{max} or of the K_d remains to be elucidated. The assay performed with the polymerisation samples produced using resin displaying polymyxin immobilised via a dimethyl adipimidate linker, suggest that the hypothesised approach is feasible but that optimisation of a number of variables is needed before definitive results can be obtained.

3.5 References

1. Boucher HW, Talbot GH, Bradley JS, Edwards JE, Gilbert D, Rice LB, et al. Bad bugs, no drugs: no ESKAPE! An update from the Infectious Diseases Society of America. Clin. Infect. Dis. 2009 Jan 1;48(1):1-12.

2. Velkov T, Thompson PE, Nation RL, Li J. Structure--activity relationships of polymyxin antibiotics. J. Med. Chem. 2010 Mar 11;53(5):1898-1916.

3. Arias CA, Murray BE. Antibiotic-resistant bugs in the 21st century--a clinical super-challenge. N. Engl. J. Med. 2009 Jan 29;360(5):439-443.

4. Zavascki AP, Goldani LZ, Li J, Nation RL. Polymyxin B for the treatment of multidrug-resistant pathogens: a critical review. J. Antimicrob. Chemother. 2007 Dec 1;60(6):1206-1215.

5. Landman D, Georgescu C, Martin DA, Quale J. Polymyxins Revisited. Clin. Microbiol. Rev. 2008 Jul 1;21(3):449-465.

6. Falagas ME, Rafailidis PI, Matthaiou DK. Resistance to polymyxins: Mechanisms, frequency and treatment options. Drug Resistance Updates. August;13(4-5):132-138.

7. Kwa AL, Tam VH, Falagas ME. Polymyxins: a review of the current status including recent developments. Ann. Acad. Med. Singap. 2008 Oct;37(10):870-883.

8. Evans M, Feola D, Rapp R. Polymyxin B sulfate and colistin: old antibiotics for emerging multiresistant gram-negative bacteria. Ann Pharmacother. 1999 Sep 1;33(9):960-967.

9. Vogler K, Studer RO. The chemistry of the polymyxin antibiotics. Experientia. 1966 Jun;22(6):345-354.

10. Orwa JA, Govaerts C, Busson R, Roets E, Van Schepdael A, Hoogmartens J. Isolation and structural characterization of polymyxin B components. Journal of Chromatography A. 2001 Apr 6;912(2):369-373.

11. Falagas ME, Kasiakou SK. Colistin: the revival of polymyxins for the management of multidrug-resistant gram-negative bacterial infections. Clin. Infect. Dis. 2005 May 1;40(9):1333-1341.

12. David SA, Balasubramanian KA, Mathan VI, Balaram P. Analysis of the binding of polymyxin B to endotoxic lipid A and core glycolipid using a fluorescent displacement probe. Biochimica et Biophysica Acta (BBA) - Lipids and Lipid Metabolism. 1992 Dec 2;1165(2):147-152.

13. Thomas CJ, Gangadhar BP, Surolia N, Surolia A. Kinetics and Mechanism of the Recognition of Endotoxin by Polymyxin B. Journal of the American Chemical Society. 1998 Dec 1;120(48):12428-12434.

14. Pristovsek P, Kidric J. Solution structure of polymyxins B and E and effect of binding to lipopolysaccharide: an NMR and molecular modeling study. J. Med. Chem. 1999 Nov 4;42(22):4604-4613.

15. Mares J, Kumaran S, Gobbo M, Zerbe O. Interactions of Lipopolysaccharide and Polymyxin Studied by NMR Spectroscopy. Journal of Biological Chemistry. 2009 Apr 24;284(17):11498 -11506.

16. Thomas CJ, Surolia N, Surolia A. Kinetic and Thermodynamic Analysis of the Interactions of 23-Residue Peptides with Endotoxin. Journal of Biological Chemistry. 2001;276(38):35701-35706.

17. Thomas CJ, Surolia A. Kinetics of the interaction of endotoxin with polymyxin B and its analogs: a surface plasmon resonance analysis. FEBS Letters. 1999 Feb 26;445(2-3):420-424.

18. Srimal S, Surolia N, Balasubramanian S, Surolia A. Titration calorimetric studies to elucidate the specificity of the interactions of polymyxin B with lipopoiysaccharides and lipid A. Biochemical Journal. 1996;315(2):679-686.

19. Brandenburg K, David A, Howe J, Koch MHJ, Andrä J, Garidel P. Temperature Dependence of the Binding of Endotoxins to the Polycationic Peptides Polymyxin B and Its Nonapeptide. Biophysical Journal. 2005 Mar;88(3):1845-1858.

20. Daugelavicius R, Bakiene E, Bamford DH. Stages of Polymyxin B Interaction with the Escherichia coli Cell Envelope. Antimicrob. Agents Chemother. 2000 Nov 1;44(11):2969-2978.

21. Rifkind D. Studies on the interaction between endotoxin and polymyxin B. J. Infect. Dis. 1967 Dec;117(5):433-438.

22. Storm DR, Rosenthal KS, Swanson PE. Polymyxin and Related Peptide Antibiotics. Annu. Rev. Biochem. 1977 Jul;46(1):723-763.

23. Tsubery H, Ofek I, Cohen S, Fridkin M. Structure–Function Studies of Polymyxin B Nonapeptide: Implications to Sensitization of Gram-Negative Bacteria#. Journal of Medicinal Chemistry. 2000;43(16):3085-3092.

24. Hancock REW, Bell A. Antibiotic uptake into gram-negative bacteria. Eur. J. Clin. Microbiol. Infect. Dis. 1988 Dec;7(6):713-720.

25. Hancock REW, Chapple DS. Peptide Antibiotics. Antimicrob Agents Chemother. 1999 Jun;43(6):1317-1323.

26. Vaara M, Vaara T. Outer membrane permeability barrier disruption by polymyxin in polymyxin-susceptible and -resistant Salmonella typhimurium. Antimicrob. Agents Chemother. 1981 Apr;19(4):578-583.

27. Warren HS, Kania SA, Siber GR. Binding and neutralization of bacterial lipopolysaccharide by colistin nonapeptide. Antimicrob. Agents Chemother. 1985 Jul 1;28(1):107-112.

28. Cajal Y, Rogers J, Berg OG, Jain MK. Intermembrane Molecular Contacts by Polymyxin B Mediate Exchange of Phospholipids†. Biochemistry. 1996 Jan 1;35(1):299-308.

29. Cajal Y, Ghanta J, Easwaran K, Surolia A, Jain MK. Specificity for the Exchange of Phospholipids Through Polymyxin B Mediated Intermembrane Molecular Contacts†. Biochemistry. 1996 Jan 1;35(18):5684-5695.

30. Clausell A, Rabanal F, Garcia-Subirats M, Asunción Alsina M, Cajal Y. Membrane association and contact formation by a synthetic analogue of polymyxin B and its fluorescent derivatives. J Phys Chem B. 2006 Mar 9;110(9):4465-4471.

31. Vaara M. Agents that increase the permeability of the outer membrane. Microbiol Rev. 1992 Sep;56(3):395-411.

32. Vaara M, Viljanen P, Vaara T, Makela P. An outer membrane-disorganizing peptide PMBN sensitizes E. coli strains to serum bactericidal action. The Journal of Immunology. 1984 May 1;132(5):2582 -2589.

33. Vaara M, Viljanen P. Binding of polymyxin B nonapeptide to gram-negative bacteria. Antimicrob Agents Chemother. 1985 Apr;27(4):548-554.

34. Clausell A, Rabanal F, Garcia-Subirats M, Asunción A, Cajal Y. Synthesis and membrane action of polymyxin B analogues. Luminescence. 2005;20(3):117-123.

35. Rose F, Heuer KU, Sibelius U, Hombach-Klonisch S, Kiss L, Seeger W, et al. Targeting Lipopolysaccharides by the Nontoxic Polymyxin B Nonapeptide Sensitizes Resistant Escherichia coli to the Bactericidal Effect of Human Neutrophils. Journal of Infectious Diseases. 2000 Jul 1;182(1):191 -199.

36. Vaara M. The outer membrane permeability-increasing action of linear analogues of polymyxin B nonapeptide. Drugs under experimental and clinical research. 1991;17(9):437.

37. Craig WA, Turner JH, Kunin CM. Prevention of the generalized Shwartzman reaction and endotoxin lethality by polymyxin B localized in tissues. Infect. Immun. 1974 Aug;10(2):287-292.

38. Tsubery H, Ofek I, Cohen S, Fridkin M. The Functional Association of Polymyxin B with Bacterial Lipopolysaccharide Is Stereospecific: Studies on Polymyxin B Nonapeptide†. Biochemistry. 2000 Oct 1;39(39):11837-11844.

39. Danner RL, Joiner KA, Rubin M, Patterson WH, Johnson N, Ayers KM, et al. Purification, toxicity, and antiendotoxin activity of polymyxin B nonapeptide. Antimicrob. Agents Chemother. 1989 Sep 1;33(9):1428-1434.

40. Tsubery H, Ofek I, Cohen S, Eisenstein M, Fridkin M. Modulation of the hydrophobic domain of polymyxin B nonapeptide: effect on outer-membrane permeabilization and lipopolysaccharide neutralization. Molecular pharmacology. 2002;62(5):1036.

41. Corrigan JJ, Kiernat JF. Effect of polymyxin B sulfate on endotoxin activity in a gram-negative septicemia model. Pediatr. Res. 1979 Jan;13(1):48-51.

42. Bhor VM, Thomas CJ, Surolia N, Surolia A. Polymyxin B: An ode to an old antidote for endotoxic shock. Mol. Biosyst. 2005;1(3):213-222.

43. Falagas ME, Kasiakou SK. Toxicity of polymyxins: a systematic review of the evidence from old and recent studies. Crit Care. 2006 Feb;10(1):R27.

44. Michalopoulos A, Falagas ME. Colistin and polymyxin B in critical care. Crit Care Clin. 2008 Apr;24(2):377-391, x.

45. Joint Formulary Committee. British National Formulary. 61st ed. Pharmaceutical Press; 2011.

46. Beringer P. The clinical use of colistin in patients with cystic fibrosis. Curr Opin Pulm Med. 2001 Nov;7(6):434-440.

47. Shoji H, Tani T, Hanasawa K, Kodama M. Extracorporeal endotoxin removal by polymyxin B immobilized fiber cartridge: designing and antiendotoxin efficacy in the clinical application. Ther Apher. 1998 Feb;2(1):3-12.

48. Tani T, Shoji H, Guadagni G, Perego A. Extracorporeal removal of endotoxin: the polymyxin B-immobilized fiber cartridge. Contrib Nephrol. 2010;167:35-44.

49. Teramoto K, Yoshiaki Nakamoto, Tetsunosuke Kunitomo, Hisataka Shoji, Toru Tani, Kazuyoshi Hanazawa, et al. Removal of Endotoxin in Blood by Polymyxin B Immobilized Polystyrene-Derivative Fiber. Therapeutic Apheresis. 2002;6(2):103-108.

50. Cruz DN, Antonelli M, Fumagalli R, Foltran F, Brienza N, Donati A, et al. Early Use of Polymyxin B Hemoperfusion in Abdominal Septic

Shock. JAMA: The Journal of the American Medical Association. 2009 Jun 17;301(23):2445 -2452.

51. Spectral Diagnostics - The Toraymyxin Polymyxin B Column [Internet]. [cited 2011 May 19];Available from: http://www.spectraldx.com/toraymyxin.html

52. Safety and Efficacy of Polymyxin B Hemoperfusion (PMX) for Septic Shock - Full Text View - ClinicalTrials.gov [Internet]. [cited 2011 May 22];Available from: http://clinicaltrials.gov/ct2/show/NCT01046669

53. Rosenthal KS, Storm DR. Disruption of the Escherichia coli outer membrane permeability barrier by immobilized polymyxin B. J. Antibiot. 1977 Dec;30(12):1087-1092.

54. LaPorte DC, Rosenthal KS, Storm DR. Inhibition of Escherichia coli growth and respiration by polymyxin B covalently attached to agarose beads. Biochemistry. 1977 Apr 1;16(8):1642-1648.

55. Schindler PRG, Teuber M. Action of Polymyxin B on Bacterial Membranes: Morphological Changes in the Cytoplasm and in the Outer Membrane of Salmonella typhimurium and Escherichia coli B. Antimicrob Agents Chemother. 1975 Jul;8(1):95–104.

56. Shafer WM. Antibacterial peptide protocols. Humana Press; 1997.

57. Rostovtsev VV, Green LG, Fokin VV, Sharpless KB. A Stepwise Huisgen Cycloaddition Process: Copper(I)-Catalyzed Regioselective "Ligation" of Azides and Terminal Alkynes. Angewandte Chemie International Edition. 2002 Jul 15;41(14):2596-2599.

58. Orwa JA, Van Gerven A, Roets E, Hoogmartens J. Liquid chromatography of polymyxin B sulphate. Journal of Chromatography A. 2000 Feb 18;870(1-2):237-243.

59. Newton BA. A fluorescent derivative of polymyxin: its preparation and use in studying the site of action of the antibiotic. J. Gen. Microbiol. 1955 Apr;12(2):226-236.

60. Moore RA, Bates NC, Hancock RE. Interaction of polycationic antibiotics with Pseudomonas aeruginosa lipopolysaccharide and lipid A studied by using dansyl-polymyxin. Antimicrob Agents Chemother. 1986 Mar;29(3):496-500.

61. Zhang L, Dhillon P, Yan H, Farmer S, Hancock REW. Interactions of Bacterial Cationic Peptide Antibiotics with Outer and Cytoplasmic Membranes of Pseudomonas aeruginosa. Antimicrob Agents Chemother. 2000 Dec;44(12):3317–3321.

62. Gmur DJ, Bredl CR, Steele SJ, Cai S, VanDevanter DR, Nardella PA. Determination of polymyxin E1 in rat plasma by high-performance liquid chromatography. J. Chromatogr. B Analyt. Technol. Biomed. Life Sci. 2003 Jun 15;789(2):365-372.

63. Vaara M, Fox J, Loidl G, Siikanen O, Apajalahti J, Hansen F, et al. Novel Polymyxin Derivatives Carrying Only Three Positive Charges Are Effective Antibacterial Agents. Antimicrob. Agents Chemother. 2008 Sep 1;52(9):3229-3236.

64. Sanger F. The free amino groups of insulin. Biochem J. 1945;39(5):507-515.

65. Bartos J, Pesez M. Spectrophotometric and fluorimetric determination of amines. Pure Appl. Chem. 1984;56(4):467-477.

66. Raetz CRH, Garrett TA, Reynolds CM, Shaw WA, Moore JD, Smith DC, et al. Kdo2-Lipid A of Escherichia coli, a defined endotoxin that activates macrophages via TLR-4. Journal of Lipid Research. 2006 May 1;47(5):1097 -1111.

67. Wilkinson SG. Composition and structure of lipopolysaccharides from Pseudomonas aeruginosa. Rev. Infect. Dis. 1983 Dec;5 Suppl 5:S941-949.

68. Brandenburg K, Arraiza MD, Lehwark-Ivetot G, Moriyon I, Zähringer U. The interaction of rough and smooth form lipopolysaccharides with polymyxins as studied by titration calorimetry. Thermochimica Acta. 2002 Oct 19;394(1-2):53-61.

69. Schindler M, Osborn MJ. Interaction of divalent cations and polymyxin B with lipopolysaccharide. Biochemistry. 1979 Oct 1;18(20):4425-4430.

70. Morrison DC, Jacobs DM. Binding of polymyxin B to the lipid A portion of bacterial lipopolysaccharides. Immunochemistry. 1976 Oct;13(10):813-818.

71. Hermanson GT. Bioconjugate Techniques. 2nd ed. Academic Press; 2008.

72. Roger R, Neilson DG. The Chemistry of Imidates. Chemical Reviews. 1961 Apr 1;61(2):179-211.

73. - Detoxi-Gel Endotoxin Removal Gel [Internet]. [cited 2011 May 19];Available from: http://www.piercenet.com/browse.cfm?fldID=02050101

74. Hartman FC, Wold F. Cross-Linking of Bovine Pancreatic Ribonuclease A with Dimethyl Adipimidate*. Biochemistry. 1967;6(8):2439-2448.

75. Kolb HC, Finn MG, Sharpless KB. Click Chemistry: Diverse Chemical Function from a Few Good Reactions. Angewandte Chemie International Edition. 2001 Jun 1;40(11):2004-2021.

76. Meldal M, Tornøe CW. Cu-Catalyzed Azide–Alkyne Cycloaddition. Chemical Reviews. 2008;108(8):2952-3015.

77. Shechter L, Wynstra J, Kurkjy RP. Glycidyl Ether Reactions with Amines. Industrial & Engineering Chemistry. 1956 Jan 1;48(1):94-97.

78. Mijovic J, Wijaya J. Reaction Kinetics of Epoxy/Amine Model Systems. The Effect of Electrophilicity of Amine Molecule. Macromolecules. 1994 Dec 1;27(26):7589-7600.

79. Aurell CA, Wistrom AO. Critical Aggregation Concentrations of Gram-Negative Bacterial Lipopolysaccharides (LPS). Biochemical and Biophysical Research Communications. 1998;253(1):119-123.

Chapter Four : Magnetite Studies

4.1 Introduction

4.1.1 General Overview

Phage display is a powerful *in vitro* tool used in the selection of peptides that possess high affinity for a target molecule. Conventional methods of screening or panning for the desired peptides rely on the immobilisation of the target molecule to a surface, typically a well of a microtiter plate or bead type structure. Phage display targeting LPS has been carried out using both immobilisation methods. The work by Noda *et al* (1), Zhu *et al* (2), Thomas *et al* (3) and Guo and Chen (4) all utilised adsorption of LPS or lipid A moieties onto the surface of multiwell plates. None of the four studies were able to enrich consensus sequence clones, although homology between the peptides in terms of the properties of the amino acid residues e.g. hydrophobicity and charge, were shown to exist. Studies conducted in 2005 and 2006 by Kim *et al* (5,6) immobilised LPS to the surface of epoxy beads which resulted in identification of identical or highly homologous peptide sequences. The authors attributed this increase in observed homology to increased variability in the conformational presentation of LPS and to the increased surface area available for interaction with phage conferred by the use of a bead-type support (5).

The initial aim of this section of work was to exploit the increased surface area conferred by bead-like supports, whilst attempting to display the LPS moiety in a more bio-representative manner. When LPS was immobilised to the epoxy bead, a variety of conformations would have resulted due to the large number of hydroxyl attachment points in the LPS moiety. Additionally the non-specific adsorption of LPS or lipid A to the wells of a microtiter plate also provides very little control over the conformation. In reality, the LPS structure is an integral component of the outer membrane of Gram-negative bacteria by virtue of its lipid

A region (7). It was hypothesised that forming a self-assembled monolayer of LPS on the surface of magnetic nanoparticles, the cellular architecture could be more closely mimicked. It was anticipated that displaying LPS on the surface of a magnetic particle would prove advantageous in the panning procedure, as no further immobilisation would be necessary as the particles would be held in position using magnetic force. Additionally the whole process should be much cleaner as the LPS-coated particles and consequently the bound phage, can simply be 'pulled out' of solution by use of a magnet, thus allowing easy separation of the bound and free fractions without the need for centrifugation. Streptavidin coated magnetic beads (e.g. MagneSphere paramagnetic particles (8)) are finding increased use in a number of phage display protocols due to the improved presentation of target and the relative ease of the process. Although the work did not progress in this direction, it was envisaged that magnetic nanoparticles could provide a useful platform for future downstream biosensing applications of the peptide-polymer recognition system.

4.1.2 Magnetite

Magnetite (Fe_3O_4), the first substance discovered to possess magnetic properties, is a ferrimagnetic iron oxide that displays the strongest magnetism of all natural minerals (9). Its magnetic properties arise from the fact that its crystal structure is composed of iron in two different oxidation states: Fe^{2+} and Fe^{3+}. These ions occupy different sub-lattices within the structure of magnetite and their magnetic moments are antiparallel, however as one moment dominates, the material possesses permanent magnetisation. If magnetite is synthesised sufficiently small (< 100 nm) the particles exist as a single domain resulting in larger magnetic susceptibilities and a loss of magnetic memory i.e. it displays superparamagnetism (10).

Magnetite with pre-defined magnetic and physicochemical properties can readily be synthesised in the laboratory (10,11). Synthesis via the co-precipitation of ferrous and ferric salts was developed by René Massart in 1981 and remains one of the most common approaches used today (12). The reaction is simple, efficient and produces large yields, however control of size and dispersity of the nanoparticles is poor (11). Careful optimisation of salt ratios, pH and temperature is needed to ensure efficient and reproducible synthesis of nanoparticles. As a consequence, over recent years research into methods to produce more defined/tuneable nanoparticles has intensified and a number of alternative methods now exist, examples of which include the use of surfactant "nanoreactors" (13), sol-gel methods (14) and high temperature thermal decomposition of organic iron precursors (15).

Iron oxides such as magnetite have found extensive use in biomedical applications due to their excellent biocompatibility and the ease of synthesis of particles with a range of useful coatings (16-19). Magnetic nanoparticles have been used as targeted drug delivery systems (20-22), as contrast agents in magnetic resonance imaging (MRI) (23,24), in the treatment of a range of cancers through the induction of hyperthermia (25,26) and also in cellular separations (18,27-29) and biosensing (30,31).

4.1.5 Aims and objectives of Chapter Four

The overall aim of this section of work was to synthesise superparamagnetic nanoparticles and investigate their utility in biological assays.

The key objectives of this work were:

1. To synthesis magnetite nanoparticles that display desirable magnetic and physicochemical properties.
2. To mimic the cellular architecture of a Gram-negative bacteria through the immobilisation of LPS on the surface of the nanoparticles.
3. To immobilise polymyxin B on the surface of the magnetite particles and evaluate the ability of the system to sequester LPS from solution.

4.2 Materials and Methods

4.2.1 Materials

All chemicals were purchased from Sigma-Aldrich, Poole, UK and were used as received unless otherwise stated. All organic solvents were of HPLC grade and were obtained from Fisher Scientific, Loughborough, UK unless otherwise stated.

4.2.2 Synthesis of magnetite nanoparticles (I)

The method of Li *et al* (32) was used to prepare water dispersible magnetite nanoparticles. Iron (III) chloride hexahydrate ($FeCl_3 \cdot 6H_2O$) was used as the single iron source for the reaction. Briefly, 10 mmol (2.70 g) $FeCl_3 \cdot 6H_2O$ was dissolved in 100 ml 2-pyrrolidone and the solution purged with nitrogen for 15 minutes. The mixture was refluxed for 10 hours under an inert atmosphere. After cooling to room temperature, an excess (~ 5 x volume) of diethyl ether was added to precipitate the magnetite, which was subsequently washed with acetone to remove residual solvent and then dried overnight to yield a crystalline, black powder.

4.2.3 Synthesis of magnetite nanoparticles (II)

The method of Sun *et al* (15) was used to prepare magnetite nanoparticles that can be dispersed in non-polar or weakly polar solvents. Iron (III) acetylacetonate ($Fe(acac)_3$) was employed as the single iron source in the reaction. Briefly, 2 mmol (706 mg) $Fe(acac)_3$, 6 mmol (1.90 ml) oleic acid, 6 mmol (1.98 ml) oleylamine and 10 mmol (2.03 g) 1,2-dodecanediol were added to 20 ml benzyl ether and the mixture stirred under a flow of nitrogen. The mixture was heated to 200

°C and maintained at this temperature for two hours before being heated to reflux (~ 300 °C) for an additional hour under an inert nitrogen atmosphere. The magnetite nanoparticles were precipitated with 40 ml ethanol. The black precipitate was re-dissolved in hexane in the presence of trace amounts (50 µl) of oleic acid and oleylamine, and centrifuged to remove undispersed residue. The supernatant was again precipitated with ethanol and centrifuged once more. The pellet was dried overnight to yield a black, crystalline powder.

4.2.4 Immobilisation of lipopolysaccharide on magnetic nanoparticles

Magnetite nanoparticles (oleic acid coated, 10 mg) were incubated with *E. coli* 0111:B4 LPS (500 µg in 1 ml water for injections) and the mixture sonicated for 3 x 15 minutes. The particles were removed magnetically and washed with 5 x 10 ml deionised water before being dried overnight at 40 °C under vacuum.

4.2.5 Raman spectroscopy

Magnetite nanoparticles were analysed by Raman spectroscopy by colleagues in the School of Chemistry, Cardiff University.

4.2.6 Immobilisation of polymyxin B on magnetite nanoparticles

Magnetite nanoparticles (oleic acid coated, 100 mg) were added to a 5 ml aqueous solution of polymyxin B (100 mg) and the mixture sonicated for 15 minutes. The nanoparticles were magnetically pulled down and the remaining solution decanted. The particles were washed with copious amounts of water before being dried overnight under vacuum at 40 °C. Control nanoparticles were prepared in the same manner, with the exclusion of polymyxin from the solution.

4.2.7 Binding assays with polymyxin modified nanoparticles

Polymyxin modified and control magnetite nanoparticles (5 mg) were incubated with various concentrations of FITC-labeled LPS from *E. coli* 0111:B4 in deionised water at room temperature for 10 minutes. Samples were subsequently subjected to magnetic force to remove the bound fraction and the fluorescence of the supernatant analysed using a FLUOstar OPTIMA platereader (BMG Labtech GmbH, Ortenburg, Germany) at an excitation wavelength of 485 nm and emission wavelength of 520 nm. All samples were prepared in triplicate.

4.2.8 Ligand exchange with 11-mercaptoundecanoic acid

Using the method of Bagaria *et al.* (33) with some modification, the oleic acid on the surface of the magnetite nanoparticles was exchanged for 11-mercaptoundecanoic acid. Briefly, 50 mg of magnetite nanoparticles suspended in 500 µl hexane were added to 2 g 11-mercaptoundecanoic acid in 20 ml cyclohexanone. The mixture was vortexed to form a homogenous suspension and heated at 100 °C for 16 hours. The particles precipitated over this time and were pulled down with magnetic force to allow for the supernatant to be discarded. Cyclohexanone was added (10 ml) and the suspension vortexed, the particles pulled down using a magnet and the supernatant discarded. This process was repeated twice with cyclohexanone, followed by two 10 ml washes with ethanol with a final 20 ml acetone wash before the particles were dried under vacuum overnight at 40 °C. The nanoparticles were analysed by FTIR.

4.2.9 Conversion of thiol groups to azides

Conversion of the thiol groups on 11-mercaptoundecanoic acid modified magnetite to azide groups was attempted using the method of

Iranpoor *et al.* (34). Magnetite nanoparticles (50 mg) were added to 6 ml dry dichloromethane. Triphenylphosphine (393 mg, 1.5 mmol), tetra-*n*-butylammonium azide (568 mg, 2 mmol) and 2,3-Dichloro-5,6-dicyanobenzoquinone (454 mg, 2 mmol) were added to the suspension, the mixture vortexed and incubated at room temperature overnight. The magnetite nanoparticles were subsequently recovered magnetically and washed with 3 x 20 ml acetone before being dried under vacuum overnight at 40 °C. The nanoparticles were analysed by FTIR.

4.3 Results and Discussion.

4.3.1 Synthesis of magnetite nanoparticles (I)

Hydrophilic magnetite nanoparticles were synthesised following the method of Li *et al* (32). Refluxing iron (III) chloride hexahydrate with 2-pyrrolidone for 10 hours successfully produced particles that were magnetic in nature and dispersible in aqueous solvents. The method however was somewhat inconsistent; several repeats were conducted that produced particles that differed in both their physical and magnetic nature. The precipitate produced following the addition of an excess of diethyl ether to the reaction mixture was sticky and tar-like and was therefore difficult to wash. As a result it was virtually impossible to remove the residual 2-pyrrolidone. The repeated washes appeared to have a detrimental effect on the coating of the particles as it became much more difficult to form a stable dispersion in water as the number of washes increased. Following the reflux reaction, the surface of the magnetite is coated with an adsorbed layer of 2-pyrrolidone molecules, coordinated to the surface of the nanoparticles via the ketone oxygen (Figure 4.1). It is therefore possible that a proportion of the 2-pyrrolidone molecules are being replaced by acetone. However, upon drying, the more volatile acetone could have been removed, thus leaving uncoated magnetite nanoparticles.

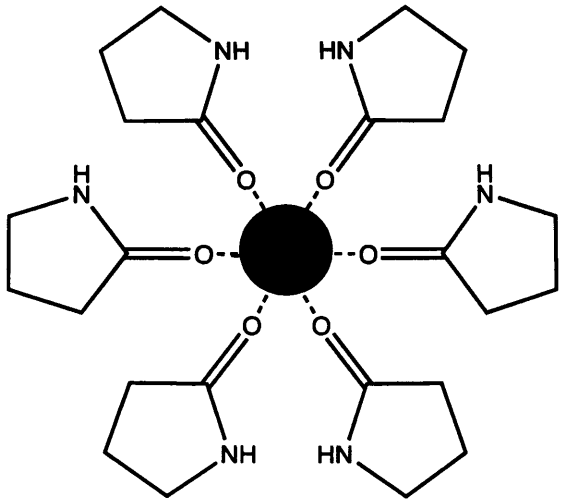

Figure 4.1: Proposed structure of 2-pyrrolidone coated nanoparticle. The oxygen atom of the 2-pyrrolidone ketone group co-ordinates with the surface of the magnetite nanoparticles (35).

It was envisaged that synthesis of hydrophilic magnetite would allow the encapsulation of the nanoparticles within the inner aqueous space of a liposome to create an artificial cell-like structure. However, the inconsistency and length of time taken to synthesise the particles, coupled with the intrinsic variability of liposomes and the encapsulation of materials within them, lead to the idea of self-assembled monolayers being utilised as an alternative way of mimicking the surface morphology of a bacterial cell.

4.3.2 Synthesis of magnetite nanoparticles (II)

The thermal decomposition of iron (III) acetylacetonate in the presence of a reducing agent (1,2 - dodecanediol) and stabilisers (oleic acid and oleylamine) reproducibly resulted in the formation of stable, oleic acid coated magnetic nanoparticles (Figure 4.2). The increased consistency observed with this method compared to that used to synthesise water

dispersible magnetite (section 4.2.2) can be attributed to the method of heating used in the experimental procedure; by heating the $Fe(acac)_3$ mixture to 200 °C and maintaining the temperature for two hours before refluxing at ~300 °C for a further hour, nucleation of the magnetite crystals is controlled thus producing monodisperse particles with consistent morphology (15,36). This in turn produces particles with the desired magnetic properties and dispersibility.

Oleic acid is a bidentate ligand that interacts with the surface of the magnetite via its carboxylate group (Figure 4.2) (37). As a result of the nature of the interaction i.e. bidentate as opposed to the monodentate nature of the 2-pyrrolidone interaction (Figure 4.1), the coating of the particles is significantly more stable and does not appear to be affected to any significant degree by the washing and centrifugation processes employed. The dispersions formed in hexane were stable and ferrofluidic in nature.

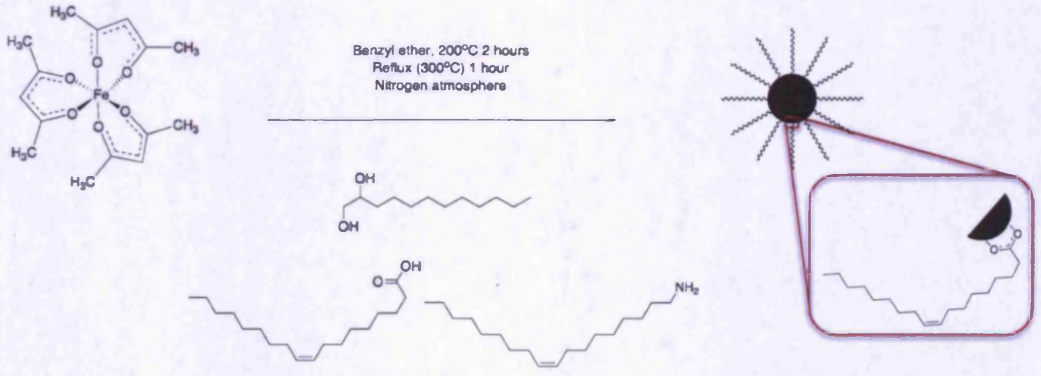

Figure 4.2: Schematic of the synthesis of magnetite nanoparticles from an iron (III) acetylacetonate precursor and the nature of the interaction between the carboxylate functionality of oleic acid and the surface of the magnetite nanoparticles.

Oleylamine has been shown to act as both a reducing agent and as a stabiliser when present as the only surfactant source in the synthesis of

magnetite (38). It is not clear how the amine would co-ordinate with the surface of the magnetite, however when an equimolar ratio of long chain acid to long chain amine is employed co-ordination of the acid group would appear to dominate. The combination of acid and amine provides good control over the growth of the particles during the synthesis (36). It is believed that the presence of an amine aids in the stabilisation of the nanoparticles by promoting the adsorption of oleic acid to the surface; it is thought that acid-base complexation leads to enhanced deprotonation of the oleic acid (39).

FTIR analysis was used to confirm the presence of oleic acid on the surface of the magnetite. The spectrum presented in Figure 4.3 is typical of oleic acid coated magnetite. The two sharp bands at 2926 and 2854 cm^{-1} are attributed to the asymmetric and symmetric stretch of CH_2 groups respectively, while the stretches observed at 1604 and 1531 cm^{-1} demonstrate the presence of a deprotonated carboxylate group (υ_{COO}- symmetric and asymmetric). The interaction can be described as chelating bidentate as the wavenumber separation between the asymmetric and symmetric stretches of the carboxylate group is less than 110 cm^{-1} (40). Additionally the spectrum shows no evidence of the characteristic carboxylic acid carbonyl stretch at ~ 1700 cm^{-1}, again suggesting the co-ordination of the deprotonated form of oleic acid at the surface of the magnetite.

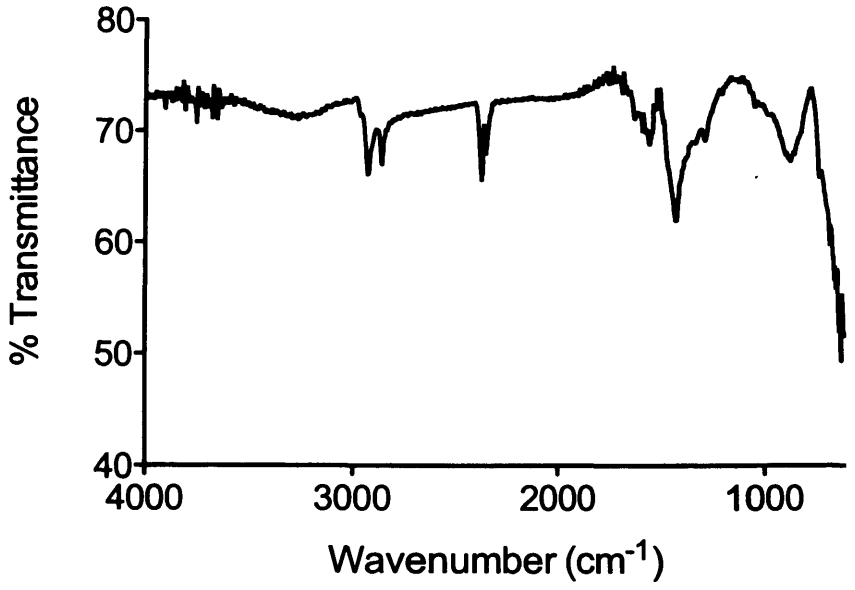

Figure 4.3: FTIR spectra of oleic acid stabilised magnetite.

4.3.3 Immobilisation of lipopolysaccharide on magnetic nanoparticles

It was hypothesised that by simply incubating magnetite with LPS under the appropriate experimental conditions, a self-assembled monolayer of LPS should form on the surface of the nanoparticles. The as-synthesised nanoparticles are stabilised with oleic acid making them hydrophobic. Under aqueous conditions and in the presence of LPS, it should be more thermodynamically favourable for the nanoparticles to become "coated" with LPS, via intercalation of lipid A with oleic acid chains, in order to disperse in the solvent. A schematic of the proposed LPS-coated nanoparticles is given in Figure 4.4.

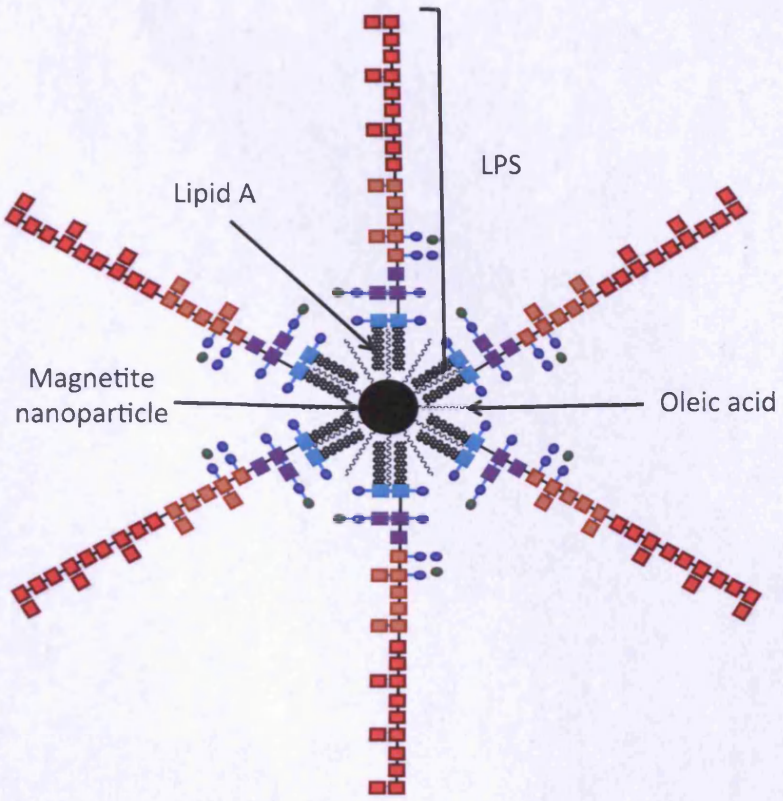

Figure 4.4: Schematic showing the proposed immobilisation of LPS on the surface of oleic acid coated magnetite nanoparticles. The lipid A region of LPS intercalates with the surface bound oleic acid group to form a self-assembled monolayer.

Self-assembled monolayers (SAMs) can be broadly thought of as the spontaneous adsorption of molecules to a surface (41,42). The most common example of the formation of self assembled monolayers is alkanethiols on the surface of gold (42) however Fu *et al,* (43) demonstrated the formation of a self assembled monolayer of lauric acid on the surface of magnetite nanoparticles, followed by the deposition of a second layer of decanoic acid molecules to form a bilayer structure. It was therefore hypothesised that a monolayer of LPS on the surface of oleic acid stabilised magnetite could be formed in a similar manner. It was anticipated that this would have a less substantial effect on the magnetic properties of the system compared to

the encapsulation of nanoparticles in the aqueous space of a liposome, since there would be a less significant change in the hydrodynamic volume of the particles and the issue of encapsulation efficiency is circumvented. During the course of this work, Piazza *et al* demonstrated the successful immobilisation of LPS on the surface of magnetic nanoparticles. They used the LPS modified particles to investigate the ability of LPS to trigger signalling via the TLR4 receptor (44).

Following sonication of the magnetite particles in an aqueous solution of *E. coli* 0111:B4, basic dispersibility tests suggested that LPS had been successfully immobilised (Figure 4.5). The control nanoparticles (OA, Figure 4.5) had been sonicated in water in the absence of LPS while the sample on the right had been sonicated in water containing 500 μg of *E. coli* 0111:B4 LPS. When LPS was present in the system, the magnetite particles became dispersible in aqueous solvents. Following extensive washing of the nanoparticles, they remained dispersible in water.

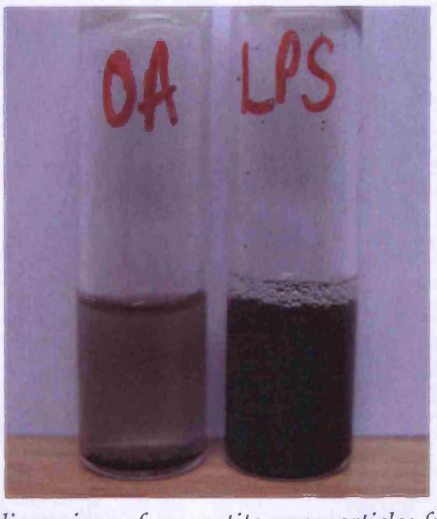

Figure 4.5: Aqueous dispersions of magnetite nanoparticles following sonication in water (left) and 500μg/ml LPS in water (right). Sonication of particles with LPS produced a stable aqueous dispersion that suggested successful immobilisation of LPS on the surface of magnetite.

The nanoparticles were analysed by Raman spectroscopy (School of Chemistry, Cardiff University) to provide further evidence for the immobilisation of LPS on the surface. Raman analysis of commercially available magnetite (Sigma-Aldrich, UK) plus LPS from *E. coli* 0111:B4 provided the reference spectra. A good spectrum was obtained for magnetite (Figure 4.6 a), however a clear spectrum could not be achieved for the LPS standard (Figure 4.6 b). This was possibly due to the presence of a large number of structurally related sugar moieties. A similar, non-distinct spectrum was obtained when the LPS coated nanoparticles were analysed (Figure 4.6 c, black line). Interestingly, if the sample was exposed to 100 % power of the argon ion laser the surface material could be visibly burnt off and the magnetite spectrum recovered (Figure 4.6 c, red line).

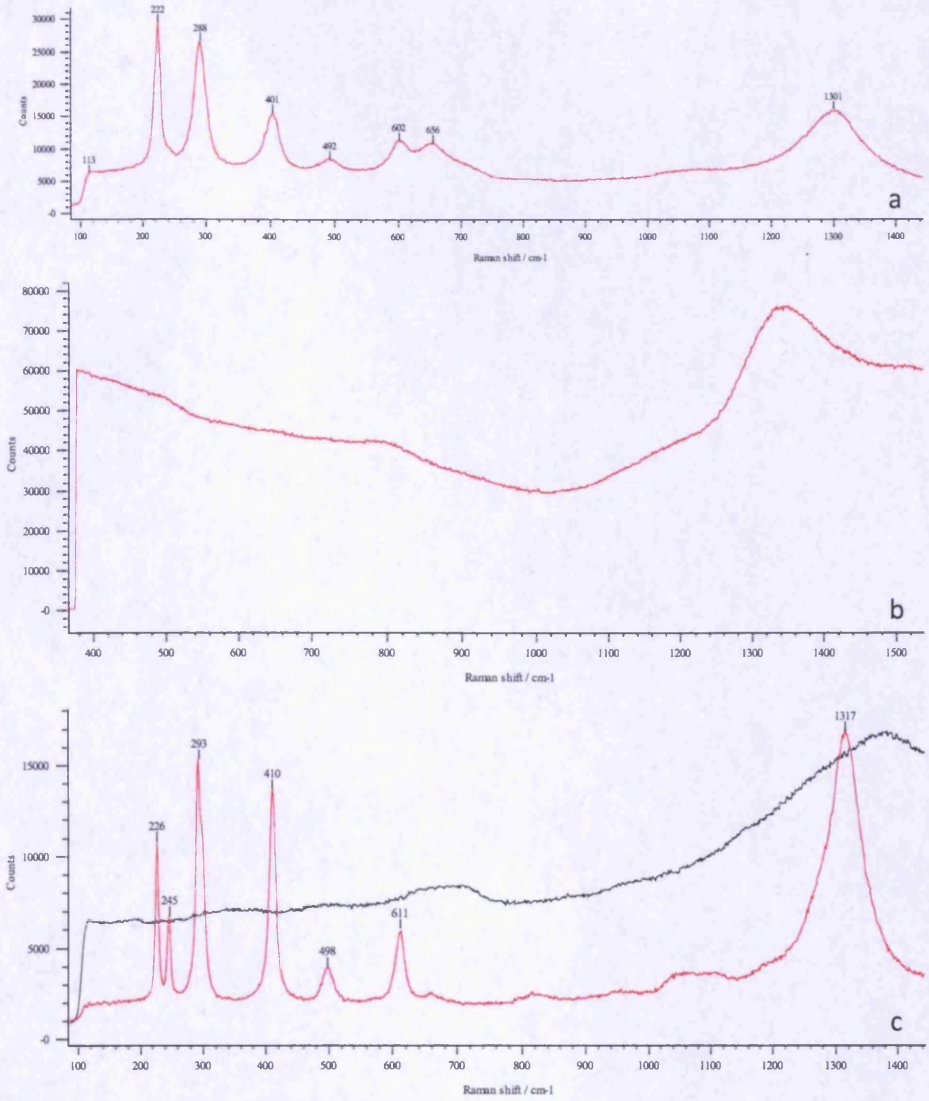

Figure 4.6: Raman spectra of magnetite from Sigma-Aldrich, UK (a), E. coli 0111:B4 LPS (b) and LPS coated magnetite (black line, c). On increasing the power of the laser, the LPS surface coating could be removed to regain the spectrum for magnetite (red line, c).

Although a good spectrum could not be obtained for the LPS standard, the fact that a similar spectrum was observed with the coated nanoparticles suggested that an LPS layer might be present. This was further supported by the observation that the spectrum for magnetite could be regained by exposing the underlying material through

burning off the outer layer. Additionally, the earlier dispersibility studies also suggested successful immobilisation. An alternative method for detecting LPS on the surface if the particles is needed to provide definitive proof of the formation of a LPS monolayer. It is anticipated that these particles will be used in a future phage display strategy (section 4.1.1) to identify high affinity peptide ligands for LPS, following further characterisation of the system.

4.3.4 Immobilisation of polymyxin B on magnetite nanoparticles

Following on from the studies with LPS, it was hypothesised that polymyxin B could be immobilised in a similar fashion. The peptide possesses a 7/8 carbon aliphatic tail, depending upon the structural isoform, that was anticipated to interact with the surface of oleic acid stabilised magnetite in the same manner proposed for LPS (Figure 4.4).

Following sonication of magnetite nanoparticles in an aqueous solution of polymyxin B, basic dispersibility tests suggested that polymyxin had been successfully immobilised (Figure 4.7). The control nanoparticles (OA, Figure 4.7) had been sonicated in water in the absence of polymyxin while the PMX sample had been sonicated in water containing the peptide. A stable aqueous dispersion of particles was achieved following extensive washing of the sample sonicated in the presence of the peptide.

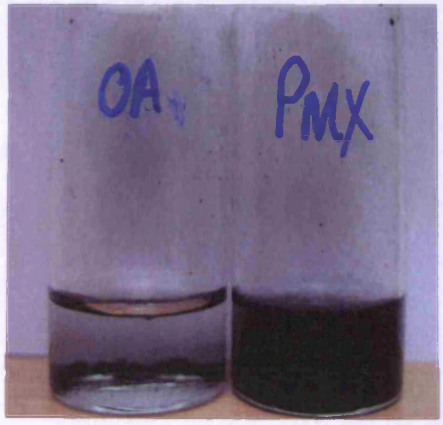

Figure 4.7: Aqueous dispersion of magnetite nanoparticles following sonication in water (left) and 100 mg / 5 ml polymyxin B in water (right). Both samples have been washed extensively with water. The polymyxin appears to "coat" the nanoparticles producing a stable dispersion in aqueous solvents.

The ability of polymyxin – magnetite nanoparticles to recognise and bind LPS in aqueous solutions was evaluated in a simple binding assay. As-synthesised oleic acid coated magnetite served as the control for the experiment. Based on the equilibrium time point assay performed with polymyxin modified Merrifield resin (Figure 3.32) and also in an attempt to minimise non-specific association of LPS with oleic acid coated magnetite, the incubation period used in the binding assay was less than 10 minutes. Figure 4.8 clearly shows increased binding of LPS to polymyxin-modified magnetite at all concentrations compared to the control nanoparticles. Apparent K_d values calculated from the binding isotherm were 0.18 μM and 1.21 μM for polymyxin and oleic acid coated magnetite respectively. The value for the polymyxin magnetite is not dissimilar to that observed with polymyxin modified Merrifield resin (0.27 μM, Figure 3.25). The immobilisation of polymyxin on magnetite is assumed to proceed via hydrophobic interactions of the acyl chain of the peptide with surface bound oleic acid, therefore all five amines from the *L*-2,4-diaminobutyric acid residues are available for

interaction with LPS. In the Merrifield system, one of the amines is involved in the immobilisation of the peptide to the resin surface and hence only four amines are free to participate in the interaction with the target. The small apparent increase in affinity observed with polymyxin magnetite may be attributable to the availability of an extra amine group.

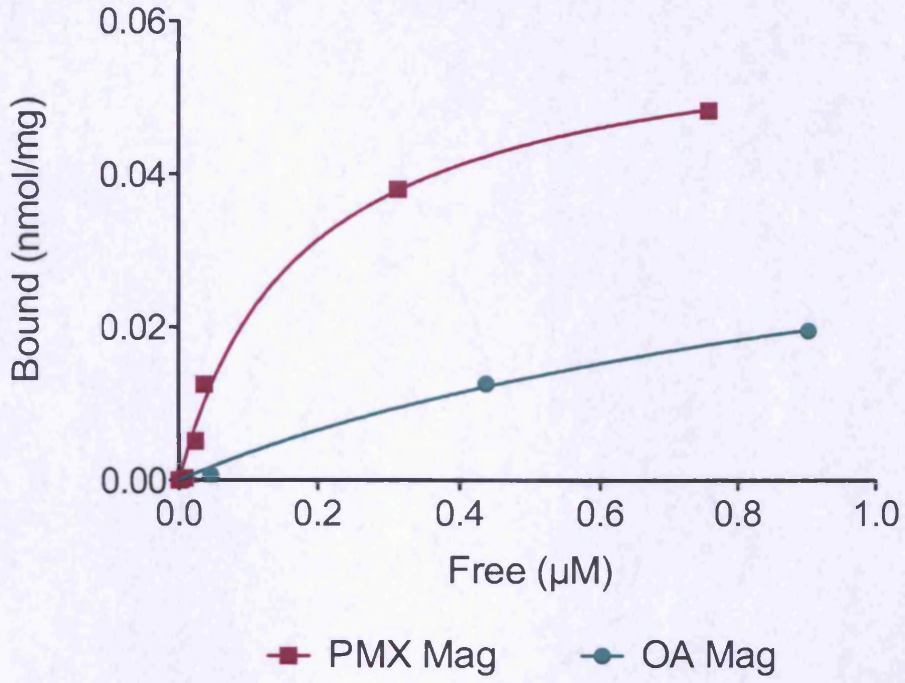

Figure 4.8: Standard binding isotherm for polymyxin modified magnetite (PMX Mag, red line) and control oleic acid coated magnetite (OA Mag, green line). In all samples 5 mg of nanoparticles were incubated with various concentrations of FITC labeled E. coli 0111:B4 LPS in a total volume of 1ml.

As discussed in Chapter One, there is a real, unmet, clinical need for a rapid diagnostic assay for sepsis. Magnetic nanoparticles have been utilised in the detection of bacteria (45,46), DNA (47) and other biological macromolecules (48,30). Binding events bring about changes in the hydrodynamic volume of the particles that in turn affects their magnetic properties. These alterations in the magnetic characteristics of

the system can be detected by measuring the magnetic susceptibility of the particles. It is therefore envisaged that the nanoparticles developed during the course of this work will be investigated as potential biosensor systems.

These studies provide preliminary data for the use of peptide modified magnetic nanoparticles in the removal of LPS from solution, however for the strategy developed thus far to be useful the stability of the peptide coating would need to be ensured. Additionally, it is anticipated that similar peptide-polymer hybrids (Chapter Three) could be grown from the surface of magnetite particles. For this to be possible an alternative method of peptide immobilisation would be needed.

4.3.5 Ligand exchange with 11-mercaptoundecanoic acid

Ligand exchange at the surface of the nanoparticles occurs readily under appropriate experimental conditions. The oleic acid groups on the surface of magnetite were substituted for a long chain, thiol-terminated acid through the incubation of particles with an excess of 11-mercaptoundecanoic acid. Following synthesis, particles were analysed by FTIR spectroscopy (Figure 4.9). The two sharp bands at 2926 and 2854 cm^{-1}, attributed to the asymmetric and symmetric stretch of CH_2 groups remained on the spectrum, while small shifts in the stretches previously observed at 1604 and 1531 cm^{-1} for oleic acid magnetite (Figure 4.3) were noted (1597 cm^{-1} and 1546 cm^{-1}). This interaction can again be described as chelating bidentate. Although no stretches indicative of thiol functionality were observed, the typical S-H stretching band at 2500 cm^{-1} is often weak and the C-S bond is normally observed below 700 cm^{-1}. The particles did however disperse in aqueous solvents following the exchange reaction (Figure 4.10),

suggesting the presence of 11-mercaptoundecanoic acid on the surface (33).

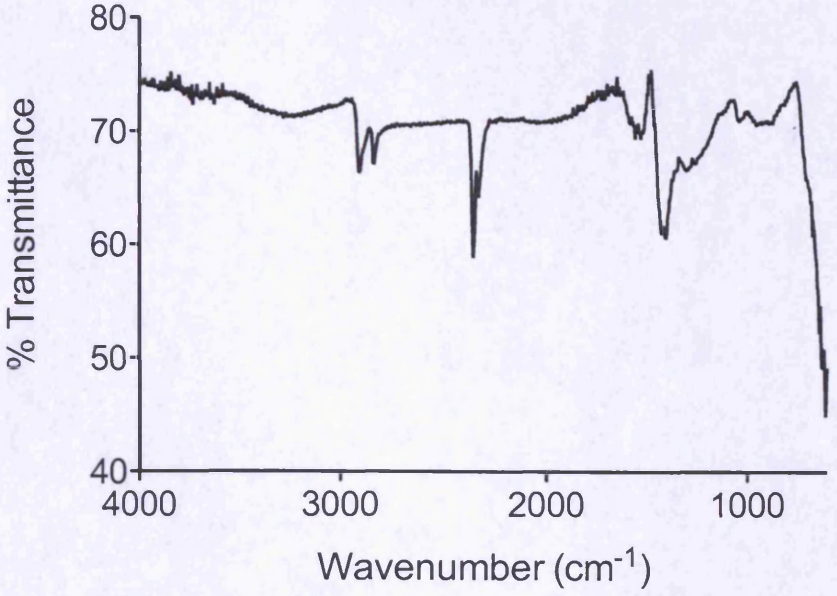

Figure 4.9: FTIR spectra of 11-mercaptoundecanoic acid coated magnetite

Figure 4.10: Aqueous dispersion of magnetite nanoparticles following the exchange of oleic acid (OA) surface groups with 11-mercaptoundecanoic acid (SH). Both samples have been washed extensively with water.

4.3.6 Conversion of thiol groups to azides

The exchange of oleic acid surface groups with 11-mercaptoundecanoic acid was conducted as it was anticipated that the thiol group could subsequently be converted to an azide using the method of Iranpoor *et al.* (34). The presence of azide functionality on the nanoparticles would have enabled attachment of polymyxin B through the "click" reaction described in section 3.2.5.2. FTIR analysis of the nanoparticles (Figure 4.11) however suggested that the reaction was unsuccessful; a characteristic azide stretch at ~ 2100 cm^{-1} was not apparent on the spectrum. Furthermore it appeared that the carboxylate stretches observed in Figures 4.3 and 4.9 have diminished, suggesting a reduced density of surface stabilising groups.

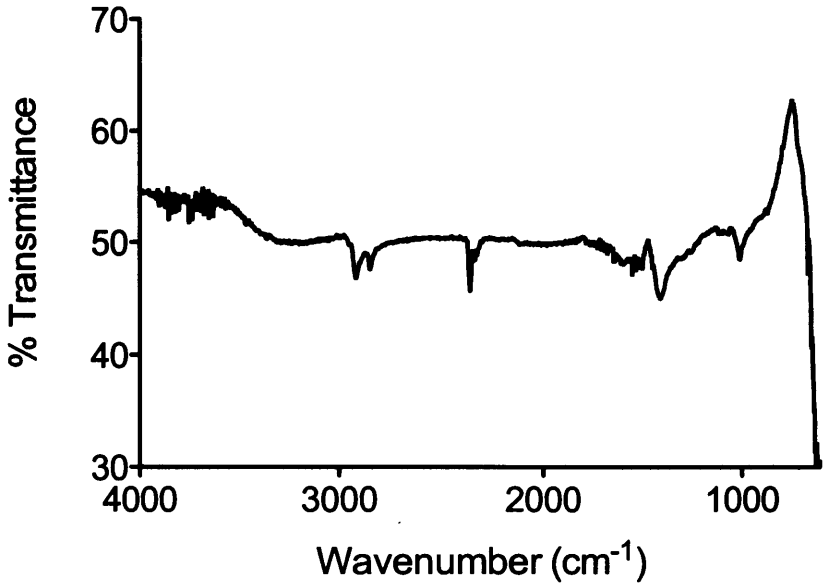

Figure 4.11: FTIR spectrum of magnetite nanoparticles following the attempted conversion of thiol groups to azides. The characteristic azide stretch at ~ 2100 cm^{-1} is absent, thus suggesting that the conversion of thiol groups to azides was unsuccessful.

The reaction used anhydrous dichloromethane as the solvent and this resulted in poor dispersibility of the thiol modified particles.

Additionally the reaction conditions, particularly the relative molar quantities of the reagents, needed to be carefully controlled to ensure that the triphenylphosphine did not reduce the azido groups to amines (Staudinger reaction, Figure 2.1). An alternative approach needs to be investigated.

4.4 Conclusions.

Magnetite nanoparticles have been successfully synthesised via the high temperature decomposition of the organic iron precursor, iron (III) acetylacetonate. They appeared to behave in a superparamagnetic manner and form stable dispersions in non-polar solvents such as hexane. It was demonstrated that LPS and polymyxin B could be immobilised on the surface of oleic acid stabilised particles using a self-assembly approach. Polymyxin-modified magnetite was shown to recognise and bind FITC labeled *E. coli* LPS with an apparent K_d of 0.18 μM. Increased binding of LPS to the peptide modified particles was observed at all concentrations compared to the oleic acid coated control particles.

4.5 Reference List.

1. Noda K, Yamasaki R, Hironaka Y, Kitagawa A. Selection of peptides that bind to the core oligosaccharide of R-form LPS from a phage-displayed heptapeptide library. FEMS Microbiology Letters. 2001;205(2):349-354.

2. Zhu Y, Ho B, Ding JL. Sequence and structural diversity in endotoxin-binding dodecapeptides. BBA-Biomembranes. 2003;1611(1-2):234-242.

3. Thomas CJ, Sharma S, Kumar G, Visweswariah SS, Surolia A. Biopanning of endotoxin-specific phage displayed peptides. Biochemical and Biophysical Research Communications. 2003;307(1):133-138.

4. Guo X, Chen RR. An improved phage display procedure for identification of lipopolysaccharide-binding peptides. Biotechnol. Prog. 2006 Apr;22(2):601-604.

5. Kim YG, Lee CS, Chung WJ, Kim E, Shin DS, Rhim JH, et al. Screening of LPS-specific peptides from a phage display library using epoxy beads. Biochemical and Biophysical Research Communications. 2005;329(1):312-317.

6. Kim Y-G, Lee C-S, Chung W-J, Kim E-M, Shin D-S, Kim J-H, et al. Selection of peptides for lipopolysaccharide binding on to epoxy beads and selective detection of Gram-negative bacteria. Biotechnol. Lett. 2006 Jan;28(2):79-84.

7. Rietschel E, Kirikae T, Schade F, Mamat U, Schmidt G, Loppnow H, et al. Bacterial endotoxin: molecular relationships of structure to activity and function. FASEB J. 1994 Feb 1;8(2):217-225.

8. Promega. Streptavidin MagneSphere® Paramagnetic Particles [Internet]. [cited 2011 Jul 1];Available from: http://www.promega.com/products/dna-and-rna-purification/rna-purification/streptavidin-magnesphere-paramagnetic-particles/

9. Harrison RJ, Dunin-Borkowski RE, Putnis A. Direct imaging of nanoscale magnetic interactions in minerals. Proceedings of the National Academy of Sciences. 2002 Dec 24;99(26):16556 -16561.

10. Lu A-H, Salabas EL, Schüth F. Magnetic nanoparticles: synthesis, protection, functionalization, and application. Angew. Chem. Int. Ed. Engl. 2007;46(8):1222-1244.

11. Laurent S, Forge D, Port M, Roch A, Robic C, Vander Elst L, et al. Magnetic Iron Oxide Nanoparticles: Synthesis, Stabilization, Vectorization, Physicochemical Characterizations, and Biological Applications. Chemical Reviews. 2008 Jun 1;108(6):2064-2110.

12. Massart R. Preparation of aqueous magnetic liquids in alkaline and acidic media. IEEE Transactions on Magnetics. 1981 Mar;17(2):1247-1248.

13. Lee Y, Lee J, Bae CJ, Park J -G, Noh H -J, Park J -H, et al. Large-Scale Synthesis of Uniform and Crystalline Magnetite Nanoparticles Using Reverse Micelles as Nanoreactors under Reflux Conditions. Advanced Functional Materials. 2005 Mar 1;15(3):503-509.

14. Xu J, Yang H, Fu W, Du K, Sui Y, Chen J, et al. Preparation and magnetic properties of magnetite nanoparticles by sol–gel method. Journal of Magnetism and Magnetic Materials. 2007 Feb;309(2):307-311.

15. Sun S, Zeng H, Robinson DB, Raoux S, Rice PM, Wang SX, et al. Monodisperse MFe2O4 (M = Fe, Co, Mn) Nanoparticles. Journal of the American Chemical Society. 2004 Jan 1;126(1):273-279.

16. Gupta AK, Gupta M. Synthesis and surface engineering of iron oxide nanoparticles for biomedical applications. Biomaterials. 2005 Jun;26(18):3995-4021.

17. Sun C, Lee JSH, Zhang M. Magnetic nanoparticles in MR imaging and drug delivery. Advanced Drug Delivery Reviews. 2008 Aug 17;60(11):1252-1265.

18. Pankhurst QA, Connolly J, Jones SK, Dobson J. Applications of magnetic nanoparticles in biomedicine. J. Phys. D: Appl. Phys. 2003 Jul;36(13):R167-R181.

19. Berry CC, Curtis ASG. Functionalisation of magnetic nanoparticles for applications in biomedicine. J. Phys. D: Appl. Phys. 2003 Jul;36(13):R198-R206.

20. Neuberger T, Schöpf B, Hofmann H, Hofmann M, von Rechenberg B. Superparamagnetic nanoparticles for biomedical applications: Possibilities and limitations of a new drug delivery system. Journal of Magnetism and Magnetic Materials. 2005 May;293(1):483-496.

21. McCarthy JR, Weissleder R. Multifunctional magnetic nanoparticles for targeted imaging and therapy. Adv. Drug Deliv. Rev. 2008 Aug 17;60(11):1241-1251.

22. Alexiou C, Arnold W, Klein RJ, Parak FG, Hulin P, Bergemann C, et al. Locoregional Cancer Treatment with Magnetic Drug Targeting. Cancer Research. 2000 Dec 1;60(23):6641 -6648.

23. Lee P-W, Hsu S-H, Wang J-J, Tsai J-S, Lin K-J, Wey S-P, et al. The characteristics, biodistribution, magnetic resonance imaging and biodegradability of superparamagnetic core-shell nanoparticles. Biomaterials. 2010 Feb;31(6):1316-1324.

24. Ito A, Shinkai M, Honda H, Kobayashi T. Medical application of functionalized magnetic nanoparticles. Journal of Bioscience and Bioengineering. 2005 Jul;100(1):1-11.

25. Jordan A, Scholz R, Wust P, Fähling H, Roland Felix. Magnetic fluid hyperthermia (MFH): Cancer treatment with AC magnetic field induced excitation of biocompatible superparamagnetic nanoparticles. Journal of Magnetism and Magnetic Materials. 1999 Jul;201(1-3):413-419.

26. Hergt R, Dutz S, Müller R, Zeisberger M. Magnetic particle hyperthermia: nanoparticle magnetism and materials development for cancer therapy. J. Phys.: Condens. Matter. 2006 Sep;18(38):S2919-S2934.

27. Kronick P, Gilpin RW. Use of superparamagnetic particles for isolation of cells. Journal of Biochemical and Biophysical Methods. 1986 Jan;12(1-2):73-80.

28. Molday RS, MacKenzie D. Immunospecific ferromagnetic iron-dextran reagents for the labeling and magnetic separation of cells. J. Immunol. Methods. 1982 Aug 13;52(3):353-367.

29. Morisada S, Miyata N, Iwahori K. Immunomagnetic separation of scum-forming bacteria using polyclonal antibody that recognizes mycolic acids. Journal of Microbiological Methods. 2002 Oct;51(2):141-148.

30. Nikitin PI, Vetoshko PM, Ksenevich TI. New type of biosensor based on magnetic nanoparticle detection. Journal of Magnetism and Magnetic Materials. 2007 Apr;311(1):445-449.

31. Chemla YR, Grossman HL, Poon Y, McDermott R, Stevens R, Alper MD, et al. Ultrasensitive magnetic biosensor for homogeneous immunoassay. Proceedings of the National Academy of Sciences. 2000 Dec 19;97(26):14268 -14272.

32. Li Z, Sun Q, Gao M. Preparation of Water-Soluble Magnetite Nanocrystals from Hydrated Ferric Salts in 2-Pyrrolidone: Mechanism Leading to Fe3O4. Angewandte Chemie. 2005 Jan 1;117(1):125-128.

33. Bagaria HG, Ada ET, Shamsuzzoha M, Nikles DE, Johnson DT. Understanding Mercapto Ligand Exchange on the Surface of FePt Nanoparticles. Langmuir. 2006;22(18):7732-7737.

34. Iranpoor N, Firouzabadi H, Akhlaghinia B, Nowrouzi N. A novel and highly selective conversion of alcohols, thiols, and silyl ethers to azides using the triphenylphosphine/2,3-dichloro-5,6-dicyanobenzoquinone(DDQ)/n-Bu4NN3 system. Tetrahedron Letters. 2004 Apr 12;45(16):3291-3294.

35. Li Z, Chen H, Bao H, Gao M. One-Pot Reaction to Synthesize Water-Soluble Magnetite Nanocrystals. Chemistry of Materials. 2004 Apr 1;16(8):1391-1393.

36. Murray CB, Sun S, Weller DK. Chemical synthesis of monodisperse and magnetic alloy nanocrystal containing thin films [Internet]. 2001 Mar 7 [cited 2011 Jun 17];Available from: http://www.freepatentsonline.com/6254662.html

37. Zhang L, He R, Gu H-C. Oleic acid coating on the monodisperse magnetite nanoparticles. Applied Surface Science. 2006 Dec 30;253(5):2611-2617.

38. Xu Z, Shen C, Hou Y, Gao H, Sun S. Oleylamine as Both Reducing Agent and Stabilizer in a Facile Synthesis of Magnetite Nanoparticles. Chemistry of Materials. 2009 May 12;21(9):1778-1780.

39. Klokkenburg M, Hilhorst J, Erné BH. Surface analysis of magnetite nanoparticles in cyclohexane solutions of oleic acid and oleylamine. Vibrational Spectroscopy. 2007;43(1):243-248.

40. Zhang L, He R, Gu H-C. Oleic acid coating on the monodisperse magnetite nanoparticles. Applied Surface Science. 2006 Dec 30;253(5):2611-2617.

41. Schreiber F. Structure and growth of self-assembling monolayers. Progress in Surface Science. November;65(5-8):151-257.

42. Love JC, Estroff LA, Kriebel JK, Nuzzo RG, Whitesides GM. Self-assembled monolayers of thiolates on metals as a form of nanotechnology. Chem. Rev. 2005;105(4):1103–1169.

43. Fu L, Dravid VP, Johnson DL. Self-assembled (SA) bilayer molecular coating on magnetic nanoparticles. Applied Surface Science. 2001;181(1-2):173-178.

44. Piazza M, Colombo M, Zanoni I, Granucci F, Tortora P, Weiss J, et al. Uniform Lipopolysaccharide (LPS)-Loaded Magnetic Nanoparticles for the Investigation of LPS–TLR4 Signaling. Angewandte Chemie International Edition. 2011 Jan 17;50(3):622-626.

45. Haik Y, Sawafta R, Ciubotaru I, Qablan A, Tan EL, Ong KG. Magnetic Techniques for Rapid Detection of Pathogens [Internet]. In: Zourob M, Elwary S, Turner A, editors. Principles of Bacterial Detection: Biosensors, Recognition Receptors and Microsystems. New York, NY: Springer New York; 2008 [cited 2011 Jul 1]. p. 415-458.Available from: http://www.springerlink.com/content/x56833245n7301v3/

46. Meyer MHF, Stehr M, Bhuju S, Krause H-J, Hartmann M, Miethe P, et al. Magnetic biosensor for the detection of Yersinia pestis. J. Microbiol. Methods. 2007 Feb;68(2):218-224.

47. Nam J-M, Stoeva SI, Mirkin CA. Bio-Bar-Code-Based DNA Detection with PCR-like Sensitivity. Journal of the American Chemical Society. 2004 May 1;126(19):5932-5933.

48. Fornara A, Johansson P, Petersson K, Gustafsson S, Qin J, Olsson E, et al. Tailored Magnetic Nanoparticles for Direct and Sensitive Detection of Biomolecules in Biological Samples. Nano Letters. 2008 Oct 8;8(10):3423-3428.

49. Spectral Diagnostics - The Toraymyxin Polymyxin B Column [Internet]. [cited 2011 May 19];Available from: http://www.spectraldx.com/toraymyxin.html

50. Safety and Efficacy of Polymyxin B Hemoperfusion (PMX) for Septic Shock - Full Text View - ClinicalTrials.gov [Internet]. [cited 2011 May 22];Available from: http://clinicaltrials.gov/ct2/show/NCT01046669

51. Raby A-C, Le Bouder E, Colmont C, Davies J, Richards P, Coles B, et al. Soluble TLR2 reduces inflammation without compromising bacterial clearance by disrupting TLR2 triggering. J. Immunol. 2009 Jul 1;183(1):506-517.

Chapter Five : General Discussion and Conclusions

5.1 General Overview of Thesis

Sepsis is the leading cause of death in non-coronary intensive care units worldwide with mortality rates of up to 50% and is a significant economic burden on the healthcare system (1). Despite this, it remains under-recognised and poorly understood because of inadequate diagnostic assays and a lack of scientifically targeted clinical treatments. LPS is ubiquitous in sepsis and its presence in the bloodstream has been correlated with a worse prognosis (2,3). With a growing number of bacteria displaying resistance to an ever-increasing number of antibiotics, diseases of infectious origin such as sepsis are likely to become more prevalent (4,5). The over-arching aim of this project was therefore to develop a peptide-polymer hybrid system capable of recognising and binding LPS in a variety of biologically relevant environments. We hypothesised that through the integration of target specific peptide receptors into the backbone of a polymer support, the issues surrounding the imprinting of biomacromolecules could be circumvented. There were a number of technological challenges associated with this project, each have been addressed in the preceding chapters of this thesis.

In Chapter Two, the development of an appropriate solid support was undertaken. Merrifield resin was selected as the support as it was anticipated that the chloromethyl functionality would allow for a multitude of chemistries to be displayed on the resins surface. Initial studies were concerned with bifunctionalisation of the resin to generate two independent chemical tethers to facilitate the attachment of a peptide species and an iniferter group. By using the Staudinger reaction

to reduce an azidomethyl intermediate, resins possessing controlled molar ratios of chloro and amino groups were produced.

Early studies were focused on achieving efficient polymerisation in ethanolic conditions as the peptide under investigation, TR401, was shown to be both stable and capable of binding its target (Texas red) in this solvent. The attachment of sodium diethyldithiocarbamate to the resin was achieved through reaction with the chloromethyl functionality and the polymerisation of an acrylamide/methylene bisacrylamide solution was demonstrated. Although the control resin was observed to also initiate polymerisation, through the photolytic cleavage of benzyl chloride to generate a reactive benzyl radical, aggregation and solution phase polymerisation was problematic. The benefits of using an iniferter species to initiate polymerisation were clear.

Modification of this system was necessary to allow for polymerisation under aqueous conditions required for the imprinting experiments with lipopolysaccharide. The diethyldithiocarbamate iniferter modified resins were not suitable for aqueous polymerisation experiments, since the resins (iniferter modified and conventional Merrifield) did not disperse in water even with continuous stirring. They aggregated at the surface of the solvent, which resulted in the formation of disc like structures after extended periods of polymerisation. At earlier time points, there was little evidence of polymerisation suggesting that possibly the dissociation of the iniferter species was slower in water than in ethanol due to the hydrophobicity of the dithiocarbamyl radical. A more hydrophilic iniferter, sodium dithiocarboxysarcosine, was synthesised and attached to the surface of the resin in a similar manner. This resin was significantly more dispersible and a stable dispersion in water could be achieved with gentle, continuous stirring.

Polymerisation experiments performed resulted in the growth of a polymer layer on the surface of the resin.

An important consideration in this study was the effect of experimental conditions on the swelling of Merrifield resin. The initial bifunctionalisation experiments were performed in DMF, a good swelling solvent for the resin. Under these conditions, elemental analysis suggested that controlled molar ratios of two chemical functionalities could be achieved but also that all chloromethyl groups could be converted to amines suggesting good access to the porous interior of the resin. Attachment of the iniferter species was carried out in ethanol and therefore the resin would have existed in a less swollen form than when DMF was used. Elemental analysis suggested that ~ 70 % of the available chloromethyl groups served as attachment points for the iniferter group. It was assumed that all of these iniferter groups would have been capable of initiating polymerisation under ethanolic conditions since the degree of swelling of the resin would have been similar, however when polymerisation was attempted in water the resin would have existed in a non-swollen state due to its hydrophobicity. Therefore it was unsurprising that the diethyldithiocarbamate resin performed poorly in the aqueous experiments since it was reasonable to assume that the majority of iniferter groups were unavailable to initiate polymerisation. Modification of the resin with the dithiocarboxysarcosine species yielded a more hydrophilic resin. However, since the iniferter was attached under aqueous conditions it was likely that the observed increase in dispersibility was a consequence of the presence of dithiocarboxysarcosine groups on the outer surface of the resin, whilst the interior surfaces of the resin were assumed to remain unmodified and hydrophobic. This resin was shown to initiate polymerisation of an aqueous acrylamide/methylene bisacrylamide solution. It was later

found that the iniferter was soluble in 50/50 methanol and DMF; conditions conducive to a swollen state. Successful attachment of iniferter was confirmed by FTIR and elemental analysis. Polymerisation experiments using this resin were not performed but warrant further investigation since the increased hydrophilicity conferred by the iniferter species may also impact on the swelling of the resin in aqueous conditions. In hindsight, a more hydrophilic solid support might have been more appropriate.

Chapter Three investigated the use of the bacterial derived peptide polymyxin B as the high affinity peptide ligand for incorporation into the peptide-polymer hybrid system described in Chapter One. Alkyne derivitisation of polymyxin B followed by immobilisation on azide modified resin via a "click" reaction successfully produced peptide modified resins. Polymyxin resin was shown to bind LPS with an apparent K_d of ~ 0.2 μM with negligible non - specific binding to azide control resin. The azidomethyl polystyrene support possessed ~ 0.2 mmol of azide groups per 100 mg, however only 7 μmoles (~ 10 mg) of peptide was estimated to be immobilised. The principle reason for this relatively low loading of polymyxin is the hydrophobicity of the resin prior to the immobilisation of the peptide. As the resin would have existed primarily in a non-swollen state under aqueous conditions, only surface azide groups would have been available for reaction. The B_{max} of polymyxin resin produced from 100 % azidomethyl polystyrene was estimated to be 0.07 $nmolmg^{-1}$ (700 $ngmg^{-1}$). If the estimated loading of polymyxin is accurate, this would suggest that at B_{max} only 1 in 1000 peptides are associated with LPS. The true significance of this is difficult to gauge as the labelling of LPS with the FITC tag is low; approximately 1 in 10 LPS molecules are labelled based on 3.80 μg of FITC per 1 mg of LPS and assuming an average molecular weight of 10,000 for LPS. A recent study by Triantafilou reports efficient labelling

of LPS (5 : 1, label : LPS) using Alexa 488 hydrazide (6). These levels of labelling would enable detection of much lower concentrations of LPS than is currently possible (current limit of detection using FITC labelled LPS is ~ 50 $ngml^{-1}$) and would allow a more accurate estimate of occupancy to be obtained.

Despite performing well in water, when binding assays were performed in serum the efficiency of the polymyxin resin was significantly reduced. In water, 5 mg of polymyxin resin bound ~ 80 % of a 1 μgml^{-1} FITC LPS solution. This was reduced to ~ 20 % when a 50/50 mix of water and foetal bovine serum (FBS) was used and to < 5 % when FBS was used alone (data not shown). Although disappointing, this result was not surprising given that LPS is bound by a number of serum proteins (specifically the high affinity lipopolysaccharide binding protein, LBP), some of which possess affinities for LPS that are orders of magnitude greater than the K_d of polymyxin. For the system to be useful in detecting LPS in *in vivo* samples, it must possess affinities equal to or greater than those displayed by endogenous proteins (i.e. low nanomolar/high picomolar range). As the K_d of polymyxin for LPS is ~ 0.2 μM it is unlikely that affinities required will be achieved through use of this peptide in the proposed hybrid system. During the course of this work, Matsumoto and colleagues identified a series of peptides displaying low nanomolar (1 - 10 nM) affinities for LPS via a phage display procedure (7). The sequence of the highest affinity 13-mer peptide is given in the paper and it is therefore anticipated that this will be made use of in future studies.

The results obtained from the proof-of-principle imprinting experiments using the cyclic and linear forms of polymyxin immobilised via "click" chemistry were somewhat disappointing. Previous attempts at imprinting using resin to which polymyxin had

been immobilised using the dimethyl adipimidate linker, demonstrated a clear imprinting effect. In that particular assay the influence of the template was clear; the amount of LPS binding to the polymyxin MIP was significantly greater than that binding to its non-imprinted antipode (polymyxin NIP). Repeating this assay with the click modified resins however failed to demonstrate a profound imprinting effect and the polymyxin MIPs (cyclic and linear) did not bind as much LPS as the respective peptide resins prior to polymerisation. The main difference between these two systems, other than the attachment chemistry, is the way in which the iniferter species were introduced as discussed in Chapter Three. Whether this is the reason for the difference in behaviour between the two assays remains to be elucidated. There are a number of complex variables that require investigation/optimisation including choice of monomer, polymerisation time, solid support and the nature and position of the peptide tether.

From a conventional imprinting perspective, it would be interesting to evaluate the approach of the Shea group used to surface imprint melittin. Amino acid sequences from melittin were modified with various lengths of hydrocarbon chains to allow for the formation of a micelle type structure in an emulsion polymerisation strategy (8). Given that LPS is naturally amphiphilic by virtue of the lipid A and polysaccharide regions, it may be possible to develop an imprinted polymer that recognises the O-antigen region of LPS as opposed to the lipid A/KDO portion of the molecule. If successful, it is envisaged that the polymer would be able to not only detect the presence of LPS but it could also potentially provide information about the causative bacterial species. This would be a significant development from a clinical perspective both in terms of diagnosis and treatment.

Chapter Four provided preliminary data for the use of peptide modified magnetic nanoparticles in the sequestration of LPS from

solution. Although the system based on Merrifield resin developed in Chapters Two and Three provided useful information about the feasibility of the proposed system, it is not immediately applicable to incorporation within a sensor platform or to a clinical setting. Magnetic nanoparticles on the other hand possess useful properties for use in both clinical and biosensing approaches. A more effective therapeutic strategy for the treatment of sepsis is urgently needed. Extracorporeal removal of LPS from the blood of septic patients using a polymyxin fibre (Toraymyxin) is the focus of a current multicenter clinical trial (9,10). This strategy has been used with some success for more than a decade in Japan, however it is likely to only remove free LPS from the blood as the affinity of LPS for polymyxin is several orders of magnitude lower than for acute phase serum proteins such as LBP and BPI (Chapter One). We hypothesise that magnetic nanoparticles displaying high affinity receptors for LPS could not only be used in a similar strategy, but also play a role in the *in vivo* sequestration of the toxin. Introduction of the magnetite nanoparticles to the systemic circulation of an infected host would hopefully reduce the immuno-stimulatory effects of LPS by acting as a decoy receptor, much like the soluble forms of CD14 and TLRs (11). Haemofiltration under a magnetic field would allow for the nanoparticles, coated with LPS, to be removed and possibly be fed into a direct sensor to allow for both treatment and rapid diagnosis. It is likely that the surface of the magnetite would require some modification to reduce the rate of clearance from the blood stream by the reticuloendothelial system.

It is anticipated that the immobilisation of LPS on the surface of magnetite particles will allow for the selection of high affinity peptide ligands via a phage display strategy. Peptides generated in this manner will be used in future studies to further investigate the utility of the peptide - polymer hybrid system. Immobilisation of polymyxin B via

the same self-assembly method used for LPS produced nanoparticles that were able to recognise and bind LPS rapidly from aqueous solutions with an apparent K_d of 0.18 μM. The system will require modification however if the peptide-polymer strategy outlined in Chapter One is to be transferred to the magnetic nanoparticles. Currently the nanoparticles are monofunctionalised with oleic acid and although initial attempts to functionalise the particles with azide groups were not obviously successful, it is anticipated that this will be readily achievable in the future.

5.2 Reference List

1. Daniels R. NHS Evidence - Emergency and Urgent Care [Internet]. 2009 [cited 2010 Nov 1];Available from: http://www.library.nhs.uk/emergency/Page.aspx?pagename=SEPSIS

2. Marshall JC, Foster D, Vincent J-L, Cook DJ, Cohen J, Dellinger RP, et al. Diagnostic and Prognostic Implications of Endotoxemia in Critical Illness: Results of the MEDIC Study. Journal of Infectious Diseases. 2004;190(3):527 -534.

3. Opal SM, Scannon PJ, Vincent J-L, White M, Carroll SF, Palardy JE, et al. Relationship between Plasma Levels of Lipopolysaccharide (LPS) and LPS-Binding Protein in Patients with Severe Sepsis and Septic Shock. Journal of Infectious Diseases. 1999 Nov 1;180(5):1584 - 1589.

4. Arias CA, Murray BE. Antibiotic-resistant bugs in the 21st century--a clinical super-challenge. N. Engl. J. Med. 2009 Jan 29;360(5):439-443.

5. Boucher HW, Talbot GH, Bradley JS, Edwards JE, Gilbert D, Rice LB, et al. Bad bugs, no drugs: no ESKAPE! An update from the Infectious Diseases Society of America. Clin. Infect. Dis. 2009 Jan 1;48(1):1-12.

6. Triantafilou K, Triantafilou M, Fernandez N. Lipopolysaccharide (LPS) labeled with Alexa 488 hydrazide as a novel probe for LPS binding studies. Cytometry. 2000 Dec 1;41(4):316-320.

7. Matsumoto M, Horiuchi Y, Yamamoto A, Ochiai M, Niwa M, Takagi T, et al. Lipopolysaccaride-binding peptides obtained by phage

display method. Journal of Microbiological Methods. 2010 Jul;82(1):54-58.

8. Zeng Z, Hoshino Y, Rodriguez A, Yoo H, Shea KJ. Synthetic Polymer Nanoparticles with Antibody-like Affinity for a Hydrophilic Peptide. ACS Nano. 2010 Jan 26;4(1):199-204.

9. Spectral Diagnostics - The Toraymyxin Polymyxin B Column [Internet]. [cited 2011 May 19];Available from: http://www.spectraldx.com/toraymyxin.html

10. Safety and Efficacy of Polymyxin B Hemoperfusion (PMX) for Septic Shock - Full Text View - ClinicalTrials.gov [Internet]. [cited 2011 May 22];Available from: http://clinicaltrials.gov/ct2/show/NCT01046669

11. Raby A-C, Le Bouder E, Colmont C, Davies J, Richards P, Coles B, et al. Soluble TLR2 reduces inflammation without compromising bacterial clearance by disrupting TLR2 triggering. J. Immunol. 2009 Jul 1;183(1):506-517.